

Susy breaking soft terms in the supersymmetric Pati-Salam landscape from Intersecting D6-Branes

Mudassar Sabir,^a Adeel Mansha,^b Tianjun Li,^{c,d,e} Zhi-Wei Wang^a

^a*School of Physics, University of Electronic Science and Technology of China, Chengdu, Sichuan 611731, P. R. China*

^b*College of Physics and Optoelectronic Engineering, Shenzhen University, Shenzhen 518060, P.R. China*

^c*CAS Key Laboratory of Theoretical Physics, Institute of Theoretical Physics, Chinese Academy of Sciences, Beijing 100190, P. R. China*

^d*School of Physical Sciences, University of Chinese Academy of Sciences, Beijing, P. R. China*

^e*School of Physics, Henan Normal University, Xinxiang 453007, P. R. China*

E-mail: mudassar.sabir@uestc.edu.cn, adeelmansha@alumni.itp.ac.cn,
tli@itp.ac.cn, zhiwei.wang@uestc.edu.cn

ABSTRACT: We investigate the supersymmetry breaking soft terms for all the viable models in the complete landscape of three-family supersymmetric Pati-Salam models arising from intersecting D6-branes on a $\mathbb{T}^6/(\mathbb{Z}_2 \times \mathbb{Z}_2)$ orientifold in type IIA string theory. The calculations are performed in the general scenario of u -moduli dominance with the s -moduli turned on, where the soft terms remain independent of the Yukawa couplings and the Wilson lines. The results for the trilinear coupling, gaugino-masses, squared-mass parameters of squarks, sleptons and Higgs depend on the brane wrapping numbers and the susy breaking parameters. We find that unlike the Yukawa couplings which remain unchanged for the models dual under the exchange of two $SU(2)$ sectors, the corresponding soft term parameters only match for the trilinear coupling and the mass of the gluino. This can be explained by the internal geometry where the Yukawa interactions depend only on the triangular areas of the worldsheet instantons while the soft terms have an additional dependence on the orientation-angles of D6-branes in the three two-tori. In the special limit of parameter space we find universal masses for the Higgs and the gauginos.

ARXIV EPRINT: [2410.09093](https://arxiv.org/abs/2410.09093)

Contents

1	Introduction	2
2	Pati-Salam model building on a $\mathbb{T}^6/(\mathbb{Z}_2 \times \mathbb{Z}_2)$ orientifold	3
2.1	Constraints from tadpole cancellation and $\mathcal{N} = 1$ supersymmetry	5
2.2	Particle spectrum	6
3	Supersymmetry breaking and $\mathcal{N} = 1$ Effective theory	7
3.1	Supersymmetry breaking via u -moduli and dilaton s	11
3.2	Soft parameters	12
3.3	Computational strategy	14
4	Susy-breaking soft terms in the Pati-Salam landscape	15
4.1	Model 13	16
4.2	Model 14	18
4.3	Model 15	20
4.4	Model 15-dual	23
4.5	Model 16	26
4.6	Model 16-dual	29
4.7	Model 17	32
4.8	Model 17-dual	35
4.9	Model 18	37
4.10	Model 18-dual	40
4.11	Model 19	42
4.12	Model 19-dual	45
4.13	Model 20	47
4.14	Model 20-dual	50
4.15	Model 21	53
4.16	Model 22	55
4.17	Model 22-dual	58
5	Discussion and conclusion	60
A	Independent supersymmetric Pati-Salam models	61

1 Introduction

In the standard model, quarks and leptons arise from chiral representations of the gauge group $SU(3)_C \times SU(2)_L \times U(1)_Y$. Intersecting D6-branes in type IIA string theory, filling the four-dimensional spacetime and extending into three compact dimensions, provide a geometric realization of standard model gauge interactions. Open strings stretched between two intersecting D6-branes act as chiral fermions [1, 2]. Family replication is readily achieved as branes generically intersect at several points. The four-dimensional gauge couplings are determined by the volumes of the cycles wrapped by D6-branes while the gravitational coupling depends on the total internal volume of the compact dimensions, thus allowing the possibility of having the string scale M_S parametrically smaller than the Planck scale M_P . Hierarchical Yukawa couplings arise from open world-sheet instantons, which are suppressed by $\exp(-A_{ijk}T)$, where A_{ijk} represents the area of the triangle formed by the intersections $\{i, j, k\}$, and T denotes the string tension.

Since realistic Yukawa textures cannot arise from a single stack of D-branes, this necessitates that the gauge group of the standard model be a direct product of unitary groups rather than a simple unitary group. Statistically, the configurations of the branes tend to favor direct products of unitary groups constructed from an even number of D-branes within the stack. This preference can be explained by the K-theory conditions [3, 4], constrained by mod 4 and thus are easier to satisfy for $U(2N)$ with $N \in \mathbb{Z}$. For example, in trinification models, there is currently no single consistent three-family model that satisfies the stringent requirements of $\mathcal{N} = 1$ supersymmetry, tadpole cancellation, and K-theory constraints [5]. Note that even if the models are consistent under the K-theory, no tadpoles and susy conditions, the viable models with realistic Yukawa textures are extremely difficult to engineer. Consequently, the left-right symmetric Pati-Salam group, $SU(4)_C \times SU(2)_L \times SU(2)_R$, stands out as the most promising option for realistic models.

The model building rules to construct supersymmetric Pati-Salam models on a $T^6/(\mathbb{Z}_2 \times \mathbb{Z}_2)$ orientifold utilizing intersecting D6-branes with the requirement of $\mathcal{N} = 1$ supersymmetry, no-tadpole constraints and ensuring K-theory conditions were laid out in [6–8]. A similar approach has been applied in more recent studies [9–13]. The complete landscape of consistent three-family $\mathcal{N} = 1$ supersymmetric Pati-Salam models containing 206,752 models has been derived in [14]. There are 33 distinct physical models with distinct gauge coupling relations up to type I and type II T-dualities. In [15], we have presented the results of Yukawa couplings for all the feasible models in this landscape, and in [16] the most realistic model explaining the fermion masses and mixings has been discussed.

In this paper, we investigate the supersymmetry breaking soft terms for all the viable three-family supersymmetric Pati-Salam models in the landscape, focusing on the u -moduli dominated scenario with the s -moduli turned on. In this setup, the soft terms remain independent of the Yukawa couplings and the Wilson lines. The results for the trilinear coupling, gaugino-masses, squared-mass parameters of squarks, sleptons and Higgs are determined by the D-brane wrapping numbers and the supersymmetry breaking parameters, which include the gravitino mass and the goldstino angles.

For any two models which are dual under the exchange of two $SU(2)$ s, the Yukawa

couplings produce identical results, however, the corresponding soft term parameters exhibit notable differences. Specifically, the trilinear coupling and the gluino mass match, whereas the other soft terms, such as bino, wino and squared masses of squarks and sleptons, differ between the dual models. This discrepancy can be understood from the underlying geometry of the compact space. While the Yukawa interactions depend solely on the triangular area of the worldsheet instantons, the soft terms are influenced by additional factors, including the orientation angles of the D6-branes on the three two-tori. As a result, dual models not only exhibit distinct gauge coupling relations but also feature different gaugino masses and soft scalar mass parameters.

Since the scale of supersymmetry breaking is still unknown, we mainly focus on generic results in the present work. Nonetheless, we have found an interesting regime of parameters where all gaugino-masses become degenerate and the Higgs mass parameter is half the gravitino-mass which determines the susy breaking scale. This special limit corresponds to setting the three goldstino angles $\{\Theta_1, \Theta_2, \Theta_3\}$ equal to $1/2$ and setting the dilaton angle $\Theta_s = -1/2$ with all CP-violating phases $\{\gamma_1, \gamma_2, \gamma_3, \gamma_s\}$ set to zero.

The contents of the paper are organized as follows. In section 2 we briefly review the rules to construct supersymmetric Pati-Salam models from stacks of intersecting D6-branes on a $\mathbb{T}^6/(\mathbb{Z}_2 \times \mathbb{Z}_2)$ orientifold. In section 3 we describe the four-dimensional effective field theory and the soft terms from supersymmetry breaking in the case of u -moduli domination with the dilaton modulus s turned on. We outline the computational strategy to calculate the susy breaking soft terms from the given wrapping numbers and the angles of D6-branes. In section 4 we systematically compute the soft terms for all viable models in the three-family Pati-Salam landscape. Finally, we conclude in section 5.

2 Pati-Salam model building on a $\mathbb{T}^6/(\mathbb{Z}_2 \times \mathbb{Z}_2)$ orientifold

$\mathbb{T}^6/(\mathbb{Z}_2 \times \mathbb{Z}_2)$ is the product of three two-tori \mathbb{T}^2 with the orbifold group $\mathbb{Z}_2 \times \mathbb{Z}_2$, having the generators θ and ω , which are respectively associated with the twist vectors $(1/2, -1/2, 0)$ and $(0, 1/2, -1/2)$ such that their action on the complex coordinates z_i is given as,

$$\begin{aligned}\theta : (z_1, z_2, z_3) &\rightarrow (-z_1, -z_2, z_3), \\ \omega : (z_1, z_2, z_3) &\rightarrow (z_1, -z_2, -z_3).\end{aligned}\tag{2.1}$$

Orientifold projection is the gauged $\Omega\mathcal{R}$ symmetry, where Ω is world-sheet parity that interchanges the left- and right-moving sectors of a closed string and swaps the two ends of an open string as,

$$\begin{aligned}\text{Closed : } \Omega : (\sigma_1, \sigma_2) &\mapsto (2\pi - \sigma_1, \sigma_2), \\ \text{Open : } \Omega : (\tau, \sigma) &\mapsto (\tau, \pi - \sigma),\end{aligned}\tag{2.2}$$

and \mathcal{R} acts as complex conjugation on coordinates z_i . This results in four different kinds of orientifold 6-planes (O6-planes) corresponding to $\Omega\mathcal{R}$, $\Omega\mathcal{R}\theta$, $\Omega\mathcal{R}\omega$, and $\Omega\mathcal{R}\theta\omega$ respectively. These orientifold projections are only consistent with either the rectangular or the tilted complex structures of the factorized two-tori. Denoting the wrapping numbers

for the rectangular and tilted tori as $n_a^i[a_i] + m_a^i[b_i]$ and $n_a^i[a'_i] + m_a^i[b_i]$ respectively, where $[a'_i] = [a_i] + \frac{1}{2}[b_i]$. Then a generic 1-cycle (n_a^i, l_a^i) satisfies $l_a^i \equiv m_a^i$ for the rectangular two-torus and $l_a^i \equiv 2\tilde{m}_a^i = 2m_a^i + n_a^i$ for the tilted two-torus such that $l_a^i - n_a^i$ is even for the tilted tori.

Note that the two different bases (n^i, l^i) and (n^i, m^i) are related as,

$$m^i = 2^{-\beta_i} l^i - \frac{\beta_i}{2} n^i, \quad \beta_i = \begin{cases} 0 & \text{rectangular } \mathbb{T}^2, \\ 1 & \text{tilted } \mathbb{T}^2. \end{cases} \quad (2.3)$$

We use the basis (n^i, l^i) to specify the model wrapping numbers in appendix A while the basis (n^i, m^i) is convenient to sketch the Yukawa textures in section 4.

The homology cycles for a stack a of N_a D6-branes along the cycle (n_a^i, l_a^i) and their $\Omega\mathcal{R}$ images a' stack of N_a D6-branes with cycles $(n_a^i, -l_a^i)$ are respectively given as,

$$\begin{aligned} [\Pi_a] &= \prod_{i=1}^3 \left(n_a^i[a_i] + 2^{-\beta_i} l_a^i[b_i] \right), \\ [\Pi_{a'}] &= \prod_{i=1}^3 \left(n_a^i[a_i] - 2^{-\beta_i} l_a^i[b_i] \right). \end{aligned} \quad (2.4)$$

The homology three-cycles, which are wrapped by the four O6-planes, are given by

$$\begin{aligned} \Omega\mathcal{R} : \quad [\Pi_{\Omega\mathcal{R}}] &= 2^3[a_1] \times [a_2] \times [a_3], \\ \Omega\mathcal{R}\omega : \quad [\Pi_{\Omega\mathcal{R}\omega}] &= -2^{3-\beta_2-\beta_3}[a_1] \times [b_2] \times [b_3], \\ \Omega\mathcal{R}\theta\omega : \quad [\Pi_{\Omega\mathcal{R}\theta\omega}] &= -2^{3-\beta_1-\beta_3}[b_1] \times [a_2] \times [b_3], \\ \Omega\mathcal{R}\theta : \quad [\Pi_{\Omega\mathcal{R}\theta}] &= -2^{3-\beta_1-\beta_2}[b_1] \times [b_2] \times [a_3]. \end{aligned} \quad (2.5)$$

The intersection numbers can be calculated in terms of wrapping numbers as,

$$\begin{aligned} I_{ab} &= [\Pi_a][\Pi_b] = 2^{-k} \prod_{i=1}^3 (n_a^i l_b^i - n_b^i l_a^i), \\ I_{ab'} &= [\Pi_a][\Pi_{b'}] = -2^{-k} \prod_{i=1}^3 (n_a^i l_b^i + n_b^i l_a^i), \\ I_{aa'} &= [\Pi_a][\Pi_{a'}] = -2^{3-k} \prod_{i=1}^3 (n_a^i l_a^i), \\ I_{aO6} &= [\Pi_a][\Pi_{O6}] = 2^{3-k} (-l_a^1 l_a^2 l_a^3 + l_a^1 n_a^2 n_a^3 + n_a^1 l_a^2 n_a^3 + n_a^1 n_a^2 l_a^3), \end{aligned} \quad (2.6)$$

where $k = \sum_{i=1}^3 \beta_i$ and $[\Pi_{O6}] = [\Pi_{\Omega\mathcal{R}}] + [\Pi_{\Omega\mathcal{R}\omega}] + [\Pi_{\Omega\mathcal{R}\theta\omega}] + [\Pi_{\Omega\mathcal{R}\theta}]$.

In order to have three families of the left chiral and right chiral standard model fields, the intersection numbers must satisfy

$$I_{ab} + I_{ab'} = 3, \quad I_{ac} = -3, \quad I_{ac'} = 0. \quad (2.7)$$

2.1 Constraints from tadpole cancellation and $\mathcal{N} = 1$ supersymmetry

Since D6-branes and O6-orientifold planes are the sources of Ramond-Ramond charges they are constrained by the Gauss's law in compact space implying the sum of D-brane and cross-cap RR-charges must vanish [17]

$$\sum_a N_a [\Pi_a] + \sum_a N_a [\Pi_{a'}] - 4[\Pi_{O6}] = 0, \quad (2.8)$$

where the last terms arise from the O6-planes, which have -4 RR charges in D6-brane charge units. RR tadpole constraint is sufficient to cancel the $SU(N_a)^3$ cubic non-Abelian anomaly while U(1) mixed gauge and gravitational anomaly or $[SU(N_a)]^2 U(1)$ gauge anomaly can be cancelled by the Green-Schwarz mechanism, mediated by untwisted RR fields [18].

Let us define the following products of wrapping numbers,

$$\begin{aligned} A_a &\equiv -n_a^1 n_a^2 n_a^3, & B_a &\equiv n_a^1 l_a^2 l_a^3, & C_a &\equiv l_a^1 n_a^2 l_a^3, & D_a &\equiv l_a^1 l_a^2 n_a^3, \\ \tilde{A}_a &\equiv -l_a^1 l_a^2 l_a^3, & \tilde{B}_a &\equiv l_a^1 n_a^2 n_a^3, & \tilde{C}_a &\equiv n_a^1 l_a^2 n_a^3, & \tilde{D}_a &\equiv n_a^1 n_a^2 l_a^3. \end{aligned} \quad (2.9)$$

Cancellation of RR tadpoles requires introducing a number of orientifold planes also called “filler branes” that trivially satisfy the four-dimensional $\mathcal{N} = 1$ supersymmetry conditions. The no-tadpole condition is given as,

$$\begin{aligned} -2^k N^{(1)} + \sum_a N_a A_a &= -2^k N^{(2)} + \sum_a N_a B_a = \\ -2^k N^{(3)} + \sum_a N_a C_a &= -2^k N^{(4)} + \sum_a N_a D_a = -16, \end{aligned} \quad (2.10)$$

where $2N^{(i)}$ is the number of filler branes wrapping along the i^{th} O6-plane. The filler branes belong to the hidden sector USp group and carry the same wrapping numbers as one of the O6-planes as shown in table 1. USp group is hence referred with respect to the non-zero A , B , C or D -type.

Orientifold action	O6-plane	$(n^1, l^1) \times (n^2, l^2) \times (n^3, l^3)$
$\Omega\mathcal{R}$	1	$(2^{\beta_1}, 0) \times (2^{\beta_2}, 0) \times (2^{\beta_3}, 0)$
$\Omega\mathcal{R}\omega$	2	$(2^{\beta_1}, 0) \times (0, -2^{\beta_2}) \times (0, 2^{\beta_3})$
$\Omega\mathcal{R}\theta\omega$	3	$(0, -2^{\beta_1}) \times (2^{\beta_2}, 0) \times (0, 2^{\beta_3})$
$\Omega\mathcal{R}\theta$	4	$(0, -2^{\beta_1}) \times (0, 2^{\beta_2}) \times (2^{\beta_3}, 0)$

Table 1: The wrapping numbers for four O6-planes.

Preserving $\mathcal{N} = 1$ supersymmetry in four dimensions after compactification from ten-dimensions restricts the rotation angle of any D6-brane with respect to the orientifold plane to be an element of $SU(3)$, i.e.

$$\theta_a^1 + \theta_a^2 + \theta_a^3 = 0 \bmod 2\pi, \quad (2.11)$$

where $\theta_a^i = \frac{1}{\pi} \arctan \left(\frac{2^{-\beta_i} l_a^i}{n_a^i} \chi_i \right)$ is the angle between the D6-brane and orientifold-plane and $\chi_i = R_i^2/R_i^1$ are the complex structure moduli of the i^{th} two-torus. $\mathcal{N} = 1$ supersymmetry conditions are given as,

$$x_A \tilde{A}_a + x_B \tilde{B}_a + x_C \tilde{C}_a + x_D \tilde{D}_a = 0, \\ \frac{A_a}{x_A} + \frac{B_a}{x_B} + \frac{C_a}{x_C} + \frac{D_a}{x_D} < 0, \quad (2.12)$$

where $x_A = \lambda$, $x_B = 2^{\beta_2+\beta_3} \cdot \lambda/\chi_2\chi_3$, $x_C = 2^{\beta_1+\beta_3} \cdot \lambda/\chi_1\chi_3$, $x_D = 2^{\beta_1+\beta_2} \cdot \lambda/\chi_1\chi_2$.

Orientifolds also have discrete D-brane RR charges classified by the \mathbb{Z}_2 K-theory groups, which are subtle and invisible by the ordinary homology [3, 19–21], which should also be taken into account [4]. The K-theory conditions are,

$$\sum_a \tilde{A}_a = \sum_a N_a \tilde{B}_a = \sum_a N_a \tilde{C}_a = \sum_a N_a \tilde{D}_a = 0 \bmod 4. \quad (2.13)$$

In our case, we avoid the nonvanishing torsion charges by taking an even number of D-branes, *i.e.*, $N_a \in 2\mathbb{Z}$.

2.2 Particle spectrum

Sector	Representation
aa	$U(N_a/2)$ vector multiplet 3 adjoint chiral multiplets
$ab + ba$	$\mathcal{M}(\frac{N_a}{2}, \frac{\bar{N}_b}{2}) = I_{ab}(\square_a, \bar{\square}_b)$
$ab' + b'a$	$\mathcal{M}(\frac{N_a}{2}, \frac{N_b}{2}) = I_{ab'}(\square_a, \square_b)$
$aa' + a'a$	$\mathcal{M}(a_{\square\square}) = \frac{1}{2}(I_{aa'} - \frac{1}{2}I_{aO6})$ $\mathcal{M}(a_{\square}) = \frac{1}{2}(I_{aa'} + \frac{1}{2}I_{aO6})$

Table 2: General spectrum for intersecting D6-branes at generic angles, where \mathcal{M} is the multiplicity, and $a_{\square\square}$ and a_{\square} denote respectively the symmetric and antisymmetric representations of $U(N_a/2)$. Positive intersection numbers in our convention refer to the left-handed chiral supermultiplets.

To have three families of the SM fermions, we need one torus to be tilted, which is chosen to be the third torus. So we have $\beta_1 = \beta_2 = 0$ and $\beta_3 = 1$. Placing the a' , b and c stacks of D6-branes on the top of each other on the third two-torus results in additional vector-like particles from $\mathcal{N} = 2$ subsectors [6]. The anomalies from three global $U(1)$ s of $U(4)_C$, $U(2)_L$ and $U(2)_R$ are cancelled by the Green-Schwarz mechanism, and the gauge fields of these $U(1)$ s obtain masses via the linear $B \wedge F$ couplings. Thus, the effective gauge symmetry is $SU(4)_C \times SU(2)_L \times SU(2)_R$.

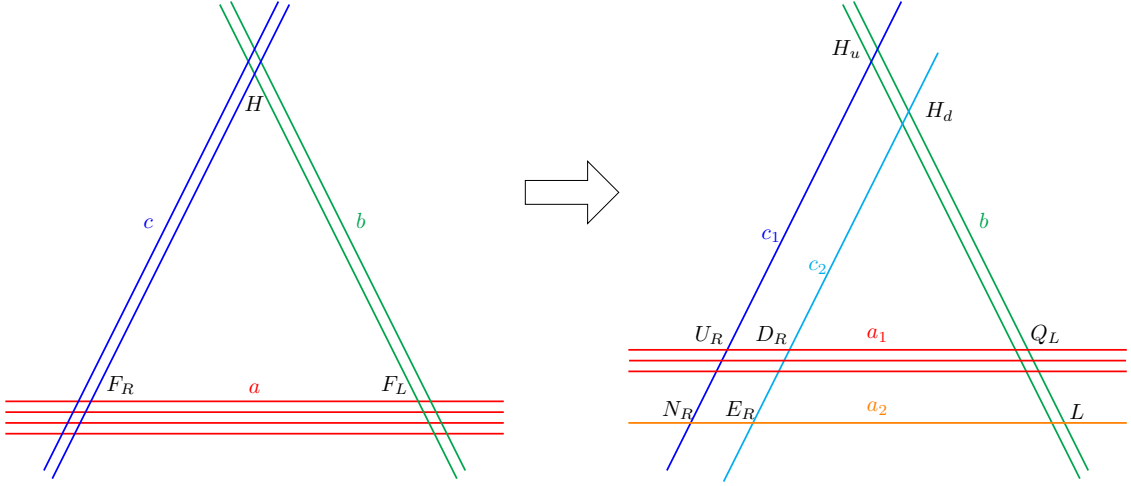


Figure 1: Pati-Salam gauge group $SU(4)_C \times SU(2)_L \times SU(2)_R$ is broken down to the standard model gauge group $SU(3)_C \times U(2)_L \times U(1)_{I_{3R}} \times U(1)_{B-L}$ via the process of brane splitting that corresponds to assigning VEVs to the adjoint scalars, which arise as open-string moduli associated with the positions of stacks a and c in the internal space.

3 Supersymmetry breaking and $\mathcal{N} = 1$ Effective theory

Pati-Salam gauge group $SU(4)_C \times SU(2)_L \times SU(2)_R$ is higgsed down to the standard model gauge group $SU(3)_C \times U(2)_L \times U(1)_{I_{3R}} \times U(1)_{B-L}$ by assigning vacuum expectation values to the adjoint scalars which arise as open-string moduli associated to the stacks a and c , see figure 1,

$$\begin{aligned} a &\rightarrow a_1 + a_2, \\ c &\rightarrow c_1 + c_2. \end{aligned} \quad (3.1)$$

Moreover, the $U(1)_{I_{3R}} \times U(1)_{B-L}$ gauge symmetry may be broken to $U(1)_Y$ by giving vacuum expectation values (VEVs) to the vector-like particles with the quantum numbers $(\mathbf{1}, \mathbf{1}, \mathbf{1}/2, -1)$ and $(\mathbf{1}, \mathbf{1}, -\mathbf{1}/2, 1)$ under the $SU(3)_C \times SU(2)_L \times U(1)_{I_{3R}} \times U(1)_{B-L}$ gauge symmetry from $a_2 c'_1$ intersections [6, 22]. This brane-splitting results in standard model quarks and leptons as [23],

$$\begin{aligned} F_L(Q_L, L_L) &\rightarrow Q_L + L, \\ F_R(Q_R, L_R) &\rightarrow U_R + D_R + E_R + N. \end{aligned} \quad (3.2)$$

Three-point Yukawa couplings for the quarks and the charged leptons can be read from the following superpotential,

$$\mathcal{W}_3 \sim Y_{ijk}^u Q_i U_j^c H_k^u + Y_{ijk}^d Q_i D_j^c H_k^d + Y_{ijk}^\nu L_i N_j^c H_k^u + Y_{ijk}^e L_i E_j^c H_k^d, \quad (3.3)$$

where Y_{ijk}^u , Y_{ijk}^d , Y_{ijk}^ν and Y_{ijk}^e are Yukawa couplings, and Q_i , U_i^c , D_i^c , L_i , N_i^c , and E_i^c are the left-handed quark doublet, right-handed up-type quarks, right-handed down-type quarks,

left-handed lepton doublet, right-handed neutrinos, and right-handed leptons, respectively. The superpotential including the four-point interactions is

$$\mathcal{W}_4 \sim \frac{1}{M_S} \left(Y_{ijkl}'^u Q_i U_j^c H_k'^u S_l^L + Y_{ijkl}'^d Q_i D_j^c H_k'^d S_l^L + Y_{ijkl}'^\nu L_i N_j^c H_k'^\nu S_l^L + Y_{ijkl}'^e L_i E_j^c H_k'^e S_l^L \right), \quad (3.4)$$

where $Y_{ijkl}'^u$, $Y_{ijkl}'^d$, $Y_{ijkl}'^\nu$, and $Y_{ijkl}'^e$ are Yukawa couplings of the four-point functions, and M_S is the string scale.

The additional exotic particles must be made superheavy to ensure gauge coupling unification at the string scale. Similar to refs. [24, 25] we can decouple the additional exotic particles except the charged chiral multiplets under $SU(4)_C$ anti-symmetric representation. These chiral multiplets can be decoupled via instanton effects in principle [26–28].

We now turn our attention toward the four dimensional low energy effective field theory. $\mathcal{N} = 1$ supergravity action is encoded by three functions viz. the gauge kinetic function f_x , the Kähler potential K and the superpotential W [29]. Each of these functions in turn depend on a dilaton modulus S , three Kähler moduli T^i and three complex structure moduli U^i .

The complex structure moduli U^i are defined as,

$$U^j = \frac{4i\chi_j + 2\beta_j\chi_j^2}{4 + \beta_j\chi_j^2}, \quad \because \chi_j \equiv \frac{R_2^j}{R_1^j}. \quad (3.5)$$

These upper case moduli in string theory basis can be transformed to lower-case s , t^i and u^i moduli in field theory basis as [30],

$$\begin{aligned} \text{Re}(s) &= \frac{e^{-\phi_4}}{2\pi} \left(\frac{\sqrt{\text{Im } U^1 \text{Im } U^2 \text{Im } U^3}}{|U^1 U^2 U^3|} \right), \\ \text{Re}(u^j) &= \frac{e^{-\phi_4}}{2\pi} \left(\sqrt{\frac{\text{Im } U^j}{\text{Im } U^k \text{Im } U^l}} \right) \left| \frac{U^k U^l}{U^j} \right|, \quad (j, k, l) = (\overline{1, 2, 3}), \\ \text{Re}(t^j) &= \frac{i\alpha'}{T^j}, \end{aligned} \quad (3.6)$$

where j denotes the j^{th} two-torus, and ϕ_4 is the four dimensional dilaton which is related to the supergravity moduli as

$$2\pi e^{\phi_4} = \left(\text{Re}(s) \text{Re}(u^1) \text{Re}(u^2) \text{Re}(u^3) \right)^{-1/4}. \quad (3.7)$$

Inverting the above formulas we can solve for U^i moduli in string theory basis in terms of s and u^i as,

$$\frac{|U^j|^2}{\text{Im}(U^j)} = \sqrt{\frac{\text{Re}(u^k) \text{Re}(u^l)}{\text{Re}(u^j) \text{Re}(s)}}, \quad (j, k, l) = (\overline{1, 2, 3}). \quad (3.8)$$

The holomorphic gauge kinetic function for any D6-brane stack x wrapping a calibrated 3-cycle is given as [7],

$$f_x = \frac{1}{2\pi\ell_s^3} \left[e^{-\phi} \int_{\Pi_x} \text{Re}(e^{-i\theta_x} \Omega_3) - i \int_{\Pi_x} C_3 \right], \quad (3.9)$$

where the integral involving 3-form Ω_3 gives,

$$\int_{\Pi_x} \Omega_3 = \frac{1}{4} \prod_{i=1}^3 (n_x^i R_1^i + 2^{-\beta_i} i l_x^i R_2^i). \quad (3.10)$$

It can then be shown that,

$$f_x = \frac{1}{4k_x} (n_x^1 n_x^2 n_x^3 s - \frac{n_x^1 l_x^2 l_x^3 u^1}{2(\beta_2+\beta_3)} - \frac{l_x^1 n_x^2 l_x^3 u^2}{2(\beta_1+\beta_3)} - \frac{l_x^1 l_x^2 n_x^3 u^3}{2(\beta_1+\beta_2)}), \quad (3.11)$$

where the factor k_x is related to the difference between the gauge couplings for $U(N_x)$ and $USp(2N_x), SO(2N_x)$ such that $k_x = 1$ for $U(N_x)$ and $k_x = 2$ for $USp(2N_x)$ or $SO(2N_x)$ [31, 32]. Since, the standard model hypercharge $U(1)_Y$ is a linear combination of several $U(1)$ s,

$$Q_Y = \frac{1}{6}Q_{a_1} + \frac{1}{2}Q_{a_2} - \frac{1}{2}Q_{c_1} - \frac{1}{2}Q_{c_2}, \quad (3.12)$$

similarly, the holomorphic gauge kinetic function for the hypercharge is also taken as a linear combination of the kinetic gauge functions from several stacks [32, 33],

$$f_Y = \frac{1}{6}f_{a_1} + \frac{1}{2}f_{a_2} + \frac{1}{2}f_{c_1} + \frac{1}{2}f_{c_2}. \quad (3.13)$$

The Kähler potential to the second order for the moduli M and open string matter fields, C_i, C_θ has the structure,

$$\begin{aligned} K(M, \bar{M}, C, \bar{C}) &= \hat{K}(M, \bar{M}) + \sum_{\text{untwisted } i,j} \tilde{K}_{C_i \bar{C}_j}(M, \bar{M}) C_i \bar{C}_j \\ &+ \sum_{\text{twisted}, \theta} \tilde{K}_{C_\theta \bar{C}_\theta}(M, \bar{M}) C_\theta \bar{C}_\theta, \end{aligned} \quad (3.14)$$

where

$$\kappa^2 \hat{K}(M, \bar{M}) = -\log(S + \bar{S}) - \sum_{i=1}^3 \log(T^i + \bar{T}^i) - \sum_{i=1}^3 \log(U^i + \bar{U}^i), \quad (3.15)$$

where $\kappa^2 = 8\pi G_N$, C_i correspond to the D-brane positions and the Wilson lines moduli arising from strings having both ends on the same stack while C_θ correspond to strings stretching between different stacks comprising 1/4 BPS branes. The untwisted moduli fields C_i, \bar{C}_j are not present in MSSM and must become heavy via higher dimensional operators¹.

Let us determine the Kähler metric $\tilde{K}_{C_\theta \bar{C}_\theta}(M, \bar{M})$ for the twisted moduli. The angles θ_x^j made by the cycle wrapped by stack of D6-branes on each of the three two-tori are related to the s and u^j moduli as,

$$\tan(\pi\theta_x^j) = \frac{2^{-\beta_j} l_x^j}{n_x^j} \chi_j = \frac{2^{-\beta_j} l_x^j}{n_x^j} \sqrt{\frac{\text{Re} u^k \text{Re} u^l}{\text{Re} u^j \text{Re} s}}, \quad (j, k, l) = (\bar{1}, 2, \bar{3}). \quad (3.16)$$

We denote the Kähler potential arising from strings stretching between stacks x and y as \tilde{K}_{xy} and $\theta_{xy}^j \equiv \theta_y^j - \theta_x^j$ denotes the angle difference between the cycles wrapped by the branes x and y on the j^{th} two-torus with the constraint $\sum_j \theta_{xy}^j = 0$.

¹D-branes wrapping rigid cycles can freeze such open string moduli [34], however such rigid cycles without discrete torsion are not present in $\mathbb{T}^6/(\mathbb{Z}_2 \times \mathbb{Z}_2)$.

Following [30, 35, 36], we find two cases for the Kähler metric for 1/4 BPS brane configurations in type IIA theory:

- $\theta_{xy}^j < 0, \theta_{xy}^k > 0, \theta_{xy}^l > 0$

$$\tilde{K}_{xy} = e^{\phi_4} e^{\gamma_E(2 - \sum_{j=1}^3 \theta_{xy}^j)} \sqrt{\frac{\Gamma(\theta_{xy}^j)}{\Gamma(1 + \theta_{xy}^j)}} \sqrt{\frac{\Gamma(1 - \theta_{xy}^k)}{\Gamma(\theta_{xy}^k)}} \sqrt{\frac{\Gamma(1 - \theta_{xy}^l)}{\Gamma(\theta_{xy}^l)}} (t^j + \bar{t}^j)^{\theta_{xy}^j} (t^k + \bar{t}^k)^{-1 + \theta_{xy}^k} (t^l + \bar{t}^l)^{-1 + \theta_{xy}^l}. \quad (3.17)$$

- $\theta_{xy}^j < 0, \theta_{xy}^k < 0, \theta_{xy}^l > 0$

$$\tilde{K}_{xy} = e^{\phi_4} e^{\gamma_E(2 + \sum_{j=1}^3 \theta_{xy}^j)} \sqrt{\frac{\Gamma(1 + \theta_{xy}^j)}{\Gamma(-\theta_{xy}^j)}} \sqrt{\frac{\Gamma(1 + \theta_{xy}^k)}{\Gamma(-\theta_{xy}^k)}} \sqrt{\frac{\Gamma(\theta_{xy}^l)}{\Gamma(1 - \theta_{xy}^l)}} (t^j + \bar{t}^j)^{-1 - \theta_{xy}^j} (t^k + \bar{t}^k)^{-1 - \theta_{xy}^k} (t^l + \bar{t}^l)^{-\theta_{xy}^l}. \quad (3.18)$$

The Kähler metric for 1/2 BPS brane configurations, which give rise to non-chiral matter in bifundamental representations like the Higgs from the $\mathcal{N} = 2$ sector, is given as,

$$\tilde{K}_{\text{Higgs}} = [(s + \bar{s})(t^1 + \bar{t}^1)(t^2 + \bar{t}^2)(u^3 + \bar{u}^3)]^{-1/2}. \quad (3.19)$$

The holomorphic superpotential is given as,

$$W(M, C) = \hat{W}(M) + \frac{1}{2} \mu_{\alpha\beta}(M) C^\alpha C^\beta + \frac{1}{6} Y_{\alpha\beta\gamma}(M) C^\alpha C^\beta C^\gamma + \dots \quad (3.20)$$

and the minimum of the tree-level F-term scalar potential of the supergravity is given by²

$$\begin{aligned} V(M, \bar{M}) &= e^{\kappa^2 \hat{K}} \left[\hat{K}^{\bar{I}J} (D_I \hat{W})^* (D_J \hat{W}) - 3 \kappa^2 |\hat{W}|^2 \right] \\ &= \hat{K}_{I\bar{J}} F^I \bar{F}^{\bar{J}} - 3 e^{\kappa^2 \hat{K}} \kappa^2 |\hat{W}|^2, \end{aligned} \quad (3.21)$$

where $D_I = \partial_I + \kappa^2 \partial_I \hat{K}$, $\hat{K}_{I\bar{J}} = \partial_{\bar{I}} \partial_J \hat{K}$, $\hat{K}^{\bar{I}J}$ is the inverse Kähler metric, and the auxiliary fields $\bar{F}^{\bar{I}}$ are,

$$\bar{F}^{\bar{I}} = \kappa^2 e^{\kappa^2 \hat{K}/2} \hat{K}^{\bar{I}J} D_J \hat{W}, \quad (3.22)$$

where the indices I, J run over the dilaton S , the complex structure moduli U^i and the Kähler moduli T^i . Thus supersymmetry is broken via F-terms from some of the hidden sector fields M acquiring VEVs, thereby generating soft terms in the observable sector [25, 35, 39]. Gravitino gets massive by absorbing goldstino via the superhiggs mechanism.

$$m_{3/2} = e^{\kappa^2 \hat{K}/2} \kappa^2 |\hat{W}|. \quad (3.23)$$

The *normalized* soft parameters viz. the gaugino mass, squared scalar mass and trilinear parameters are given by [40],

$$\begin{aligned} M_x &= \frac{1}{2 \text{Re } f_x} (F^I \partial_I f_x), \\ m_{xy}^2 &= m_{3/2}^2 + V_0 - \sum_{\bar{I}, J} \bar{F}^{\bar{I}} F^J \partial_{\bar{I}} \partial_J \log(\tilde{K}_{xy}), \\ A_{xyz} &= F^I \left[\hat{K}_I + \partial_I \log(Y_{xyz}) - \partial_I \log(\tilde{K}_{xy} \tilde{K}_{yz} \tilde{K}_{zx}) \right], \end{aligned} \quad (3.24)$$

²In our analysis we assume that D-terms do not affect the soft terms [37, 38].

where V_0 is the VEV of the scalar potential.

Although it appears that soft terms may depend on the Yukawa couplings via the superpotential, however these are *not* the physical Yukawa couplings which exponentially depend on the worldsheet area. Both are related by the following relation,

$$Y_{xyz}^{\text{phys}} = Y_{xyz} \frac{\hat{W}^*}{|\hat{W}|} e^{\kappa^2 \hat{K}/2} (\tilde{K}_{xy} \tilde{K}_{yz} \tilde{K}_{zx})^{-1/2}. \quad (3.25)$$

To calculate the soft terms from supersymmetry breaking we ignore the cosmological constant V_0 and introduce the following VEVs for the auxiliary fields (3.22) for the s , t^i and u^i moduli [41],

$$\begin{aligned} F^s &= 2\sqrt{3}Cm_{3/2}\text{Re}(s)\Theta_s e^{-i\gamma_s}, \\ F^{\{u,t\}^i} &= 2\sqrt{3}Cm_{3/2} \left(\text{Re}(u^i)\Theta_i^u e^{-i\gamma_i^u} + \text{Re}(t^i)\Theta_i^t e^{-i\gamma_i^t} \right), \end{aligned} \quad (3.26)$$

Here, the factors γ_s and γ_i denote the CP-violating phases of the moduli. The constant C is given by the gravitino-mass $m_{3/2}$ and the cosmological constant V_0 as $C^2 = 1 + \frac{V_0}{3m_{3/2}^2}$. Θ_s and $\Theta_i^{t,u}$ are the goldstino angles which determine the degree to which supersymmetry breaking is being dominated by any of the dilaton s , complex structure (u^i) and Kähler (t^i) moduli constrained by the relation,

$$\sum_{i=1}^3 (|\Theta_i^u|^2 + |\Theta_i^t|^2) + |\Theta_s|^2 = 1. \quad (3.27)$$

Unlike the s or u -moduli dominant supersymmetry breaking, the case of t -moduli dominant susy breaking depends on the physical Yukawa couplings via the area of the triangles. Accordingly we shall concentrate on the general scenario with the u -moduli dominated supersymmetry breaking with dilaton-modulus s turned on, $F^s \neq 0$. We set the cosmological constant, V_0 to be zero.

3.1 Supersymmetry breaking via u -moduli and dilaton s

Supersymmetry breaking via u -moduli including a non-zero VEV for the dilaton s results in the following auxiliary fields (3.26),

$$F^{s,u^i} = \sqrt{3}m_{3/2}[(s + \bar{s})\Theta_s e^{-i\gamma_s} + (u^i + \bar{u}^i)\Theta_i e^{-i\gamma_i}]. \quad (3.28)$$

To calculate the soft terms, we need to know the derivatives of the Kähler potential with respect to u^i . Defining $\tilde{K}_{xy} \equiv e^{\phi_4} \tilde{K}_{xy}^0$ and using (3.17) and (3.18), we compute the derivatives with respect to u^i as,

$$\frac{\partial \log \tilde{K}_{xy}}{\partial u^i} = \sum_{j=1}^3 \frac{\partial \log \tilde{K}_{xy}^0}{\partial \theta_{xy}^j} \frac{\partial \theta_{xy}^j}{\partial u^i} - \frac{1}{4(u^i + \bar{u}^i)}, \quad (3.29)$$

$$\frac{\partial^2 \log \tilde{K}_{xy}}{\partial u^i \partial \bar{u}^j} = \sum_{k=1}^3 \left(\frac{\partial \log \tilde{K}_{xy}^0}{\partial \theta_{xy}^k} \frac{\partial^2 \theta_{xy}^k}{\partial u^i \partial \bar{u}^j} + \frac{\partial^2 \log \tilde{K}_{xy}^0}{\partial (\theta_{xy}^k)^2} \frac{\partial \theta_{xy}^k}{\partial u^i} \frac{\partial \theta_{xy}^k}{\partial \bar{u}^j} + \frac{\delta_{ij}}{4(u^i + \bar{u}^i)^2} \right). \quad (3.30)$$

From the Kähler potential in (3.18), we have

$$\Psi(\theta_{xy}^j) \equiv \frac{\partial \log \tilde{K}_{xy}^0}{\partial \theta_{xy}^j} = \gamma_E + \frac{1}{2} \frac{d}{d\theta_{xy}^j} \log \Gamma(1 - \theta_{xy}^j) - \frac{1}{2} \frac{d}{d\theta_{xy}^j} \log \Gamma(\theta_{xy}^j) - \log(t^j + \bar{t}^j), \quad (3.31)$$

$$\Psi'(\theta_{xy}^j) \equiv \frac{\partial^2 \log \tilde{K}_{xy}^0}{\partial (\theta_{xy}^j)^2} = \frac{d\Psi(\theta_{xy}^j)}{d\theta_{xy}^j}. \quad (3.32)$$

The first derivative of the angle differences θ_{xy}^j are defined as,

$$\theta_{xy}^{j,k} \equiv (u^k + \bar{u}^k) \frac{\partial \theta_{xy}^j}{\partial u^k} = \begin{cases} \left[-\frac{1}{4\pi} \sin(2\pi\theta^j)\right]_y^x, & j = k \\ \left[\frac{1}{4\pi} \sin(2\pi\theta^j)\right]_y^x, & j \neq k \end{cases} \quad (3.33)$$

$$\theta_{xy}^{j,s} \equiv (s + \bar{s}) \frac{\partial \theta_{xy}^j}{\partial s} = -\frac{1}{4\pi} [\sin(2\pi\theta^j)]_y^x, \quad (3.34)$$

where $[f(\theta^j)]_y^x = f(\theta_x^j) - f(\theta_y^j)$.

And the second order derivatives of the angle differences are,

$$\theta_{xy}^{j,k\bar{l}} \equiv (u^k + \bar{u}^k)(u^l + \bar{u}^l) \frac{\partial^2 \theta_{xy}^j}{\partial u^k \partial \bar{u}^l} = \begin{cases} \frac{1}{16\pi} [\sin(4\pi\theta^j) + 4\sin(2\pi\theta^j)]_y^x, & j = k = l \\ \frac{1}{16\pi} [\sin(4\pi\theta^j) - 4\sin(2\pi\theta^j)]_y^x, & j \neq k = l \\ -\frac{1}{16\pi} [\sin(4\pi\theta^j)]_y^x, & j = k \neq l \text{ or } j = l \neq k \\ \frac{1}{16\pi} [\sin(4\pi\theta^j)]_y^x, & j \neq k \neq l \neq j \end{cases} \quad (3.35)$$

where $k, l \neq s$. While the terms associated with the dilaton s are given as,

$$\theta_{xy}^{j,k\bar{s}} \equiv (u^k + \bar{u}^k)(s + \bar{s}) \frac{\partial^2 \theta_{xy}^j}{\partial u^k \partial \bar{s}} = \begin{cases} \frac{1}{16\pi} [\sin 4\pi\theta^j]_y^x, & j = k \\ -\frac{1}{16\pi} [\sin 4\pi\theta^j]_y^x, & j \neq k, \end{cases} \quad (3.36)$$

and

$$\theta_{xy}^{j,s\bar{s}} \equiv (s + \bar{s})(s + \bar{s}) \frac{\partial^2 \theta_{xy}^j}{\partial s \partial \bar{s}} = \frac{1}{16\pi} [\sin 4\pi\theta^j + 4\sin(2\pi\theta^j)]_y^x. \quad (3.37)$$

3.2 Soft parameters

Substituting above parametrizations (3.28)-(3.32) in the general formulas (3.24), the soft parameters are found as follows:

- Gaugino mass parameters:

$$M_x = \frac{-\sqrt{3}m_{3/2}}{4\text{Re}f_x} \left[\sum_{j=1}^3 \text{Re}(u^j) \Theta_j e^{-i\gamma_j} 2^{-(\beta_k + \beta_l)} n_x^j l_x^k l_x^l + \Theta_s \text{Re}(s) e^{-i\gamma_0} n_x^1 n_x^2 n_x^3 \right],$$

$$(j, k, l) = (\overline{1}, 2, 3). \quad (3.38)$$

Bino mass parameter is then related to the linear combination of the gaugino masses for each stack as,

$$M_Y = \frac{1}{f_Y} \sum_x c_x f_x M_x, \quad (3.39)$$

where the coefficients c_x correspond to the linear combination of $U(1)$ factors which define the hypercharge, $U(1)_Y = \sum c_x U(1)_x$, cf. (3.13).

- Trilinear parameters:

$$A_{xyz} = -\sqrt{3}m_{3/2} \sum_{j=1}^4 \left[\Theta_j e^{-i\gamma_j} \left(\frac{1}{2} + \sum_{k=1}^3 \theta_{xy}^{k,j} \Psi(\theta_{xy}^k) + \sum_{k=1}^3 \theta_{zx}^{k,j} \Psi(\theta_{zx}^k) \right) \right] + \frac{\sqrt{3}}{2} m_{3/2} (\Theta_3 e^{-i\gamma_3} + \Theta_s e^{-i\gamma_s}), \quad (3.40)$$

where $j = 4$ corresponds to Θ_s and x, y , and z label those stacks of branes whose intersections define the corresponding fields present in the trilinear coupling. Since the differences of the angles may be negative $\theta_{xy} = \theta_y - \theta_x$, it is useful to define the sign parameter,

$$\eta_{xy} = \prod_{i=1}^3 (-1)^{1-H(\theta_{xy}^i)}, \quad H(x) = \begin{cases} 0, & x < 0 \\ 1, & x \geq 0 \end{cases} \quad (3.41)$$

where the value $\eta_{xy} = -1$ indicates that only one of the angle differences is negative while $\eta_{xy} = +1$ indicates that two of the angle differences are negative.

- Squarks and sleptons mass-squared (1/4 BPS scalars):

$$m_{xy}^2 = m_{3/2}^2 \left[1 - 3 \sum_{m,n=1}^4 \Theta_m \Theta_n e^{-i(\gamma_m - \gamma_n)} \left(\frac{\delta_{mn}}{4} + \sum_{j=1}^3 (\theta_{xy}^{j,m\bar{n}} \Psi(\theta_{xy}^j) + \theta_{xy}^{j,m} \theta_{xy}^{j,\bar{n}} \Psi'(\theta_{xy}^j)) \right) \right], \quad (3.42)$$

where $\Theta_4 \equiv \Theta_s$ and the functions $\Psi(\theta_{xy}) = \frac{\partial \log(e^{-\phi_4} \tilde{K}_{xy})}{\partial \theta_{xy}}$ in the case of $\eta_{xy} = -1$ are

if $\theta_{xy} < 0$:

$$\Psi(\theta_{xy}^j) = -\gamma_E + \frac{1}{2} \frac{d}{d\theta_{xy}^j} \log \Gamma(-\theta_{xy}^j) - \frac{1}{2} \frac{d}{d\theta_{xy}^j} \log \Gamma(1 + \theta_{xy}^j) + \log(t^j + \bar{t}^j)$$

if $\theta_{xy} > 0$:

$$\Psi(\theta_{xy}^j) = -\gamma_E + \frac{1}{2} \frac{d}{d\theta_{xy}^j} \log \Gamma(1 - \theta_{xy}^j) - \frac{1}{2} \frac{d}{d\theta_{xy}^j} \log \Gamma(\theta_{xy}^j) + \log(t^j + \bar{t}^j), \quad (3.43)$$

and in the case of $\eta_{xy} = +1$ are

if $\theta_{xy} < 0$:

$$\Psi(\theta_{xy}^j) = \gamma_E + \frac{1}{2} \frac{d}{d\theta_{xy}^j} \log \Gamma(1 + \theta_{xy}^j) - \frac{1}{2} \frac{d}{d\theta_{xy}^j} \log \Gamma(-\theta_{xy}^j) - \log(t^j + \bar{t}^j)$$

if $\theta_{xy} > 0$:

$$\Psi(\theta_{xy}^j) = \gamma_E + \frac{1}{2} \frac{d}{d\theta_{xy}^j} \log \Gamma(\theta_{xy}^j) - \frac{1}{2} \frac{d}{d\theta_{xy}^j} \log \Gamma(1 - \theta_{xy}^j) - \log(t^j + \bar{t}^j), \quad (3.44)$$

and $\Psi'(\theta_{xy})$ is just the derivative $\Psi'(\theta_{xy}) = \frac{d\Psi(\theta_{xy})}{d\theta_{xy}^j}$.

- Higgs mass-squared (1/2 BPS scalar):

$$m_H^2 = m_{3/2}^2 \left[1 - \frac{3}{2} (|\Theta_3|^2 + |\Theta_s|^2) \right]. \quad (3.45)$$

3.3 Computational strategy

For any given model we first analyze the structure of three-point Yukawa couplings in that model by considering the triplets $(a, b, c)_i$ on each of the two-tori $i = 1, 2, 3$. Not all models can incorporate the standard model fermion-mass hierarchies due to the generic rank-one problem. Only the models containing the required number of Higgs pairs from either from bulk or from $\mathcal{N} = 2$ subsector on a single two-torus are viable to incorporate the Yukawa couplings [15].

Once a model is viable to generate fermion masses, we consider it to compute the relevant soft terms from supersymmetry breaking in the general case of u -moduli dominance with dilaton modulus s turned on.

We first need to calculate the complex structure moduli U^i (3.5) in string theory basis and the corresponding u^i -moduli and s -modulus in the supergravity basis from (3.6). We also need to compute the gauge kinetic functions $\{f_a, f_b, f_c\}$ (3.11) for each of three D6-brane stacks to calculate the bino mass (3.39). Finally, using the computed $\{M_a, M_b, M_c\}$ for the relevant triplet intersection of the particular model, we can obtain the gaugino masses, $\{M_Y, M_b, M_a\} \equiv \{M_{\tilde{B}}, M_{\tilde{W}}, M_{\tilde{g}}\}$, for the respective gauge groups $U(1)_Y$, $SU(2)_L$ and $SU(3)_C$.

Next, to calculate the trilinear coupling we first tabulate the various angles (3.16) with respect to the orientifold plane made by the cycle wrapped by each stack of D6-brane on each of the three two-tori. Care needs to be taken in evaluating the multivalued arctan function to avoid infinities. Furthermore, unlike the gauge kinetic function (3.11), that is even under the orientifold action for any D-brane stack, the angles (and the differences of the angles $\theta_{xy}^i = \theta_y^i - \theta_x^i$) change signs which makes the computation quite involved. For example, the three-point Yukawa couplings for Model 22 and Model 22-dual are completely different even though the models are dual under the exchange of b and c stacks.

In order to account for the negative angle differences it is convenient to define the sign function σ_{xy}^i which was first introduced in [12], which is -1 only for negative angle difference and $+1$ otherwise,

$$\sigma_{xy}^i \equiv (-1)^{1-H(\theta_{xy}^i)}, \quad (3.46)$$

where $H(x)$ is the unit step function. And the function η_{xy} (3.41) can thus be defined by taking the product on the torus index i as,

$$\eta_{xy} \equiv \prod_{i=1}^3 \sigma_{xy}^i. \quad (3.47)$$

Using the above defined σ_{xy}^i and η_{xy} , we can readily write the four cases of functions $\Psi(\theta_{xy})$ defined in (3.43) and (3.44) into a single expression as,

$$\Psi(\theta_{xy}^j) = \eta_{xy} \left(\frac{1}{2} \psi^{(0)}(\sigma_{xy}^i \theta_{xy}^j) + \frac{1}{2} \psi^{(0)}(1 - \sigma_{xy}^i \theta_{xy}^j) + \gamma_E - \log(t^j + \bar{t}^j) \right), \quad (3.48)$$

where $\psi^{(0)}(z)$ is called the digamma function defined as the derivative of the logarithm of the gamma function. The successive derivatives of the $\log \Gamma(z)$ yield the polygamma

function $\psi^{(n)}(z)$ as,

$$\psi^{(n-1)}(z) = \frac{d^{(n)}}{dz^{(n)}} \log \Gamma(z), \quad (3.49)$$

with the following properties,

$$\begin{aligned} \frac{d}{dz} \psi^{(0)}(\pm z) &= \pm \psi^{(1)}(\pm z), \\ \frac{d}{dz} \psi^{(0)}(1 \pm z) &= \pm \psi^{(1)}(1 \pm z). \end{aligned} \quad (3.50)$$

Similarly, the derivative $\Psi'(\theta_{xy}^j) = \frac{d\Psi(\theta_{xy}^j)}{d\theta_{xy}^j}$ can be expressed succinctly as,

$$\Psi'(\theta_{xy}^j) = \eta_{xy} \sigma_{xy}^i \left(\frac{1}{2} \psi^{(1)}(\sigma_{xy}^i \theta_{xy}^j) + \frac{1}{2} \psi^{(1)}(1 - \sigma_{xy}^i \theta_{xy}^j) \right), \quad (3.51)$$

where we have utilized the property (3.50) and have neglected the contribution of the t -moduli.

Lastly, by making use of appropriate Kronecker deltas and defining $u^4 \equiv s$, we can express the various cases of the first and second derivatives of the angles as,

$$\begin{aligned} \theta_{xy}^{i,m} &\equiv (u^m + \bar{u}^m) \frac{\partial \theta_{xy}^i}{\partial u^m} = (-1)^{\delta_{m,4}} (-1)^{\delta_{i,j}} \frac{\sin(2\pi \theta^i)}{4\pi} \Big|_y^x, \\ i &= 1, 2, 3; \quad m = 1, 2, 3, 4. \end{aligned} \quad (3.52)$$

$$\begin{aligned} \theta_{xy}^{i,mn} &\equiv (u^m + \bar{u}^m)(u^n + \bar{u}^n) \frac{\partial^2 \theta_{xy}^i}{\partial u^m \partial \bar{u}^n} \\ &= \delta_{m,n} \frac{\sin(4\pi \theta^i) + (-1)^{(1-\delta_{4,m})(1-\delta_{i,m})} 4 \sin(2\pi \theta^i)}{16\pi} \Big|_y^x \\ &\quad + (1 - \delta_{m,n}) (-1)^{(1-\delta_{4,m})(1-\delta_{4,n})(\delta_{i,m}+\delta_{i,n})} (-1)^{1-\delta_{i,m}-\delta_{i,n}} \frac{\sin(4\pi \theta^i)}{16\pi} \Big|_y^x \\ i &= 1, 2, 3; \quad m, n = 1, 2, 3, 4. \end{aligned} \quad (3.53)$$

Utilizing these results the trilinear coupling (3.40) and the sleptons and the squarks mass-squared parameters (3.42) are computed while ignoring the CP-violating phases $\{\gamma_1, \gamma_2, \gamma_3, \gamma_s\}$.

4 Susy-breaking soft terms in the Pati-Salam landscape

In appendix A we tabulate all 33 independent three-family supersymmetric Pati-Salam models with distinct allowed gauge coupling relations. The complete perturbative particle spectra for all models in the landscape have been listed in the appendix B of ref. [15].

We find that the first sixteen models viz. 1, 1-dual, 2, 3, 3-dual, 4, 5, 6, 7, 8, 9, 9-dual, 10, 11, 11-dual, and 12 do not possess the correct form of three-point Yukawa textures to generate the fermion masses on a single two-torus. Therefore, we will only focus on the remaining models where viable three-point Yukawa interactions are possible.

4.1 Model 13

In Model 13 the three-point Yukawa couplings arise from the triplet intersections from the branes a , b and c on the first two-torus with 3 pairs of Higgs from the bulk³. Yukawa matrices for the Model 13 are of rank 3 and the three intersections required to form the disk diagrams for the Yukawa couplings all occur on the first torus as shown in figure 2.

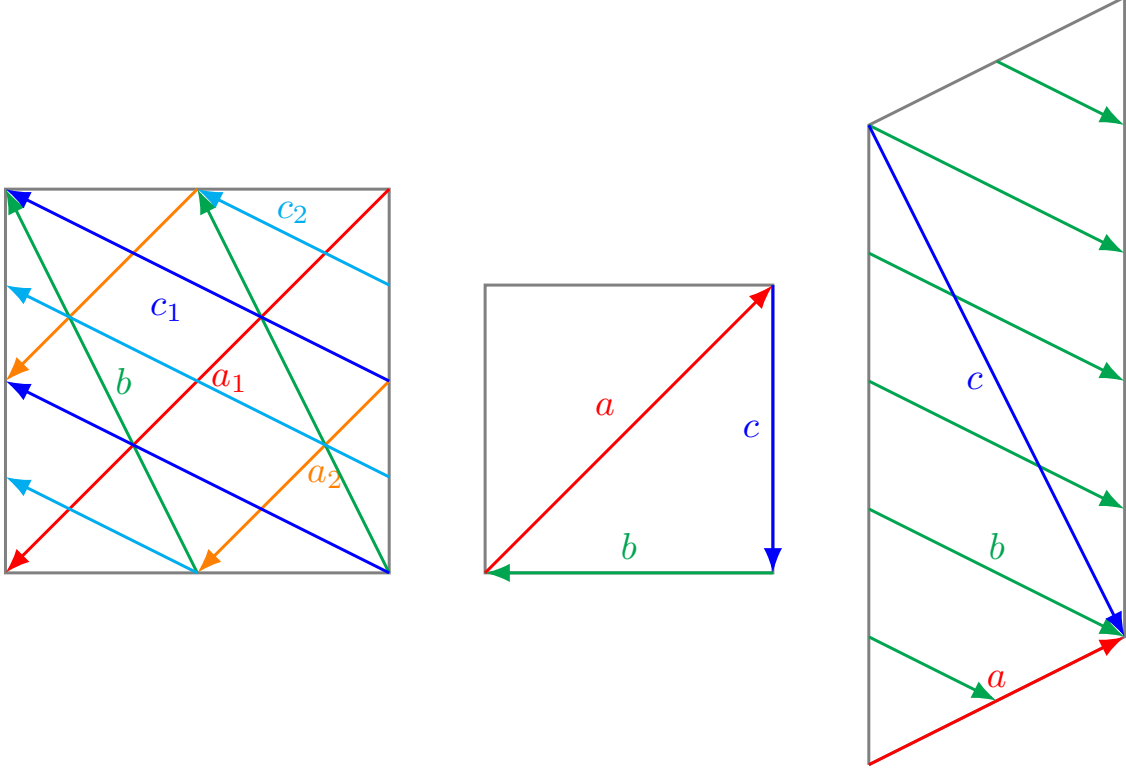


Figure 2: Brane configuration for the three two-tori in Model 13 where the third two-torus is tilted. Fermion mass hierarchies result from the intersections on the first two-torus.

13	θ^1	θ^2	θ^3
a	$\tan^{-1}\left(\frac{1}{\sqrt{5}}\right)$	$-\tan^{-1}\left(\frac{2}{\sqrt{5}}\right)$	$-\tan^{-1}\left(\frac{1}{2\sqrt{5}}\right)$
b	$\tan^{-1}\left(\frac{11}{\sqrt{5}}\right)$	0	$\frac{\pi}{2}$
c	$\tan^{-1}(2\sqrt{5})$	$\tan^{-1}\left(\frac{2}{\sqrt{5}}\right)$	$-\tan^{-1}(2\sqrt{5})$

Table 3: The angles with respect to the orientifold plane made by the cycle wrapped by stack of D6-branes on each of the three two-tori in Model 13.

³This is the only model in the landscape with 3 adjoint scalars from the bulk. Unlike the Higgs from the $\mathcal{N} = 2$ sector which are insensitive to the bulk moduli, the tiny Yukawa couplings from the bulk Higgs are argued to be related to the infinite distance limit [42] in the moduli space where a light of tower states, dubbed gonions [2], appears signalling the decompactification of one or two compact dimensions [43].

The complex structure moduli U^i (3.5) are given as,

$$\{U^1, U^2, U^3\} = \left\{ \frac{i}{\sqrt{5}}, \frac{11i}{\sqrt{5}}, \frac{4}{21} (10 + i\sqrt{5}) \right\}, \quad (4.1)$$

and the corresponding u -moduli and s -modulus in supergravity basis from (3.6) are,

$$\begin{aligned} \{u^1, u^2, u^3\} &= \left\{ \frac{\sqrt[4]{5}\sqrt{11}e^{-\phi_4}}{\pi}, \frac{\sqrt[4]{5}e^{-\phi_4}}{\sqrt{11}\pi}, \frac{\sqrt{11}e^{-\phi_4}}{4 \cdot 5^{3/4}\pi} \right\}, \\ s &= \frac{\sqrt[4]{5}e^{-\phi_4}}{4\sqrt{11}\pi}. \end{aligned} \quad (4.2)$$

Using (3.11) and the values from the table 36, the gauge kinetic function becomes,

$$\{f_a, f_b, f_c\} = \left\{ \frac{63e^{-\phi_4}}{8 \cdot 5^{3/4}\sqrt{11}\pi}, \frac{9\sqrt[4]{5}e^{-\phi_4}}{16\sqrt{11}\pi}, \frac{21\sqrt{11}e^{-\phi_4}}{16 \cdot 5^{3/4}\pi} \right\}, \quad (4.3)$$

To calculate the gaugino masses $\{M_Y, M_b, M_a\}$ for the respective gauge groups $U(1)_Y$, $SU(2)_L$, and $SU(3)_C$, we first compute $\{M_a, M_b, M_c\}$ using (3.38) as,

$$\begin{aligned} M_a &= \frac{m_{3/2}(110\Theta_1 + 10\Theta_2 + 11\Theta_3 + 5\Theta_4)}{42\sqrt{3}}, \\ M_b &= \frac{m_{3/2}(4\Theta_2 - 5\Theta_4)}{3\sqrt{3}}, \\ M_c &= \frac{m_{3/2}(20\Theta_1 + \Theta_3)}{7\sqrt{3}}. \end{aligned} \quad (4.4)$$

Next, to compute the trilinear coupling and the sleptons mass-squared we require the angles, the differences of angles and their first and second order derivatives with respect to the moduli. In table 3 we show the angles (3.16) made by the cycles wrapped by each stack of D6-branes with respect to the orientifold plane on each two-torus. The differences of the angles, $\theta_{xy}^i = \theta_y^i - \theta_x^i$ are,

$$\begin{bmatrix} \{0., 0., 0.\} & \{0.132923, -0.228657, 0.378919\} & \{0.642663, 0.0589537, 0.298383\} \\ \{-0.132923, 0.228657, -0.378919\} & \{0., 0., 0.\} & \{0.50974, 0.287611, -0.080536\} \\ \{-0.642663, -0.0589537, -0.298383\} & \{-0.50974, -0.287611, 0.080536\} & \{0., 0., 0.\} \end{bmatrix} \quad (4.5)$$

To account for the negative angle differences we employ the sign function σ_{xy}^i , which is -1 only for negative angle difference and $+1$ otherwise,

$$\sigma_{xy}^i = \begin{pmatrix} \{1, 1, 1\} & \{1, -1, 1\} & \{1, 1, 1\} \\ \{-1, 1, -1\} & \{1, 1, 1\} & \{1, 1, -1\} \\ \{-1, -1, -1\} & \{-1, -1, 1\} & \{1, 1, 1\} \end{pmatrix}, \quad (4.6)$$

and the function η_{xy} is evaluated by taking the product on the torus index i as,

$$\eta_{xy} = \begin{pmatrix} 1 & -1 & 1 \\ 1 & 1 & -1 \\ -1 & 1 & 1 \end{pmatrix}. \quad (4.7)$$

Using the values of σ_{xy}^i and η_{xy} in (3.48) we can compute the four cases of functions $\Psi(\theta_{xy})$ defined in (3.43) and (3.44). Similarly we calculate the derivative $\Psi'(\theta_{xy}^j) = \frac{d\Psi(\theta_{xy}^j)}{d\theta_{xy}^j}$ using equations (3.51), (3.3), (3.53) and the properties of digamma function $\psi^{(0)}(z)$ (3.50) while neglecting the contribution of the t -moduli.

Utilizing above results while ignoring the CP-violating phases γ_m , the gaugino masses; the trilinear coupling (3.40); and the squared-masses of squarks and sleptons (3.42) are obtained as,

$$\begin{aligned}
M_{\tilde{B}} &\equiv M_Y = m_{3/2} \left(\frac{176\Theta_1 + 4\Theta_2 + 11\Theta_3 + 2\Theta_4}{63\sqrt{3}} \right), \\
M_{\tilde{W}} &\equiv M_b = m_{3/2} \left(\frac{4\Theta_2 - 5\Theta_4}{3\sqrt{3}} \right), \\
M_{\tilde{g}} &\equiv M_a = m_{3/2} \left(\frac{110\Theta_1 + 10\Theta_2 + 11\Theta_3 + 5\Theta_4}{42\sqrt{3}} \right), \\
A_0 &\equiv A_{abc} = m_{3/2} \left(-0.557548\Theta_1 - 1.13015\Theta_2 + 0.418029\Theta_3 - 0.462383\Theta_4 \right), \\
m_L^2 &\equiv m_{ab}^2 = m_{3/2}^2 \left(0.185098\Theta_1^2 - 0.0411881\Theta_1\Theta_2 - 1.44927\Theta_1\Theta_3 - 1.45644\Theta_1\Theta_4 \right. \\
&\quad \left. + 1.06435\Theta_2^2 - 0.969753\Theta_2\Theta_3 - 0.386382\Theta_2\Theta_4 - 0.290557\Theta_3^2 \right. \\
&\quad \left. + 0.395625\Theta_3\Theta_4 - 1.0645\Theta_4^2 + 1 \right), \\
m_R^2 &\equiv m_{ac}^2 = m_{3/2}^2 \left(-2.63181\Theta_1^2 + 0.77203\Theta_1\Theta_2 + 1.29272\Theta_1\Theta_3 + 1.47197\Theta_1\Theta_4 \right. \\
&\quad \left. - 2.51929\Theta_2^2 + 1.29272\Theta_2\Theta_3 + 0.844287\Theta_2\Theta_4 - 2.34591\Theta_3^2 \right. \\
&\quad \left. - 0.0442256\Theta_3\Theta_4 - 0.0470486\Theta_4^2 + 1 \right). \tag{4.8}
\end{aligned}$$

All soft terms are subject to the constraint (3.27).

4.2 Model 14

In Model 14 the three-point Yukawa couplings arise from the triplet intersections from the branes a , b and c on the second two-torus with 6 pairs of Higgs from the $\mathcal{N} = 2$ sector. Yukawa matrices for the Model 14 are of rank 3 and the three intersections required to form the disk diagrams for the Yukawa couplings all occur on the second torus as shown in figure 3.

14	θ^1	θ^2	θ^3
a	$\frac{3\pi}{4}$	0	$\frac{\pi}{2}$
b	0	$\frac{\pi}{4}$	$\frac{3\pi}{4}$
c	$\frac{\pi}{4}$	$\frac{3\pi}{4}$	$\frac{3\pi}{4}$

Table 4: The angles with respect to the orientifold plane made by the cycle wrapped by stack of D6-branes on each of the three two-tori in Model 14.

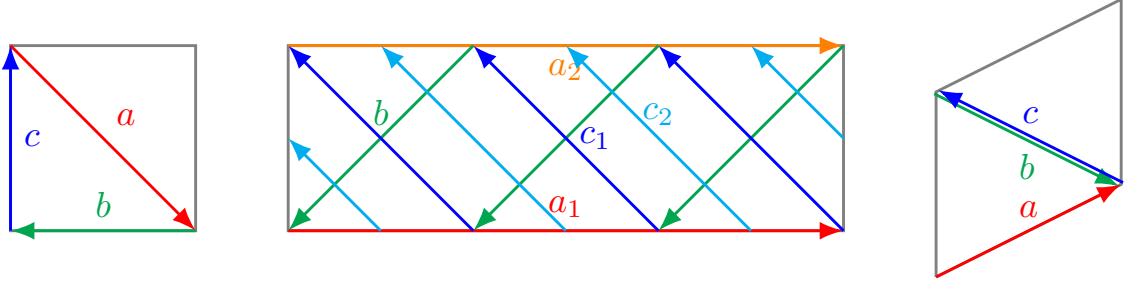


Figure 3: Brane configuration for the three two-tori in Model 14 where the third two-torus is tilted. Fermion mass hierarchies result from the intersections on the second two-torus.

The complex structure moduli U^i (3.5) are given as,

$$\{U^1, U^2, U^3\} = \left\{ i, \frac{i}{3}, 1 + i \right\}, \quad (4.9)$$

and the corresponding u -moduli and s -modulus in supergravity basis from (3.6) are,

$$\begin{aligned} \{u^1, u^2, u^3\} &= \left\{ \frac{e^{-\phi_4}}{\sqrt{6}\pi}, \frac{\sqrt{\frac{3}{2}}e^{-\phi_4}}{\pi}, \frac{e^{-\phi_4}}{2\sqrt{6}\pi} \right\}, \\ s &= \frac{\sqrt{\frac{3}{2}}e^{-\phi_4}}{2\pi}. \end{aligned} \quad (4.10)$$

Using (3.11) and the values from the table 37, the gauge kinetic function becomes,

$$\{f_a, f_b, f_c\} = \left\{ \frac{\sqrt{\frac{3}{2}}e^{-\phi_4}}{4\pi}, \frac{\sqrt{\frac{3}{2}}e^{-\phi_4}}{4\pi}, \frac{\sqrt{\frac{3}{2}}e^{-\phi_4}}{4\pi} \right\}, \quad (4.11)$$

To calculate the gaugino masses $\{M_Y, M_b, M_a\}$ for the respective gauge groups $U(1)_Y$, $SU(2)_L$, and $SU(3)_C$, we first compute $\{M_a, M_b, M_c\}$ using (3.38) as,

$$\begin{aligned} M_a &= \frac{1}{2}\sqrt{3}m_{3/2}(\Theta_2 - \Theta_4), \\ M_b &= \frac{1}{2}\sqrt{3}m_{3/2}(\Theta_1 - \Theta_4), \\ M_c &= \frac{1}{2}\sqrt{3}m_{3/2}(\Theta_2 + \Theta_3). \end{aligned} \quad (4.12)$$

Next, to compute the trilinear coupling and the sleptons mass-squared we require the angles, the differences of angles and their first and second order derivatives with respect to the moduli. In table 4 we show the angles (3.16) made by the cycles wrapped by each stack of D6-branes with respect to the orientifold plane on each two-torus. The differences of the angles, $\theta_{xy}^i = \theta_y^i - \theta_x^i$ are,

$$\begin{bmatrix} \{0., 0., 0.\} & \{-0.0730092, 0.643806, -0.570796\} & \{0.356194, 0.356194, -0.429204\} \\ \{0.0730092, -0.643806, 0.570796\} & \{0., 0., 0.\} & \{0.429204, -0.287611, 0.141593\} \\ \{-0.356194, -0.356194, 0.429204\} & \{-0.429204, 0.287611, -0.141593\} & \{0., 0., 0.\} \end{bmatrix} \quad (4.13)$$

To account for the negative angle differences we employ the sign function σ_{xy}^i , which is -1 only for negative angle difference and $+1$ otherwise,

$$\sigma_{xy}^i = \begin{pmatrix} \{1, 1, 1\} & \{-1, 1, -1\} & \{1, 1, -1\} \\ \{1, -1, 1\} & \{1, 1, 1\} & \{1, -1, 1\} \\ \{-1, -1, 1\} & \{-1, 1, -1\} & \{1, 1, 1\} \end{pmatrix}, \quad (4.14)$$

and the function η_{xy} is evaluated by taking the product on the torus index i as,

$$\eta_{xy} = \begin{pmatrix} 1 & 1 & -1 \\ -1 & 1 & -1 \\ 1 & 1 & 1 \end{pmatrix}. \quad (4.15)$$

Using the values of σ_{xy}^i and η_{xy} in (3.48) we can compute the four cases of functions $\Psi(\theta_{xy})$ defined in (3.43) and (3.44). Similarly we calculate the derivative $\Psi'(\theta_{xy}^j) = \frac{d\Psi(\theta_{xy}^j)}{d\theta_{xy}^j}$ using equations (3.51), (3.3), (3.53) and the properties of digamma function $\psi^{(0)}(z)$ (3.50) while neglecting the contribution of the t -moduli.

Utilizing above results while ignoring the CP-violating phases γ_m , the gaugino masses; the trilinear coupling (3.40); and the squared-masses of squarks and sleptons (3.42) are obtained as,

$$\begin{aligned} M_{\tilde{B}} &\equiv M_Y = m_{3/2} \left(\frac{1}{10} \sqrt{3} (5\Theta_2 + 3\Theta_3 - 2\Theta_4) \right), \\ M_{\tilde{W}} &\equiv M_b = m_{3/2} \left(\frac{1}{2} \sqrt{3} (\Theta_1 - \Theta_4) \right), \\ M_{\tilde{g}} &\equiv M_a = m_{3/2} \left(\frac{1}{2} \sqrt{3} (\Theta_2 - \Theta_4) \right), \\ A_0 &\equiv A_{abc} = m_{3/2} \left(-0.444661\Theta_1 - 1.36219\Theta_2 + 0.260871\Theta_3 - 0.186075\Theta_4 \right), \\ m_L^2 &\equiv m_{ab}^2 = m_{3/2}^2 \left(-0.0689562\Theta_1^2 + 1.52807\Theta_1\Theta_2 - 0.25782\Theta_1\Theta_3 - 0.582907\Theta_1\Theta_4 \right. \\ &\quad \left. - 0.127855\Theta_2^2 + 0.31395\Theta_2\Theta_3 - 0.623439\Theta_2\Theta_4 - 2.04994\Theta_3^2 \right. \\ &\quad \left. + 1.23441\Theta_3\Theta_4 - 0.809377\Theta_4^2 + 1 \right), \\ m_R^2 &\equiv m_{ac}^2 = m_{3/2}^2 \left(-2.28519\Theta_1^2 - 1.00169\Theta_1\Theta_2 + 0.506454\Theta_1\Theta_3 + 1.26634\Theta_1\Theta_4 \right. \\ &\quad \left. - 0.637087\Theta_2^2 + 1.13601\Theta_2\Theta_3 + 0.140834\Theta_2\Theta_4 - 0.0262168\Theta_3^2 \right. \\ &\quad \left. - 1.1866\Theta_3\Theta_4 - 0.492648\Theta_4^2 + 1 \right). \end{aligned} \quad (4.16)$$

All soft terms are subject to the constraint (3.27).

4.3 Model 15

In Model 15 the three-point Yukawa couplings arise from the triplet intersections from the branes a , b and c on the first two-torus with 6 pairs of Higgs from the $\mathcal{N} = 2$ sector. Yukawa matrices for the Model 15 are of rank 3 and the three intersections required to form the disk diagrams for the Yukawa couplings all occur on the first torus as shown in figure 4.

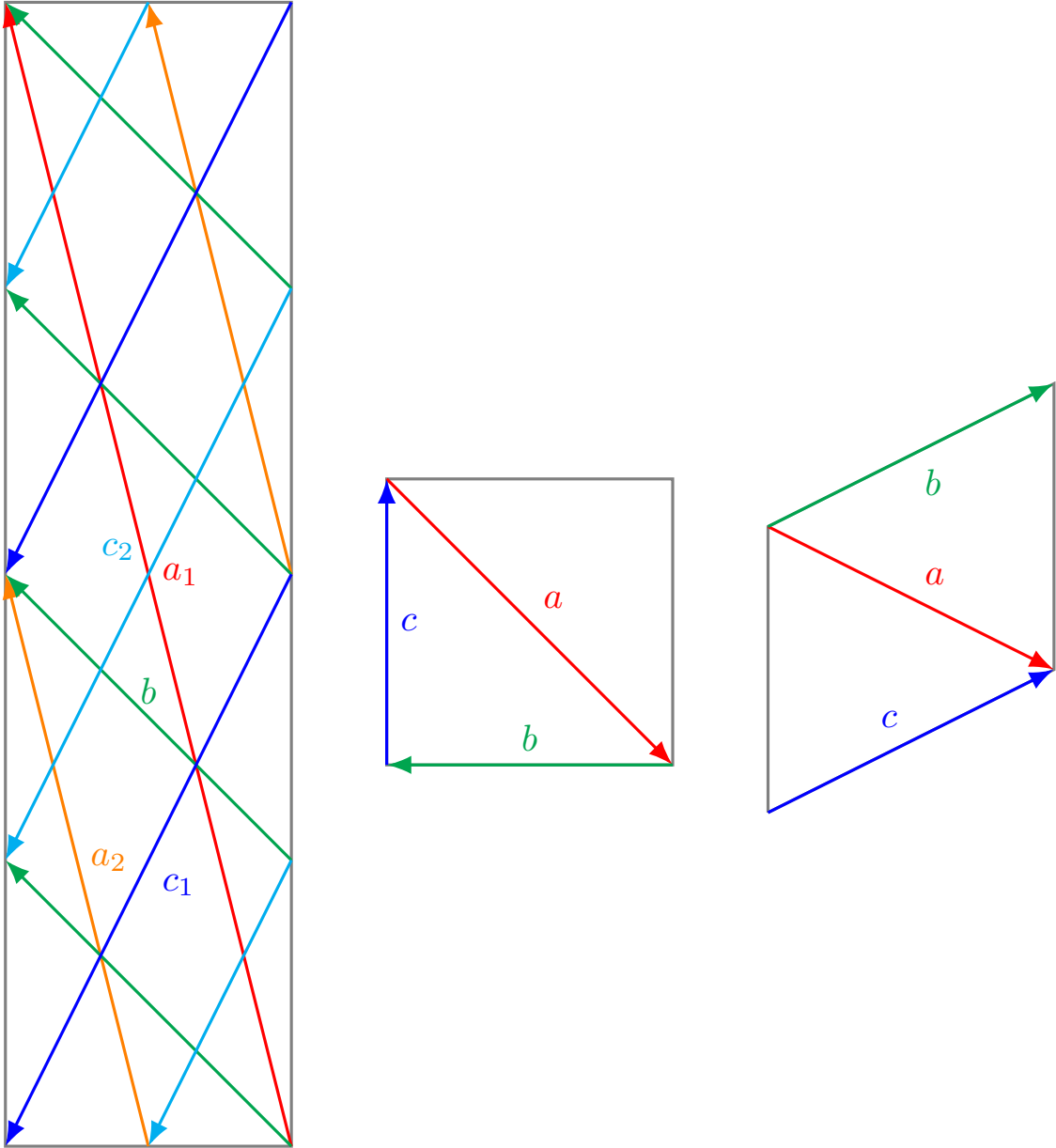


Figure 4: Brane configuration for the three two-tori in Model 15 where the third two-torus is tilted. Fermion mass hierarchies result from the intersections on the first two-torus.

The complex structure moduli U^i (3.5) are given as,

$$\{U^1, U^2, U^3\} = \left\{ 2i\sqrt{2}, \frac{5i}{\sqrt{2}}, \frac{2}{3} (1 + i\sqrt{2}) \right\}, \quad (4.17)$$

15	θ^1	θ^2	θ^3
a	$-\tan^{-1}(2\sqrt{2})$	$-\tan^{-1}\left(\frac{1}{\sqrt{2}}\right)$	$\tan^{-1}(\sqrt{2})$
b	$-\tan^{-1}\left(\frac{5}{\sqrt{2}}\right)$	0	$\frac{\pi}{2}$
c	$-\tan^{-1}\left(\frac{1}{\sqrt{2}}\right)$	$\tan^{-1}\left(\frac{1}{\sqrt{2}}\right)$	$\tan^{-1}\left(\frac{1}{\sqrt{2}}\right)$

Table 5: The angles with respect to the orientifold plane made by the cycle wrapped by stack of D6-branes on each of the three two-tori in Model 15.

and the corresponding u -moduli and s -modulus in supergravity basis from (3.6) are,

$$\{u^1, u^2, u^3\} = \left\{ \frac{\sqrt{5}e^{-\phi_4}}{2 \cdot 2^{3/4}\pi}, \frac{\sqrt[4]{2}e^{-\phi_4}}{\sqrt{5}\pi}, \frac{\sqrt{5}e^{-\phi_4}}{2^{3/4}\pi} \right\},$$

$$s = \frac{e^{-\phi_4}}{2 \cdot 2^{3/4}\sqrt{5}\pi}. \quad (4.18)$$

Using (3.11) and the values from the table 38, the gauge kinetic function becomes,

$$\{f_a, f_b, f_c\} = \left\{ \frac{27e^{-\phi_4}}{16 \cdot 2^{3/4}\sqrt{5}\pi}, \frac{3e^{-\phi_4}}{4 \cdot 2^{3/4}\sqrt{5}\pi}, \frac{3\sqrt{5}e^{-\phi_4}}{8 \cdot 2^{3/4}\pi} \right\}, \quad (4.19)$$

To calculate the gaugino masses $\{M_Y, M_b, M_a\}$ for the respective gauge groups $U(1)_Y$, $SU(2)_L$, and $SU(3)_C$, we first compute $\{M_a, M_b, M_c\}$ using (3.38) as,

$$M_a = \frac{m_{3/2}(5\Theta_1 + 4\Theta_2 + 20\Theta_3 + 2\Theta_4)}{9\sqrt{3}},$$

$$M_b = \frac{m_{3/2}(\Theta_2 - 2\Theta_4)}{\sqrt{3}},$$

$$M_c = \frac{m_{3/2}(\Theta_1 + 2\Theta_3)}{\sqrt{3}}. \quad (4.20)$$

Next, to compute the trilinear coupling and the sleptons mass-squared we require the angles, the differences of angles and their first and second order derivatives with respect to the moduli. In table 5 we show the angles (3.16) made by the cycles wrapped by each stack of D6-branes with respect to the orientifold plane on each two-torus. The differences of the angles, $\theta_{xy}^i = \theta_y^i - \theta_x^i$ are,

$$\begin{bmatrix} \{0., 0., 0.\} & \{-0.38452, -0.563254, 0.230959\} & \{-0.0969093, -0.13405, 0.230959\} \\ \{0.38452, 0.563254, -0.230959\} & \{0., 0., 0.\} & \{0.287611, 0.429204, 0.\} \\ \{0.0969093, 0.13405, -0.230959\} & \{-0.287611, -0.429204, 0.\} & \{0., 0., 0.\} \end{bmatrix} \quad (4.21)$$

To account for the negative angle differences we employ the sign function σ_{xy}^i , which is -1 only for negative angle difference and $+1$ otherwise,

$$\sigma_{xy}^i = \begin{pmatrix} \{1, 1, 1\} & \{-1, -1, 1\} & \{-1, -1, 1\} \\ \{1, 1, -1\} & \{1, 1, 1\} & \{1, 1, 1\} \\ \{1, 1, -1\} & \{-1, -1, 1\} & \{1, 1, 1\} \end{pmatrix}, \quad (4.22)$$

and the function η_{xy} is evaluated by taking the product on the torus index i as,

$$\eta_{xy} = \begin{pmatrix} 1 & 1 & 1 \\ -1 & 1 & 1 \\ -1 & 1 & 1 \end{pmatrix}. \quad (4.23)$$

Using the values of σ_{xy}^i and η_{xy} in (3.48) we can compute the four cases of functions $\Psi(\theta_{xy})$ defined in (3.43) and (3.44). Similarly we calculate the derivative $\Psi'(\theta_{xy}^j) = \frac{d\Psi(\theta_{xy}^j)}{d\theta_{xy}^j}$ using equations (3.51), (3.3), (3.53) and the properties of digamma function $\psi^{(0)}(z)$ (3.50) while neglecting the contribution of the t -moduli.

Utilizing above results while ignoring the CP-violating phases γ_m , the gaugino masses; the trilinear coupling (3.40); and the squared-masses of squarks and sleptons (3.42) are obtained as,

$$\begin{aligned} M_{\tilde{B}} &\equiv M_Y = m_{3/2} \left(\frac{10\Theta_1 + 2\Theta_2 + 25\Theta_3 + \Theta_4}{12\sqrt{3}} \right), \\ M_{\tilde{W}} &\equiv M_b = m_{3/2} \left(\frac{\Theta_2 - 2\Theta_4}{\sqrt{3}} \right), \\ M_{\tilde{g}} &\equiv M_a = m_{3/2} \left(\frac{5\Theta_1 + 4\Theta_2 + 20\Theta_3 + 2\Theta_4}{9\sqrt{3}} \right), \\ A_0 &\equiv A_{abc} = m_{3/2} \left(-0.863715\Theta_1 + 0.764882\Theta_2 - 1.2303\Theta_3 - 0.402914\Theta_4 \right), \\ m_L^2 &\equiv m_{ab}^2 = m_{3/2}^2 \left(-1.47868\Theta_1^2 - 0.544215\Theta_1\Theta_2 + 2.13294\Theta_1\Theta_3 + 0.574711\Theta_1\Theta_4 \right. \\ &\quad \left. - 2.39151\Theta_2^2 + 1.01424\Theta_2\Theta_3 + 1.98343\Theta_2\Theta_4 + 0.200897\Theta_3^2 \right. \\ &\quad \left. - 1.60235\Theta_3\Theta_4 - 1.24227\Theta_4^2 + 1 \right), \\ m_R^2 &\equiv m_{ac}^2 = m_{3/2}^2 \left(-0.93815\Theta_1^2 - 0.630132\Theta_1\Theta_2 + 1.49955\Theta_1\Theta_3 + 1.27302\Theta_1\Theta_4 \right. \\ &\quad \left. - 2.84613\Theta_2^2 + 1.49955\Theta_2\Theta_3 + 1.28512\Theta_2\Theta_4 - 0.482776\Theta_3^2 \right. \\ &\quad \left. - 1.68827\Theta_3\Theta_4 - 0.472685\Theta_4^2 + 1 \right). \end{aligned} \quad (4.24)$$

All soft terms are subject to the constraint (3.27).

4.4 Model 15-dual

In Model 15-dual the three-point Yukawa couplings arise from the triplet intersections from the branes a , b and c on the second two-torus with 6 pairs of Higgs from the $\mathcal{N} = 2$ sector. Yukawa matrices for the Model 15-dual are of rank 3 and the three intersections required to

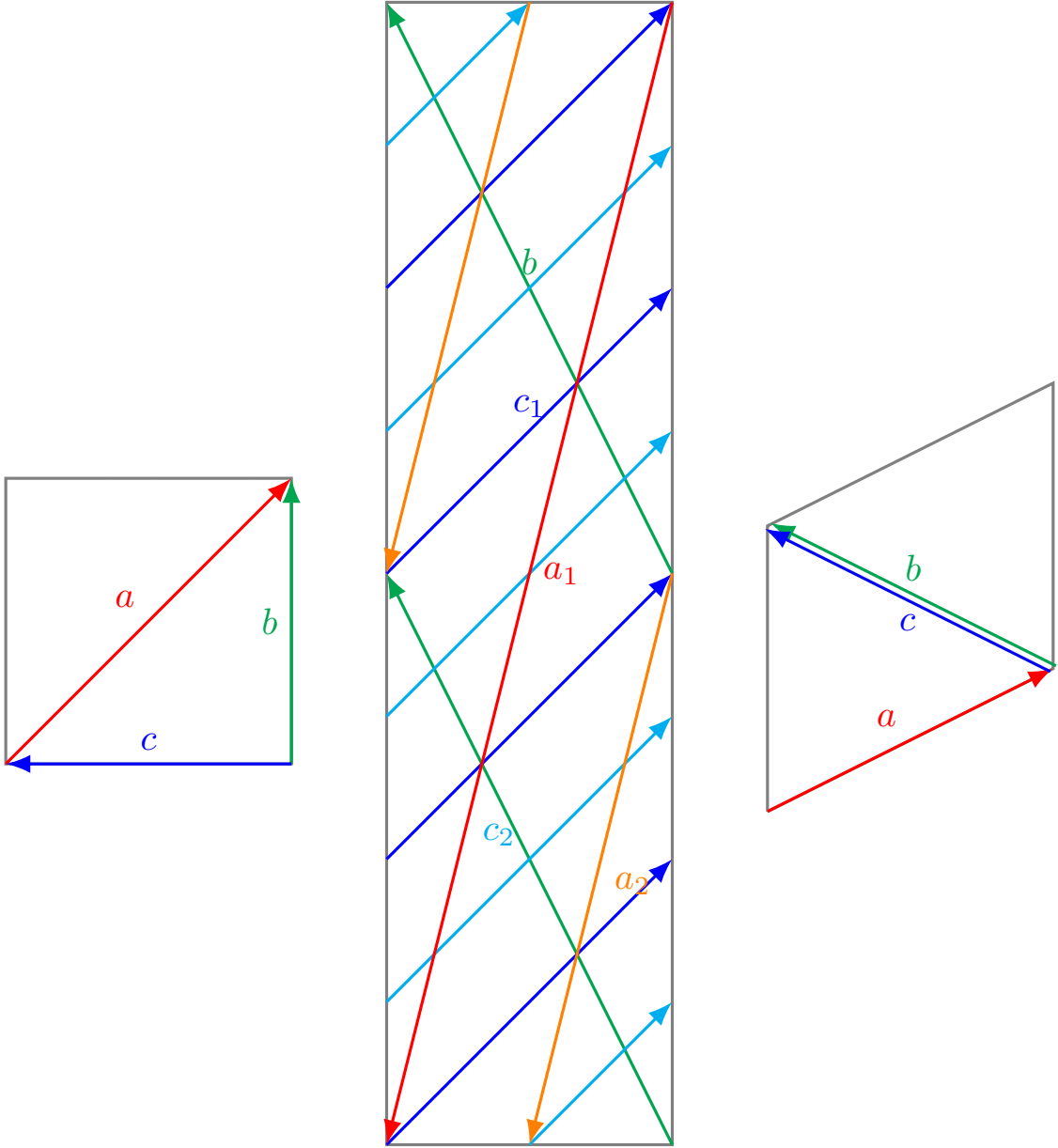


Figure 5: Brane configuration for the three two-tori in Model 15-dual where the third two-torus is tilted. Fermion mass hierarchies result from the intersections on the second two-torus.

form the disk diagrams for the Yukawa couplings all occur on the second torus as shown in figure 5.

The complex structure moduli U^i (3.5) are given as,

$$\{U^1, U^2, U^3\} = \left\{ \frac{5i}{\sqrt{2}}, 2i\sqrt{2}, \frac{2}{3} (1 + i\sqrt{2}) \right\}, \quad (4.25)$$

15-dual	θ^1	θ^2	θ^3
a	$\tan^{-1}\left(\frac{5}{\sqrt{2}}\right)$	$\frac{\pi}{2}$	0
b	$\tan^{-1}(2\sqrt{2})$	$-\tan^{-1}(\sqrt{2})$	$\tan^{-1}\left(\frac{1}{\sqrt{2}}\right)$
c	$\tan^{-1}\left(\frac{1}{\sqrt{2}}\right)$	$-\tan^{-1}\left(\frac{1}{\sqrt{2}}\right)$	$-\tan^{-1}\left(\frac{1}{\sqrt{2}}\right)$

Table 6: The angles with respect to the orientifold plane made by the cycle wrapped by stack of D6-branes on each of the three two-tori in Model 15-dual.

and the corresponding u -moduli and s -modulus in supergravity basis from (3.6) are,

$$\{u^1, u^2, u^3\} = \left\{ \frac{\sqrt[4]{2}e^{-\phi_4}}{\sqrt{5}\pi}, \frac{\sqrt{5}e^{-\phi_4}}{2 \cdot 2^{3/4}\pi}, \frac{\sqrt{5}e^{-\phi_4}}{2^{3/4}\pi} \right\},$$

$$s = \frac{e^{-\phi_4}}{2 \cdot 2^{3/4}\sqrt{5}\pi}. \quad (4.26)$$

Using (3.11) and the values from the table 39, the gauge kinetic function becomes,

$$\{f_a, f_b, f_c\} = \left\{ \frac{27e^{-\phi_4}}{16 \cdot 2^{3/4}\sqrt{5}\pi}, \frac{3\sqrt{5}e^{-\phi_4}}{8 \cdot 2^{3/4}\pi}, \frac{3e^{-\phi_4}}{4 \cdot 2^{3/4}\sqrt{5}\pi} \right\}, \quad (4.27)$$

To calculate the gaugino masses $\{M_Y, M_b, M_a\}$ for the respective gauge groups $U(1)_Y$, $SU(2)_L$, and $SU(3)_C$, we first compute $\{M_a, M_b, M_c\}$ using (3.38) as,

$$M_a = \frac{m_{3/2}(4\Theta_1 + 5\Theta_2 + 20\Theta_3 + 2\Theta_4)}{9\sqrt{3}},$$

$$M_b = \frac{m_{3/2}(\Theta_2 + 2\Theta_3)}{\sqrt{3}},$$

$$M_c = \frac{m_{3/2}(\Theta_1 - 2\Theta_4)}{\sqrt{3}}. \quad (4.28)$$

Next, to compute the trilinear coupling and the sleptons mass-squared we require the angles, the differences of angles and their first and second order derivatives with respect to the moduli. In table 6 we show the angles (3.16) made by the cycles wrapped by each stack of D6-branes with respect to the orientifold plane on each two-torus. The differences of the angles, $\theta_{xy}^i = \theta_y^i - \theta_x^i$ are,

$$\left[\begin{array}{ccc} \{0., 0., 0.\} & \{0.275643, 0.0969093, -0.0893668\} & \{-0.153561, 0.526113, -0.0893668\} \\ \{-0.275643, -0.0969093, 0.0893668\} & \{0., 0., 0.\} & \{-0.429204, 0.429204, 0.\} \\ \{0.153561, -0.526113, 0.0893668\} & \{0.429204, -0.429204, 0.\} & \{0., 0., 0.\} \end{array} \right] \quad (4.29)$$

To account for the negative angle differences we employ the sign function σ_{xy}^i , which is -1 only for negative angle difference and $+1$ otherwise,

$$\sigma_{xy}^i = \begin{pmatrix} \{1, 1, 1\} & \{1, 1, -1\} & \{-1, 1, -1\} \\ \{-1, -1, 1\} & \{1, 1, 1\} & \{-1, 1, 1\} \\ \{1, -1, 1\} & \{1, -1, 1\} & \{1, 1, 1\} \end{pmatrix}, \quad (4.30)$$

and the function η_{xy} is evaluated by taking the product on the torus index i as,

$$\eta_{xy} = \begin{pmatrix} 1 & -1 & 1 \\ 1 & 1 & -1 \\ -1 & -1 & 1 \end{pmatrix}. \quad (4.31)$$

Using the values of σ_{xy}^i and η_{xy} in (3.48) we can compute the four cases of functions $\Psi(\theta_{xy})$ defined in (3.43) and (3.44). Similarly we calculate the derivative $\Psi'(\theta_{xy}^j) = \frac{d\Psi(\theta_{xy}^j)}{d\theta_{xy}^j}$ using equations (3.51), (3.3), (3.53) and the properties of digamma function $\psi^{(0)}(z)$ (3.50) while neglecting the contribution of the t -moduli.

Utilizing above results while ignoring the CP-violating phases γ_m , the gaugino masses; the trilinear coupling (3.40); and the squared-masses of squarks and sleptons (3.42) are obtained as,

$$\begin{aligned} M_{\tilde{B}} &\equiv M_Y = m_{3/2} \left(\frac{2\Theta_1 + \Theta_2 + 4\Theta_3 - 2\Theta_4}{3\sqrt{3}} \right), \\ M_{\tilde{W}} &\equiv M_b = m_{3/2} \left(\frac{\Theta_2 + 2\Theta_3}{\sqrt{3}} \right), \\ M_{\tilde{g}} &\equiv M_a = m_{3/2} \left(\frac{4\Theta_1 + 5\Theta_2 + 20\Theta_3 + 2\Theta_4}{9\sqrt{3}} \right), \\ A_0 &\equiv A_{abc} = m_{3/2} \left(-0.0762806\Theta_1 - 1.65577\Theta_2 + 0.222917\Theta_3 - 0.222917\Theta_4 \right), \\ m_L^2 &\equiv m_{ab}^2 = m_{3/2}^2 \left(-2.50015\Theta_1^2 - 1.28868\Theta_1\Theta_2 + 0.56326\Theta_1\Theta_3 + 1.78275\Theta_1\Theta_4 \right. \\ &\quad \left. - 0.272045\Theta_2^2 + 1.18291\Theta_2\Theta_3 + 0.336724\Theta_2\Theta_4 + 0.10754\Theta_3^2 \right. \\ &\quad \left. - 2.1859\Theta_3\Theta_4 - 0.202498\Theta_4^2 + 1 \right), \\ m_R^2 &\equiv m_{ac}^2 = m_{3/2}^2 \left(-0.229829\Theta_1^2 + 1.01289\Theta_1\Theta_2 - 0.749437\Theta_1\Theta_3 - 1.33965\Theta_1\Theta_4 \right. \\ &\quad \left. + 0.277823\Theta_2^2 - 0.150917\Theta_2\Theta_3 - 0.779826\Theta_2\Theta_4 - 1.85574\Theta_3^2 \right. \\ &\quad \left. + 1.9101\Theta_3\Theta_4 - 0.7735\Theta_4^2 + 1 \right). \end{aligned} \quad (4.32)$$

All soft terms are subject to the constraint (3.27).

4.5 Model 16

In Model 16 the three-point Yukawa couplings arise from the triplet intersections from the branes a , b and c on the first two-torus with 6 pairs of Higgs from the $\mathcal{N} = 2$ sector. Yukawa matrices for the Model 16 are of rank 3 and the three intersections required to form

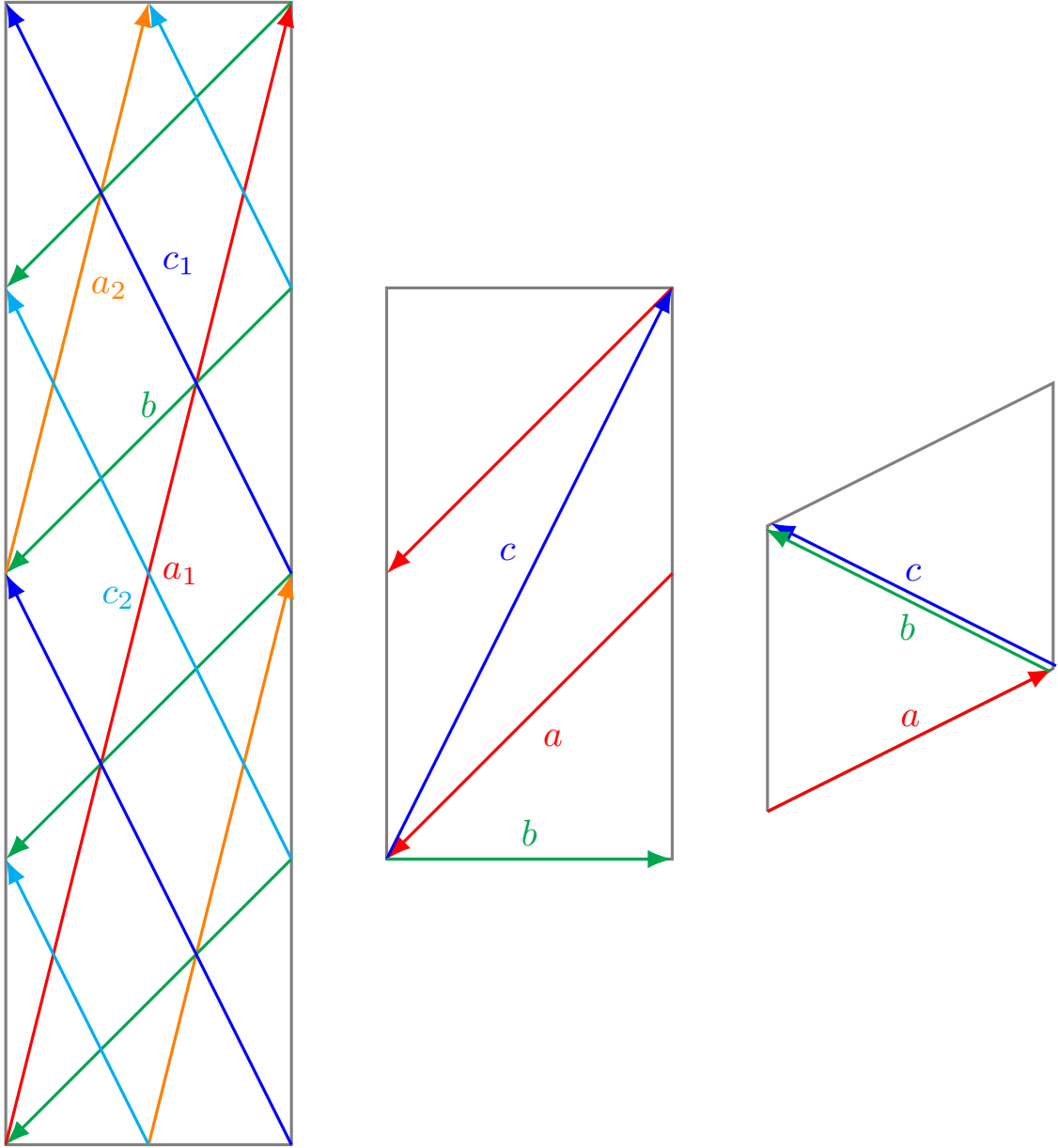


Figure 6: Brane configuration for the three two-tori in Model 16 where the third two-torus is tilted. Fermion mass hierarchies result from the intersections on the first two-torus.

the disk diagrams for the Yukawa couplings all occur on the first torus as shown in figure 6.

The complex structure moduli U^i (3.5) are given as,

$$\{U^1, U^2, U^3\} = \left\{ i\sqrt{\frac{13}{2}}, 2i\sqrt{26}, \frac{2}{45} \left(13 + 4i\sqrt{26} \right) \right\}, \quad (4.33)$$

16	θ^1	θ^2	θ^3
a	$\tan^{-1}\left(\sqrt{\frac{13}{2}}\right)$	$\tan^{-1}\left(\frac{\sqrt{\frac{13}{2}}}{4}\right)$	$-\tan^{-1}\left(\frac{\sqrt{\frac{13}{2}}}{2}\right)$
b	$\tan^{-1}(\sqrt{26})$	0	$\tan^{-1}(2\sqrt{26})$
c	$\tan^{-1}\left(\frac{\sqrt{\frac{13}{2}}}{4}\right)$	$-\tan^{-1}\left(\frac{\sqrt{\frac{13}{2}}}{4}\right)$	$-\tan^{-1}\left(\frac{\sqrt{\frac{13}{2}}}{4}\right)$

Table 7: The angles with respect to the orientifold plane made by the cycle wrapped by stack of D6-branes on each of the three two-tori in Model 16.

and the corresponding u -moduli and s -modulus in supergravity basis from (3.6) are,

$$\{u^1, u^2, u^3\} = \left\{ \frac{\sqrt[4]{13}e^{-\phi_4}}{2^{3/4}\pi}, \frac{\sqrt[4]{13}e^{-\phi_4}}{4 \cdot 2^{3/4}\pi}, \frac{\sqrt[4]{26}e^{-\phi_4}}{\pi} \right\},$$

$$s = \frac{e^{-\phi_4}}{26^{3/4}\pi}. \quad (4.34)$$

Using (3.11) and the values from the table 40, the gauge kinetic function becomes,

$$\{f_a, f_b, f_c\} = \left\{ \frac{135e^{-\phi_4}}{16 \cdot 26^{3/4}\pi}, \frac{45e^{-\phi_4}}{32 \cdot 26^{3/4}\pi}, \frac{315e^{-\phi_4}}{32 \cdot 26^{3/4}\pi} \right\}, \quad (4.35)$$

To calculate the gaugino masses $\{M_Y, M_b, M_a\}$ for the respective gauge groups $U(1)_Y$, $SU(2)_L$, and $SU(3)_C$, we first compute $\{M_a, M_b, M_c\}$ using (3.38) as,

$$M_a = \frac{m_{3/2}(26\Theta_1 + 13\Theta_2 + 8(13\Theta_3 + \Theta_4))}{45\sqrt{3}},$$

$$M_b = \frac{m_{3/2}(13\Theta_2 - 32\Theta_4)}{15\sqrt{3}},$$

$$M_c = \frac{m_{3/2}(104\Theta_1 - 13\Theta_2 + 208\Theta_3 - 16\Theta_4)}{105\sqrt{3}}. \quad (4.36)$$

Next, to compute the trilinear coupling and the sleptons mass-squared we require the angles, the differences of angles and their first and second order derivatives with respect to the moduli. In table 7 we show the angles (3.16) made by the cycles wrapped by each stack of D6-branes with respect to the orientifold plane on each two-torus. The differences of the angles, $\theta_{xy}^i = \theta_y^i - \theta_x^i$ are,

$$\left[\begin{array}{ccc} \{0., 0., 0.\} & \{0.228854, -0.235545, 0.0066917\} & \{0.0389882, 0.237505, 0.0066917\} \\ \{-0.228854, 0.235545, -0.0066917\} & \{0., 0., 0.\} & \{-0.189865, 0.473051, 0.\} \\ \{-0.0389882, -0.237505, -0.0066917\} & \{0.189865, -0.473051, 0.\} & \{0., 0., 0.\} \end{array} \right] \quad (4.37)$$

To account for the negative angle differences we employ the sign function σ_{xy}^i , which is -1 only for negative angle difference and $+1$ otherwise,

$$\sigma_{xy}^i = \begin{pmatrix} \{1, 1, 1\} & \{1, -1, 1\} & \{1, 1, 1\} \\ \{-1, 1, -1\} & \{1, 1, 1\} & \{-1, 1, 1\} \\ \{-1, -1, -1\} & \{1, -1, 1\} & \{1, 1, 1\} \end{pmatrix}, \quad (4.38)$$

and the function η_{xy} is evaluated by taking the product on the torus index i as,

$$\eta_{xy} = \begin{pmatrix} 1 & -1 & 1 \\ 1 & 1 & -1 \\ -1 & -1 & 1 \end{pmatrix}. \quad (4.39)$$

Using the values of σ_{xy}^i and η_{xy} in (3.48) we can compute the four cases of functions $\Psi(\theta_{xy})$ defined in (3.43) and (3.44). Similarly we calculate the derivative $\Psi'(\theta_{xy}^j) = \frac{d\Psi(\theta_{xy}^j)}{d\theta_{xy}^j}$ using equations (3.51), (3.3), (3.53) and the properties of digamma function $\psi^{(0)}(z)$ (3.50) while neglecting the contribution of the t -moduli.

Utilizing above results while ignoring the CP-violating phases γ_m , the gaugino masses; the trilinear coupling (3.40); and the squared-masses of squarks and sleptons (3.42) are obtained as,

$$\begin{aligned} M_{\tilde{B}} &\equiv M_Y = m_{3/2} \left(\frac{416\Theta_1 + 13\Theta_2 + 1040\Theta_3 - 16\Theta_4}{495\sqrt{3}} \right), \\ M_{\tilde{W}} &\equiv M_b = m_{3/2} \left(\frac{13\Theta_2 - 32\Theta_4}{15\sqrt{3}} \right), \\ M_{\tilde{g}} &\equiv M_a = m_{3/2} \left(\frac{26\Theta_1 + 13\Theta_2 + 8(13\Theta_3 + \Theta_4)}{45\sqrt{3}} \right), \\ A_0 &\equiv A_{abc} = m_{3/2} \left(-0.674714\Theta_1 - 1.05734\Theta_2 - 0.296892\Theta_3 + 0.296892\Theta_4 \right), \\ m_L^2 &\equiv m_{ab}^2 = m_{3/2}^2 \left(0.357659\Theta_1^2 + 0.87063\Theta_1\Theta_2 - 1.16965\Theta_1\Theta_3 - 0.902287\Theta_1\Theta_4 \right. \\ &\quad \left. - 0.152099\Theta_2^2 - 0.139037\Theta_2\Theta_3 - 1.26422\Theta_2\Theta_4 - 0.463359\Theta_3^2 \right. \\ &\quad \left. + 1.81488\Theta_3\Theta_4 - 2.03894\Theta_4^2 + 1 \right), \\ m_R^2 &\equiv m_{ac}^2 = m_{3/2}^2 \left(-2.30496\Theta_1^2 - 0.638749\Theta_1\Theta_2 + 0.0264302\Theta_1\Theta_3 + 1.87359\Theta_1\Theta_4 \right. \\ &\quad \left. - 1.13248\Theta_2^2 + 0.518024\Theta_2\Theta_3 + 0.292916\Theta_2\Theta_4 - 0.63835\Theta_3^2 \right. \\ &\quad \left. - 1.58299\Theta_3\Theta_4 - 0.0912327\Theta_4^2 + 1 \right). \end{aligned} \quad (4.40)$$

All soft terms are subject to the constraint (3.27).

4.6 Model 16-dual

In Model 16-dual the three-point Yukawa couplings arise from the triplet intersections from the branes a , b and c on the first two-torus with 6 pairs of Higgs from the $\mathcal{N} = 2$ sector. Yukawa matrices for the Model 16-dual are of rank 3 and the three intersections required to

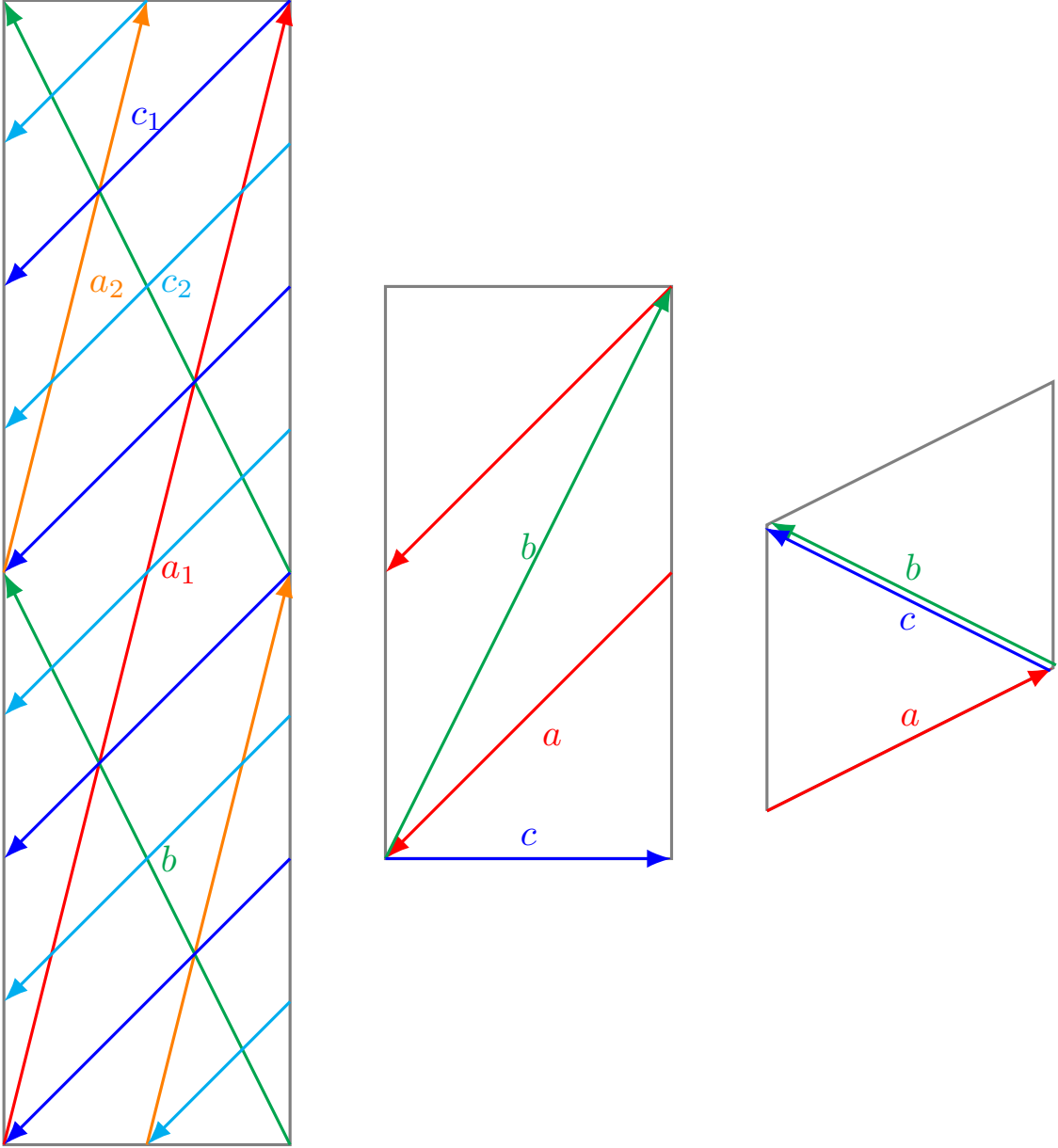


Figure 7: Brane configuration for the three two-tori in Model 16-dual where the third two-torus is tilted. Fermion mass hierarchies result from the intersections on the first two-torus.

form the disk diagrams for the Yukawa couplings all occur on the first torus as shown in figure 7.

The complex structure moduli U^i (3.5) are given as,

$$\{U^1, U^2, U^3\} = \left\{ i\sqrt{\frac{13}{2}}, 2i\sqrt{26}, \frac{2}{45} \left(13 + 4i\sqrt{26} \right) \right\}, \quad (4.41)$$

16-dual	θ^1	θ^2	θ^3
a	$\tan^{-1}\left(\sqrt{\frac{13}{2}}\right)$	$-\tan^{-1}\left(\frac{\sqrt{\frac{13}{2}}}{2}\right)$	$\tan^{-1}\left(\frac{\sqrt{\frac{13}{2}}}{4}\right)$
b	$\tan^{-1}(\sqrt{26})$	$\tan^{-1}(2\sqrt{26})$	0
c	$\tan^{-1}\left(\frac{\sqrt{\frac{13}{2}}}{4}\right)$	$-\tan^{-1}\left(\frac{\sqrt{\frac{13}{2}}}{4}\right)$	$-\tan^{-1}\left(\frac{\sqrt{\frac{13}{2}}}{4}\right)$

Table 8: The angles with respect to the orientifold plane made by the cycle wrapped by stack of D6-branes on each of the three two-tori in Model 16-dual.

and the corresponding u -moduli and s -modulus in supergravity basis from (3.6) are,

$$\{u^1, u^2, u^3\} = \left\{ \frac{\sqrt[4]{13}e^{-\phi_4}}{2^{3/4}\pi}, \frac{\sqrt[4]{13}e^{-\phi_4}}{4 \cdot 2^{3/4}\pi}, \frac{\sqrt[4]{26}e^{-\phi_4}}{\pi} \right\},$$

$$s = \frac{e^{-\phi_4}}{26^{3/4}\pi}. \quad (4.42)$$

Using (3.11) and the values from the table 41, the gauge kinetic function becomes,

$$\{f_a, f_b, f_c\} = \left\{ \frac{135e^{-\phi_4}}{16 \cdot 26^{3/4}\pi}, \frac{315e^{-\phi_4}}{32 \cdot 26^{3/4}\pi}, \frac{45e^{-\phi_4}}{32 \cdot 26^{3/4}\pi} \right\}, \quad (4.43)$$

To calculate the gaugino masses $\{M_Y, M_b, M_a\}$ for the respective gauge groups $U(1)_Y$, $SU(2)_L$, and $SU(3)_C$, we first compute $\{M_a, M_b, M_c\}$ using (3.38) as,

$$M_a = \frac{m_{3/2}(26\Theta_1 + 13\Theta_2 + 8(13\Theta_3 + \Theta_4))}{45\sqrt{3}},$$

$$M_b = \frac{m_{3/2}(104\Theta_1 - 13\Theta_2 + 208\Theta_3 - 16\Theta_4)}{105\sqrt{3}},$$

$$M_c = \frac{m_{3/2}(13\Theta_2 - 32\Theta_4)}{15\sqrt{3}}. \quad (4.44)$$

Next, to compute the trilinear coupling and the sleptons mass-squared we require the angles, the differences of angles and their first and second order derivatives with respect to the moduli. In table 8 we show the angles (3.16) made by the cycles wrapped by each stack of D6-branes with respect to the orientifold plane on each two-torus. The differences of the angles, $\theta_{xy}^i = \theta_y^i - \theta_x^i$ are,

$$\left[\begin{array}{ccc} \{0., 0., 0.\} & \{0.0389882, 0.237505, 0.0066917\} & \{0.228854, -0.235545, 0.0066917\} \\ \{-0.0389882, -0.237505, -0.0066917\} & \{0., 0., 0.\} & \{0.189865, -0.473051, 0.\} \\ \{-0.228854, 0.235545, -0.0066917\} & \{-0.189865, 0.473051, 0.\} & \{0., 0., 0.\} \end{array} \right] \quad (4.45)$$

To account for the negative angle differences we employ the sign function σ_{xy}^i , which is -1 only for negative angle difference and $+1$ otherwise,

$$\sigma_{xy}^i = \begin{pmatrix} \{1, 1, 1\} & \{1, 1, 1\} & \{1, -1, 1\} \\ \{-1, -1, -1\} & \{1, 1, 1\} & \{1, -1, 1\} \\ \{-1, 1, -1\} & \{-1, 1, 1\} & \{1, 1, 1\} \end{pmatrix}, \quad (4.46)$$

and the function η_{xy} is evaluated by taking the product on the torus index i as,

$$\eta_{xy} = \begin{pmatrix} 1 & 1 & -1 \\ -1 & 1 & -1 \\ 1 & -1 & 1 \end{pmatrix}. \quad (4.47)$$

Using the values of σ_{xy}^i and η_{xy} in (3.48) we can compute the four cases of functions $\Psi(\theta_{xy})$ defined in (3.43) and (3.44). Similarly we calculate the derivative $\Psi'(\theta_{xy}^j) = \frac{d\Psi(\theta_{xy}^j)}{d\theta_{xy}^j}$ using equations (3.51), (3.3), (3.53) and the properties of digamma function $\psi^{(0)}(z)$ (3.50) while neglecting the contribution of the t -moduli.

Utilizing above results while ignoring the CP-violating phases γ_m , the gaugino masses; the trilinear coupling (3.40); and the squared-masses of squarks and sleptons (3.42) are obtained as,

$$\begin{aligned} M_{\tilde{B}} &\equiv M_Y = m_{3/2} \left(\frac{104\Theta_1 + 91\Theta_2 + 416\Theta_3 - 64\Theta_4}{225\sqrt{3}} \right), \\ M_{\tilde{W}} &\equiv M_b = m_{3/2} \left(\frac{104\Theta_1 - 13\Theta_2 + 208\Theta_3 - 16\Theta_4}{105\sqrt{3}} \right), \\ M_{\tilde{g}} &\equiv M_a = m_{3/2} \left(\frac{26\Theta_1 + 13\Theta_2 + 8(13\Theta_3 + \Theta_4)}{45\sqrt{3}} \right), \\ A_0 &\equiv A_{abc} = m_{3/2} \left(-0.674714\Theta_1 - 1.05734\Theta_2 - 0.296892\Theta_3 + 0.296892\Theta_4 \right), \\ m_L^2 &\equiv m_{ab}^2 = m_{3/2}^2 \left(-2.30496\Theta_1^2 - 0.638749\Theta_1\Theta_2 + 0.0264302\Theta_1\Theta_3 + 1.87359\Theta_1\Theta_4 \right. \\ &\quad \left. - 1.13248\Theta_2^2 + 0.518024\Theta_2\Theta_3 + 0.292916\Theta_2\Theta_4 - 0.63835\Theta_3^2 \right. \\ &\quad \left. - 1.58299\Theta_3\Theta_4 - 0.0912327\Theta_4^2 + 1 \right), \\ m_R^2 &\equiv m_{ac}^2 = m_{3/2}^2 \left(0.357659\Theta_1^2 + 0.87063\Theta_1\Theta_2 - 1.16965\Theta_1\Theta_3 - 0.902287\Theta_1\Theta_4 \right. \\ &\quad \left. - 0.152099\Theta_2^2 - 0.139037\Theta_2\Theta_3 - 1.26422\Theta_2\Theta_4 - 0.463359\Theta_3^2 \right. \\ &\quad \left. + 1.81488\Theta_3\Theta_4 - 2.03894\Theta_4^2 + 1 \right). \end{aligned} \quad (4.48)$$

All soft terms are subject to the constraint (3.27).

4.7 Model 17

In Model 17 the three-point Yukawa couplings arise from the triplet intersections from the branes a , b and c on the second two-torus with 9 pairs of Higgs from the $\mathcal{N} = 2$ sector. Yukawa matrices for the Model 17 are of rank 3 and the three intersections required to

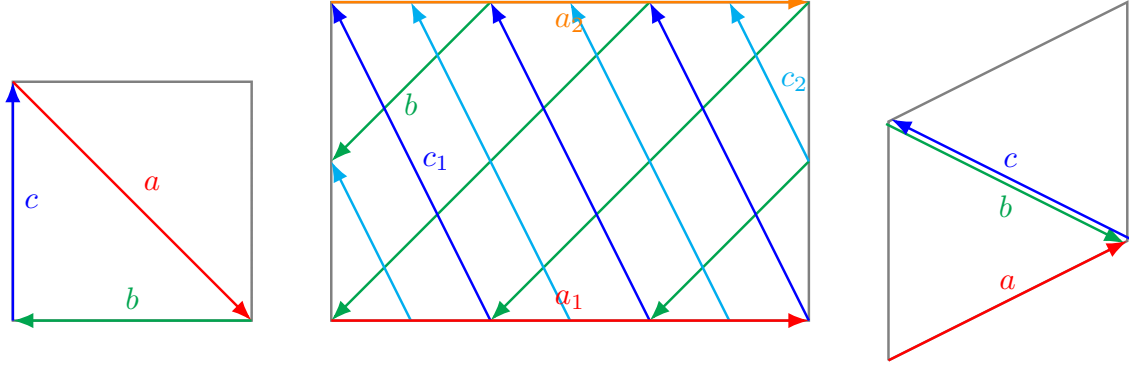


Figure 8: Brane configuration for the three two-tori in Model 17 where the third two-torus is tilted. Fermion mass hierarchies result from the intersections on the second two-torus.

17	θ^1	θ^2	θ^3
a	$-\tan^{-1}\left(\frac{1}{\sqrt{2}}\right)$	0	$\frac{\pi}{2}$
b	0	$\tan^{-1}\left(\frac{1}{\sqrt{2}}\right)$	$-\tan^{-1}(\sqrt{2})$
c	$\tan^{-1}\left(\frac{1}{\sqrt{2}}\right)$	$-\tan^{-1}\left(\frac{1}{\sqrt{2}}\right)$	$-\tan^{-1}\left(\frac{1}{\sqrt{2}}\right)$

Table 9: The angles with respect to the orientifold plane made by the cycle wrapped by stack of D6-branes on each of the three two-tori in Model 17.

form the disk diagrams for the Yukawa couplings all occur on the second torus as shown in figure 8.

The complex structure moduli U^i (3.5) are given as,

$$\{U^1, U^2, U^3\} = \left\{ \frac{i}{\sqrt{2}}, \frac{i\sqrt{2}}{3}, \frac{2}{3}(1 + i\sqrt{2}) \right\}, \quad (4.49)$$

and the corresponding u -moduli and s -modulus in supergravity basis from (3.6) are,

$$\begin{aligned} \{u^1, u^2, u^3\} &= \left\{ \frac{e^{-\phi_4}}{\sqrt[4]{2}\sqrt{3}\pi}, \frac{\sqrt{3}e^{-\phi_4}}{2\sqrt[4]{2}\pi}, \frac{e^{-\phi_4}}{2\sqrt[4]{2}\sqrt{3}\pi} \right\}, \\ s &= \frac{\sqrt{3}e^{-\phi_4}}{2\sqrt[4]{2}\pi}. \end{aligned} \quad (4.50)$$

Using (3.11) and the values from the table 42, the gauge kinetic function becomes,

$$\{f_a, f_b, f_c\} = \left\{ \frac{3\sqrt{3}e^{-\phi_4}}{16\sqrt[4]{2}\pi}, \frac{3\sqrt{3}e^{-\phi_4}}{8\sqrt[4]{2}\pi}, \frac{3\sqrt{3}e^{-\phi_4}}{16\sqrt[4]{2}\pi} \right\}, \quad (4.51)$$

To calculate the gaugino masses $\{M_Y, M_b, M_a\}$ for the respective gauge groups $U(1)_Y$,

$SU(2)_L$, and $SU(3)_C$, we first compute $\{M_a, M_b, M_c\}$ using (3.38) as,

$$\begin{aligned} M_a &= \frac{m_{3/2}(\Theta_2 - 2\Theta_4)}{\sqrt{3}}, \\ M_b &= \frac{m_{3/2}(\Theta_1 - 2\Theta_4)}{\sqrt{3}}, \\ M_c &= \frac{m_{3/2}(\Theta_2 + 2\Theta_3)}{\sqrt{3}}. \end{aligned} \quad (4.52)$$

Next, to compute the trilinear coupling and the sleptons mass-squared we require the angles, the differences of angles and their first and second order derivatives with respect to the moduli. In table 9 we show the angles (3.16) made by the cycles wrapped by each stack of D6-branes with respect to the orientifold plane on each two-torus. The differences of the angles, $\theta_{xy}^i = \theta_y^i - \theta_x^i$ are,

$$\begin{bmatrix} \{0., 0., 0.\} & \{-0.242928, 0.473887, -0.230959\} & \{0.186276, 0.186276, -0.0893668\} \\ \{0.242928, -0.473887, 0.230959\} & \{0., 0., 0.\} & \{0.429204, -0.287611, 0.141593\} \\ \{-0.186276, -0.186276, 0.0893668\} & \{-0.429204, 0.287611, -0.141593\} & \{0., 0., 0.\} \end{bmatrix} \quad (4.53)$$

To account for the negative angle differences we employ the sign function σ_{xy}^i , which is -1 only for negative angle difference and $+1$ otherwise,

$$\sigma_{xy}^i = \begin{pmatrix} \{1, 1, 1\} & \{-1, 1, -1\} & \{1, 1, -1\} \\ \{1, -1, 1\} & \{1, 1, 1\} & \{1, -1, 1\} \\ \{-1, -1, 1\} & \{-1, 1, -1\} & \{1, 1, 1\} \end{pmatrix}, \quad (4.54)$$

and the function η_{xy} is evaluated by taking the product on the torus index i as,

$$\eta_{xy} = \begin{pmatrix} 1 & 1 & -1 \\ -1 & 1 & -1 \\ 1 & 1 & 1 \end{pmatrix}. \quad (4.55)$$

Using the values of σ_{xy}^i and η_{xy} in (3.48) we can compute the four cases of functions $\Psi(\theta_{xy})$ defined in (3.43) and (3.44). Similarly we calculate the derivative $\Psi'(\theta_{xy}^j) = \frac{d\Psi(\theta_{xy}^j)}{d\theta_{xy}^j}$ using equations (3.51), (3.3), (3.53) and the properties of digamma function $\psi^{(0)}(z)$ (3.50) while neglecting the contribution of the t -moduli.

Utilizing above results while ignoring the CP-violating phases γ_m , the gaugino masses; the trilinear coupling (3.40); and the squared-masses of squarks and sleptons (3.42) are

obtained as,

$$\begin{aligned}
M_{\tilde{B}} &\equiv M_Y = m_{3/2} \left(\frac{5\Theta_2 + 6\Theta_3 - 4\Theta_4}{5\sqrt{3}} \right), \\
M_{\tilde{W}} &\equiv M_b = m_{3/2} \left(\frac{\Theta_1 - 2\Theta_4}{\sqrt{3}} \right), \\
M_{\tilde{g}} &\equiv M_a = m_{3/2} \left(\frac{\Theta_2 - 2\Theta_4}{\sqrt{3}} \right), \\
A_0 &\equiv A_{abc} = m_{3/2} \left(-0.128593\Theta_1 - 1.64721\Theta_2 - 0.107781\Theta_3 + 0.151538\Theta_4 \right), \\
m_L^2 &\equiv m_{ab}^2 = m_{3/2}^2 \left(0.36917\Theta_1^2 + 0.669259\Theta_1\Theta_2 - 0.840813\Theta_1\Theta_3 - 1.82443\Theta_1\Theta_4 \right. \\
&\quad \left. + 0.375979\Theta_2^2 - 0.820669\Theta_2\Theta_3 - 0.733709\Theta_2\Theta_4 - 0.929866\Theta_3^2 \right. \\
&\quad \left. + 1.7274\Theta_3\Theta_4 - 1.1538\Theta_4^2 + 1 \right), \\
m_R^2 &\equiv m_{ac}^2 = m_{3/2}^2 \left(-2.2278\Theta_1^2 - 2.22881\Theta_1\Theta_2 + 0.0357856\Theta_1\Theta_3 + 1.61629\Theta_1\Theta_4 \right. \\
&\quad \left. + 0.395725\Theta_2^2 + 0.464088\Theta_2\Theta_3 + 0.503187\Theta_2\Theta_4 + 0.535193\Theta_3^2 \right. \\
&\quad \left. - 3.12602\Theta_3\Theta_4 + 0.309973\Theta_4^2 + 1 \right). \tag{4.56}
\end{aligned}$$

All soft terms are subject to the constraint (3.27).

4.8 Model 17-dual

In Model 17-dual the three-point Yukawa couplings arise from the triplet intersections from the branes a , b and c on the second two-torus with 9 pairs of Higgs from the $\mathcal{N} = 2$ sector. Yukawa matrices for the Model 17-dual are of rank 3 and the three intersections required to form the disk diagrams for the Yukawa couplings all occur on the second torus as shown in figure 9.

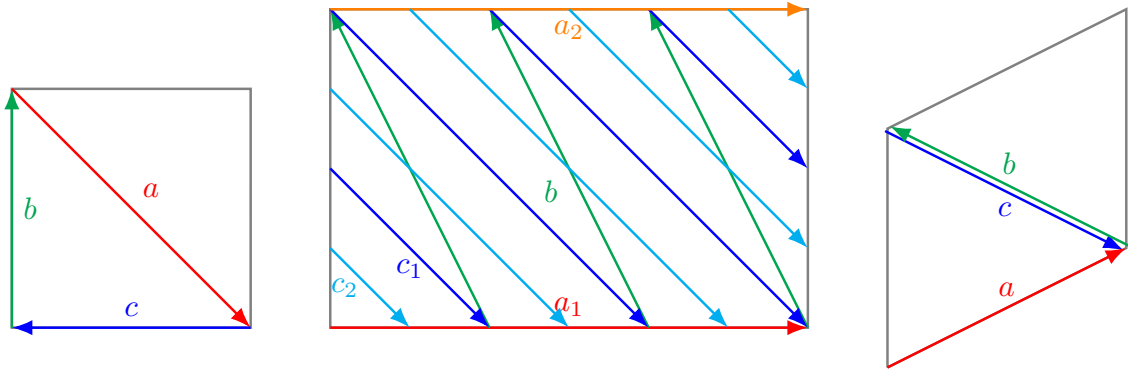


Figure 9: Brane configuration for the three two-tori in Model 17-dual where the third two-torus is tilted. Fermion mass hierarchies result from the intersections on the second two-torus.

17-dual	θ^1	θ^2	θ^3
a	$-\tan^{-1}\left(\frac{1}{\sqrt{2}}\right)$	$\frac{\pi}{2}$	0
b	0	$-\tan^{-1}(\sqrt{2})$	$\tan^{-1}\left(\frac{1}{\sqrt{2}}\right)$
c	$\tan^{-1}\left(\frac{1}{\sqrt{2}}\right)$	$-\tan^{-1}\left(\frac{1}{\sqrt{2}}\right)$	$-\tan^{-1}\left(\frac{1}{\sqrt{2}}\right)$

Table 10: The angles with respect to the orientifold plane made by the cycle wrapped by stack of D6-branes on each of the three two-tori in Model 17-dual.

The complex structure moduli U^i (3.5) are given as,

$$\{U^1, U^2, U^3\} = \left\{ \frac{i}{\sqrt{2}}, \frac{i\sqrt{2}}{3}, \frac{2}{3}(1 + i\sqrt{2}) \right\}, \quad (4.57)$$

and the corresponding u -moduli and s -modulus in supergravity basis from (3.6) are,

$$\begin{aligned} \{u^1, u^2, u^3\} &= \left\{ \frac{e^{-\phi_4}}{\sqrt[4]{2}\sqrt{3}\pi}, \frac{\sqrt{3}e^{-\phi_4}}{2\sqrt[4]{2}\pi}, \frac{e^{-\phi_4}}{2\sqrt[4]{2}\sqrt{3}\pi} \right\}, \\ s &= \frac{\sqrt{3}e^{-\phi_4}}{2\sqrt[4]{2}\pi}. \end{aligned} \quad (4.58)$$

Using (3.11) and the values from the table 43, the gauge kinetic function becomes,

$$\{f_a, f_b, f_c\} = \left\{ \frac{3\sqrt{3}e^{-\phi_4}}{16\sqrt[4]{2}\pi}, \frac{3\sqrt{3}e^{-\phi_4}}{16\sqrt[4]{2}\pi}, \frac{3\sqrt{3}e^{-\phi_4}}{8\sqrt[4]{2}\pi} \right\}, \quad (4.59)$$

To calculate the gaugino masses $\{M_Y, M_b, M_a\}$ for the respective gauge groups $U(1)_Y$, $SU(2)_L$, and $SU(3)_C$, we first compute $\{M_a, M_b, M_c\}$ using (3.38) as,

$$\begin{aligned} M_a &= \frac{m_{3/2}(\Theta_2 - 2\Theta_4)}{\sqrt{3}}, \\ M_b &= \frac{m_{3/2}(\Theta_2 + 2\Theta_3)}{\sqrt{3}}, \\ M_c &= \frac{m_{3/2}(\Theta_1 - 2\Theta_4)}{\sqrt{3}}. \end{aligned} \quad (4.60)$$

Next, to compute the trilinear coupling and the sleptons mass-squared we require the angles, the differences of angles and their first and second order derivatives with respect to the moduli. In table 10 we show the angles (3.16) made by the cycles wrapped by each stack of D6-branes with respect to the orientifold plane on each two-torus. The differences of the angles, $\theta_{xy}^i = \theta_y^i - \theta_x^i$ are,

$$\begin{bmatrix} \{0., 0., 0.\} & \{0.186276, 0.186276, -0.0893668\} & \{-0.242928, 0.473887, -0.230959\} \\ \{-0.186276, -0.186276, 0.0893668\} & \{0., 0., 0.\} & \{-0.429204, 0.287611, -0.141593\} \\ \{0.242928, -0.473887, 0.230959\} & \{0.429204, -0.287611, 0.141593\} & \{0., 0., 0.\} \end{bmatrix} \quad (4.61)$$

To account for the negative angle differences we employ the sign function σ_{xy}^i , which is -1 only for negative angle difference and $+1$ otherwise,

$$\sigma_{xy}^i = \begin{pmatrix} \{1, 1, 1\} & \{1, 1, -1\} & \{-1, 1, -1\} \\ \{-1, -1, 1\} & \{1, 1, 1\} & \{-1, 1, -1\} \\ \{1, -1, 1\} & \{1, -1, 1\} & \{1, 1, 1\} \end{pmatrix}, \quad (4.62)$$

and the function η_{xy} is evaluated by taking the product on the torus index i as,

$$\eta_{xy} = \begin{pmatrix} 1 & -1 & 1 \\ 1 & 1 & 1 \\ -1 & -1 & 1 \end{pmatrix}. \quad (4.63)$$

Using the values of σ_{xy}^i and η_{xy} in (3.48) we can compute the four cases of functions $\Psi(\theta_{xy})$ defined in (3.43) and (3.44). Similarly we calculate the derivative $\Psi'(\theta_{xy}^j) = \frac{d\Psi(\theta_{xy}^j)}{d\theta_{xy}^j}$ using equations (3.51), (3.3), (3.53) and the properties of digamma function $\psi^{(0)}(z)$ (3.50) while neglecting the contribution of the t -moduli.

Utilizing above results while ignoring the CP-violating phases γ_m , the gaugino masses; the trilinear coupling (3.40); and the squared-masses of squarks and sleptons (3.42) are obtained as,

$$\begin{aligned} M_{\tilde{B}} &\equiv M_Y = m_{3/2} \left(\frac{3\Theta_1 + \Theta_2 - 8\Theta_4}{4\sqrt{3}} \right), \\ M_{\tilde{W}} &\equiv M_b = m_{3/2} \left(\frac{\Theta_2 + 2\Theta_3}{\sqrt{3}} \right), \\ M_{\tilde{g}} &\equiv M_a = m_{3/2} \left(\frac{\Theta_2 - 2\Theta_4}{\sqrt{3}} \right), \\ A_0 &\equiv A_{abc} = m_{3/2} \left(-0.128593\Theta_1 - 1.64721\Theta_2 - 0.107781\Theta_3 + 0.151538\Theta_4 \right), \\ m_L^2 &\equiv m_{ab}^2 = m_{3/2}^2 \left(-2.2278\Theta_1^2 - 2.22881\Theta_1\Theta_2 + 0.0357856\Theta_1\Theta_3 + 1.61629\Theta_1\Theta_4 \right. \\ &\quad \left. + 0.395725\Theta_2^2 + 0.464088\Theta_2\Theta_3 + 0.503187\Theta_2\Theta_4 + 0.535193\Theta_3^2 \right. \\ &\quad \left. - 3.12602\Theta_3\Theta_4 + 0.309973\Theta_4^2 + 1 \right), \\ m_R^2 &\equiv m_{ac}^2 = m_{3/2}^2 \left(0.36917\Theta_1^2 + 0.669259\Theta_1\Theta_2 - 0.840813\Theta_1\Theta_3 - 1.82443\Theta_1\Theta_4 \right. \\ &\quad \left. + 0.375979\Theta_2^2 - 0.820669\Theta_2\Theta_3 - 0.733709\Theta_2\Theta_4 - 0.929866\Theta_3^2 \right. \\ &\quad \left. + 1.7274\Theta_3\Theta_4 - 1.1538\Theta_4^2 + 1 \right). \end{aligned} \quad (4.64)$$

All soft terms are subject to the constraint (3.27).

4.9 Model 18

In Model 18 the three-point Yukawa couplings arise from the triplet intersections from the branes a , b and c on the first two-torus with 9 pairs of Higgs from the $\mathcal{N} = 2$ sector. Yukawa matrices for the Model 18 are of rank 3 and the three intersections required to

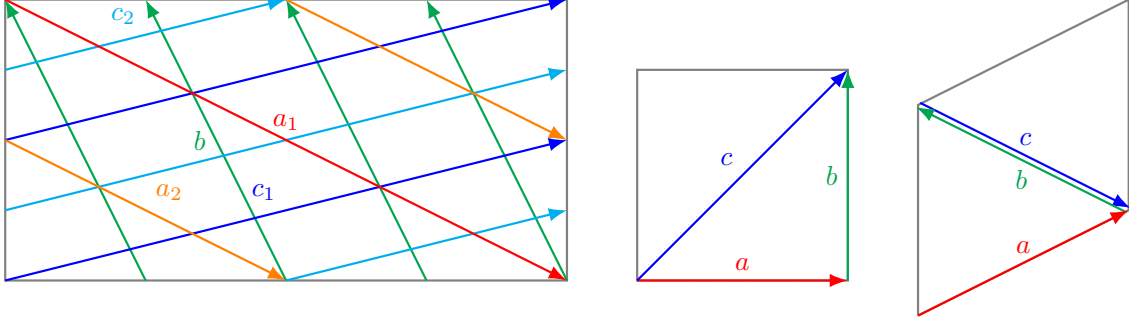


Figure 10: Brane configuration for the three two-tori in Model 18 where the third two-torus is tilted. Fermion mass hierarchies result from the intersections on the first two-torus.

18	θ^1	θ^2	θ^3
a	$-\tan^{-1}\left(\frac{1}{2}\right)$	$-\tan^{-1}(2)$	$\tan^{-1}\left(\frac{1}{4}\right)$
b	0	$\frac{\pi}{2}$	$\tan^{-1}\left(\frac{2}{9}\right)$
c	$\tan^{-1}\left(\frac{1}{2}\right)$	$-\tan^{-1}\left(\frac{1}{2}\right)$	$-\tan^{-1}\left(\frac{1}{2}\right)$

Table 11: The angles with respect to the orientifold plane made by the cycle wrapped by stack of D6-branes on each of the three two-tori in Model 18.

form the disk diagrams for the Yukawa couplings all occur on the first torus as shown in figure 10.

The complex structure moduli U^i (3.5) are given as,

$$\{U^1, U^2, U^3\} = \left\{ \frac{i}{2}, \frac{2i}{9}, \frac{2}{5} + \frac{4i}{5} \right\}, \quad (4.65)$$

and the corresponding u -moduli and s -modulus in supergravity basis from (3.6) are,

$$\begin{aligned} \{u^1, u^2, u^3\} &= \left\{ \frac{e^{-\phi_4}}{3\pi}, \frac{3e^{-\phi_4}}{4\pi}, \frac{e^{-\phi_4}}{6\pi} \right\}, \\ s &= \frac{3e^{-\phi_4}}{2\pi}. \end{aligned} \quad (4.66)$$

Using (3.11) and the values from the table 44, the gauge kinetic function becomes,

$$\{f_a, f_b, f_c\} = \left\{ \frac{15e^{-\phi_4}}{32\pi}, \frac{5e^{-\phi_4}}{24\pi}, \frac{85e^{-\phi_4}}{96\pi} \right\}, \quad (4.67)$$

To calculate the gaugino masses $\{M_Y, M_b, M_a\}$ for the respective gauge groups $U(1)_Y$,

$SU(2)_L$, and $SU(3)_C$, we first compute $\{M_a, M_b, M_c\}$ using (3.38) as,

$$\begin{aligned} M_a &= \frac{1}{5}\sqrt{3}m_{3/2}(\Theta_2 - 4\Theta_4), \\ M_b &= \frac{1}{5}\sqrt{3}m_{3/2}(\Theta_1 + 4\Theta_3), \\ M_c &= \frac{1}{85}\sqrt{3}m_{3/2}(8\Theta_1 + 9\Theta_2 - 4(\Theta_3 + 18\Theta_4)). \end{aligned} \quad (4.68)$$

Next, to compute the trilinear coupling and the sleptons mass-squared we require the angles, the differences of angles and their first and second order derivatives with respect to the moduli. In table 11 we show the angles (3.16) made by the cycles wrapped by each stack of D6-branes with respect to the orientifold plane on each two-torus. The differences of the angles, $\theta_{xy}^i = \theta_y^i - \theta_x^i$ are,

$$\begin{bmatrix} \{0., 0., 0.\} & \{-0.501908, 0.570796, 0.214297\} & \{-0.291374, 0.218669, 0.0727048\} \\ \{0.501908, -0.570796, -0.214297\} & \{0., 0., 0.\} & \{0.210535, -0.352127, -0.141593\} \\ \{0.291374, -0.218669, -0.0727048\} & \{-0.210535, 0.352127, 0.141593\} & \{0., 0., 0.\} \end{bmatrix} \quad (4.69)$$

To account for the negative angle differences we employ the sign function σ_{xy}^i , which is -1 only for negative angle difference and $+1$ otherwise,

$$\sigma_{xy}^i = \begin{pmatrix} \{1, 1, 1\} & \{-1, 1, 1\} & \{-1, 1, 1\} \\ \{1, -1, -1\} & \{1, 1, 1\} & \{1, -1, -1\} \\ \{1, -1, -1\} & \{-1, 1, 1\} & \{1, 1, 1\} \end{pmatrix}, \quad (4.70)$$

and the function η_{xy} is evaluated by taking the product on the torus index i as,

$$\eta_{xy} = \begin{pmatrix} 1 & -1 & -1 \\ 1 & 1 & 1 \\ 1 & -1 & 1 \end{pmatrix}. \quad (4.71)$$

Using the values of σ_{xy}^i and η_{xy} in (3.48) we can compute the four cases of functions $\Psi(\theta_{xy})$ defined in (3.43) and (3.44). Similarly we calculate the derivative $\Psi'(\theta_{xy}^j) = \frac{d\Psi(\theta_{xy}^j)}{d\theta_{xy}^j}$ using equations (3.51), (3.3), (3.53) and the properties of digamma function $\psi^{(0)}(z)$ (3.50) while neglecting the contribution of the t -moduli.

Utilizing above results while ignoring the CP-violating phases γ_m , the gaugino masses; the trilinear coupling (3.40); and the squared-masses of squarks and sleptons (3.42) are

obtained as,

$$\begin{aligned}
M_{\tilde{B}} &\equiv M_Y = m_{3/2} \left(\frac{1}{115} \sqrt{3} (8\Theta_1 + 15\Theta_2 - 4(\Theta_3 + 24\Theta_4)) \right), \\
M_{\tilde{W}} &\equiv M_b = m_{3/2} \left(\frac{1}{5} \sqrt{3} (\Theta_1 + 4\Theta_3) \right), \\
M_{\tilde{g}} &\equiv M_a = m_{3/2} \left(\frac{1}{5} \sqrt{3} (\Theta_2 - 4\Theta_4) \right), \\
A_0 &\equiv A_{abc} = m_{3/2} \left(-1.82708\Theta_1 - 1.50614\Theta_2 + 1.42587\Theta_3 + 0.175299\Theta_4 \right), \\
m_L^2 &\equiv m_{ab}^2 = m_{3/2}^2 \left(0.730534\Theta_1^2 + 0.131797\Theta_1\Theta_2 - 1.01748\Theta_1\Theta_3 - 1.17062\Theta_1\Theta_4 \right. \\
&\quad \left. + 0.144867\Theta_2^2 - 1.16345\Theta_2\Theta_3 - 0.752402\Theta_2\Theta_4 - 0.846416\Theta_3^2 \right. \\
&\quad \left. + 0.832553\Theta_3\Theta_4 - 0.848056\Theta_4^2 + 1 \right), \\
m_R^2 &\equiv m_{ac}^2 = m_{3/2}^2 \left(0.72924\Theta_1^2 + 0.0000979797\Theta_1\Theta_2 - 0.60321\Theta_1\Theta_3 - 2.56141\Theta_1\Theta_4 \right. \\
&\quad \left. + 0.759033\Theta_2^2 - 2.39659\Theta_2\Theta_3 - 0.388307\Theta_2\Theta_4 - 1.82808\Theta_3^2 \right. \\
&\quad \left. + 1.44981\Theta_3\Theta_4 + 0.339613\Theta_4^2 + 1 \right). \tag{4.72}
\end{aligned}$$

All soft terms are subject to the constraint (3.27).

4.10 Model 18-dual

In Model 18-dual the three-point Yukawa couplings arise from the triplet intersections from the branes a , b and c on the first two-torus with 9 pairs of Higgs from the $\mathcal{N} = 2$ sector. Yukawa matrices for the Model 18-dual are of rank 3 and the three intersections required to form the disk diagrams for the Yukawa couplings all occur on the first torus as shown in figure 11.

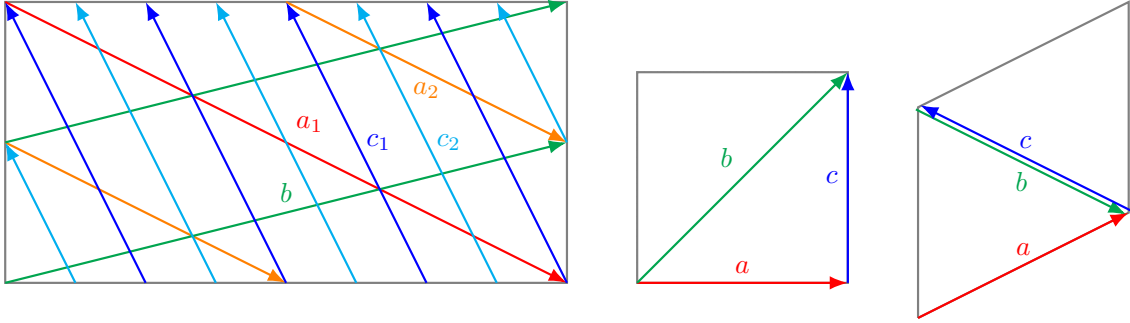


Figure 11: Brane configuration for the three two-tori in Model 18-dual where the third two-torus is tilted. Fermion mass hierarchies result from the intersections on the first two-torus.

The complex structure moduli U^i (3.5) are given as,

$$\{U^1, U^2, U^3\} = \left\{ \frac{i}{2}, \frac{2i}{9}, \frac{2}{5} + \frac{4i}{5} \right\}, \tag{4.73}$$

18-dual	θ^1	θ^2	θ^3
a	$-\tan^{-1}\left(\frac{1}{2}\right)$	$\tan^{-1}\left(\frac{1}{4}\right)$	$-\tan^{-1}(2)$
b	0	$\tan^{-1}\left(\frac{2}{9}\right)$	$\frac{\pi}{2}$
c	$\tan^{-1}\left(\frac{1}{2}\right)$	$-\tan^{-1}\left(\frac{1}{2}\right)$	$-\tan^{-1}\left(\frac{1}{2}\right)$

Table 12: The angles with respect to the orientifold plane made by the cycle wrapped by stack of D6-branes on each of the three two-tori in Model 18-dual.

and the corresponding u -moduli and s -modulus in supergravity basis from (3.6) are,

$$\{u^1, u^2, u^3\} = \left\{ \frac{e^{-\phi_4}}{3\pi}, \frac{3e^{-\phi_4}}{4\pi}, \frac{e^{-\phi_4}}{6\pi} \right\},$$

$$s = \frac{3e^{-\phi_4}}{2\pi}. \quad (4.74)$$

Using (3.11) and the values from the table 45, the gauge kinetic function becomes,

$$\{f_a, f_b, f_c\} = \left\{ \frac{15e^{-\phi_4}}{32\pi}, \frac{85e^{-\phi_4}}{96\pi}, \frac{5e^{-\phi_4}}{24\pi} \right\}, \quad (4.75)$$

To calculate the gaugino masses $\{M_Y, M_b, M_a\}$ for the respective gauge groups $U(1)_Y$, $SU(2)_L$, and $SU(3)_C$, we first compute $\{M_a, M_b, M_c\}$ using (3.38) as,

$$M_a = \frac{1}{5}\sqrt{3}m_{3/2}(\Theta_2 - 4\Theta_4),$$

$$M_b = \frac{1}{85}\sqrt{3}m_{3/2}(8\Theta_1 + 9\Theta_2 - 4(\Theta_3 + 18\Theta_4)),$$

$$M_c = \frac{1}{5}\sqrt{3}m_{3/2}(\Theta_1 + 4\Theta_3). \quad (4.76)$$

Next, to compute the trilinear coupling and the sleptons mass-squared we require the angles, the differences of angles and their first and second order derivatives with respect to the moduli. In table 12 we show the angles (3.16) made by the cycles wrapped by each stack of D6-branes with respect to the orientifold plane on each two-torus. The differences of the angles, $\theta_{xy}^i = \theta_y^i - \theta_x^i$ are,

$$\left[\begin{array}{ccc} \{0., 0., 0.\} & \{-0.291374, 0.218669, 0.0727048\} & \{-0.501908, 0.570796, 0.214297\} \\ \{0.291374, -0.218669, -0.0727048\} & \{0., 0., 0.\} & \{-0.210535, 0.352127, 0.141593\} \\ \{0.501908, -0.570796, -0.214297\} & \{0.210535, -0.352127, -0.141593\} & \{0., 0., 0.\} \end{array} \right] \quad (4.77)$$

To account for the negative angle differences we employ the sign function σ_{xy}^i , which is -1 only for negative angle difference and $+1$ otherwise,

$$\sigma_{xy}^i = \begin{pmatrix} \{1, 1, 1\} & \{-1, 1, 1\} & \{-1, 1, 1\} \\ \{1, -1, -1\} & \{1, 1, 1\} & \{-1, 1, 1\} \\ \{1, -1, -1\} & \{1, -1, -1\} & \{1, 1, 1\} \end{pmatrix}, \quad (4.78)$$

and the function η_{xy} is evaluated by taking the product on the torus index i as,

$$\eta_{xy} = \begin{pmatrix} 1 & -1 & -1 \\ 1 & 1 & -1 \\ 1 & 1 & 1 \end{pmatrix}. \quad (4.79)$$

Using the values of σ_{xy}^i and η_{xy} in (3.48) we can compute the four cases of functions $\Psi(\theta_{xy})$ defined in (3.43) and (3.44). Similarly we calculate the derivative $\Psi'(\theta_{xy}^j) = \frac{d\Psi(\theta_{xy}^j)}{d\theta_{xy}^j}$ using equations (3.51), (3.3), (3.53) and the properties of digamma function $\psi^{(0)}(z)$ (3.50) while neglecting the contribution of the t -moduli.

Utilizing above results while ignoring the CP-violating phases γ_m , the gaugino masses; the trilinear coupling (3.40); and the squared-masses of squarks and sleptons (3.42) are obtained as,

$$\begin{aligned} M_{\tilde{B}} &\equiv M_Y = m_{3/2} \left(\frac{1}{25} \sqrt{3} (2\Theta_1 + 3\Theta_2 + 8\Theta_3 - 12\Theta_4) \right), \\ M_{\tilde{W}} &\equiv M_b = m_{3/2} \left(\frac{1}{85} \sqrt{3} (8\Theta_1 + 9\Theta_2 - 4(\Theta_3 + 18\Theta_4)) \right), \\ M_{\tilde{g}} &\equiv M_a = m_{3/2} \left(\frac{1}{5} \sqrt{3} (\Theta_2 - 4\Theta_4) \right), \\ A_0 &\equiv A_{abc} = m_{3/2} \left(-1.82708\Theta_1 - 1.50614\Theta_2 + 1.42587\Theta_3 + 0.175299\Theta_4 \right), \\ m_L^2 &\equiv m_{ab}^2 = m_{3/2}^2 \left(0.72924\Theta_1^2 + 0.0000979797\Theta_1\Theta_2 - 0.60321\Theta_1\Theta_3 - 2.56141\Theta_1\Theta_4 \right. \\ &\quad \left. + 0.759033\Theta_2^2 - 2.39659\Theta_2\Theta_3 - 0.388307\Theta_2\Theta_4 - 1.82808\Theta_3^2 \right. \\ &\quad \left. + 1.44981\Theta_3\Theta_4 + 0.339613\Theta_4^2 + 1 \right), \\ m_R^2 &\equiv m_{ac}^2 = m_{3/2}^2 \left(0.730534\Theta_1^2 + 0.131797\Theta_1\Theta_2 - 1.01748\Theta_1\Theta_3 - 1.17062\Theta_1\Theta_4 \right. \\ &\quad \left. + 0.144867\Theta_2^2 - 1.16345\Theta_2\Theta_3 - 0.752402\Theta_2\Theta_4 - 0.846416\Theta_3^2 \right. \\ &\quad \left. + 0.832553\Theta_3\Theta_4 - 0.848056\Theta_4^2 + 1 \right). \end{aligned} \quad (4.80)$$

All soft terms are subject to the constraint (3.27).

4.11 Model 19

In Model 19 the three-point Yukawa couplings arise from the triplet intersections from the branes a , b and c on the first two-torus with 9 pairs of Higgs from the $\mathcal{N} = 2$ sector. Yukawa matrices for the Model 19 are of rank 3 and the three intersections required to form the disk diagrams for the Yukawa couplings all occur on the first torus as shown in figure 12.

The complex structure moduli U^i (3.5) are given as,

$$\{U^1, U^2, U^3\} = \left\{ i\sqrt{\frac{7}{23}}, i\sqrt{161}, \frac{8}{135} (28 + i\sqrt{161}) \right\}, \quad (4.81)$$

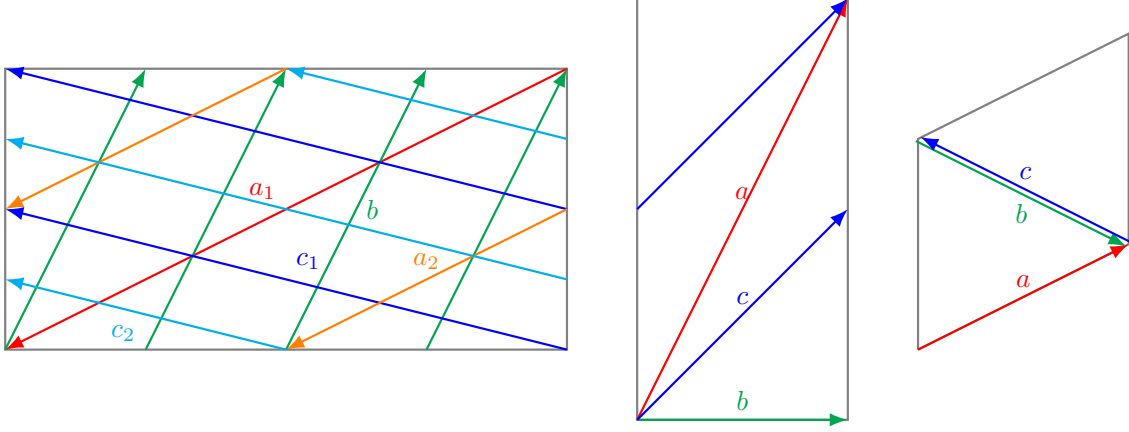


Figure 12: Brane configuration for the three two-tori in Model 19 where the third two-torus is tilted. Fermion mass hierarchies result from the intersections on the first two-torus.

19	θ^1	θ^2	θ^3
a	$\tan^{-1}\left(\sqrt{\frac{7}{23}}\right)$	$\tan^{-1}\left(4\sqrt{\frac{7}{23}}\right)$	$-\tan^{-1}\left(\frac{\sqrt{\frac{7}{23}}}{2}\right)$
b	$\tan^{-1}\left(\sqrt{161}\right)$	0	$\tan^{-1}\left(\frac{\sqrt{161}}{2}\right)$
c	$\tan^{-1}\left(4\sqrt{\frac{7}{23}}\right)$	$-\tan^{-1}\left(4\sqrt{\frac{7}{23}}\right)$	$-\tan^{-1}\left(4\sqrt{\frac{7}{23}}\right)$

Table 13: The angles with respect to the orientifold plane made by the cycle wrapped by stack of D6-branes on each of the three two-tori in Model 19.

and the corresponding u -moduli and s -modulus in supergravity basis from (3.6) are,

$$\{u^1, u^2, u^3\} = \left\{ \frac{\sqrt{2}\sqrt[4]{161}e^{-\phi_4}}{\pi}, \frac{\sqrt{2}\sqrt[4]{7}e^{-\phi_4}}{23^{3/4}\pi}, \frac{\sqrt[4]{161}e^{-\phi_4}}{4\sqrt{2}\pi} \right\},$$

$$s = \frac{\sqrt[4]{23}e^{-\phi_4}}{4\sqrt{2}7^{3/4}\pi}. \quad (4.82)$$

Using (3.11) and the values from the table 46, the gauge kinetic function becomes,

$$\{f_a, f_b, f_c\} = \left\{ \frac{405e^{-\phi_4}}{8\sqrt{2}161^{3/4}\pi}, \frac{135e^{-\phi_4}}{16\sqrt{2}161^{3/4}\pi}, \frac{1485e^{-\phi_4}}{16\sqrt{2}161^{3/4}\pi} \right\}, \quad (4.83)$$

To calculate the gaugino masses $\{M_Y, M_b, M_a\}$ for the respective gauge groups $U(1)_Y$, $SU(2)_L$, and $SU(3)_C$, we first compute $\{M_a, M_b, M_c\}$ using (3.38) as,

$$M_a = \frac{m_{3/2}(644\Theta_1 + 28\Theta_2 + 23(7\Theta_3 + \Theta_4))}{270\sqrt{3}},$$

$$M_b = \frac{m_{3/2}(112\Theta_2 - 23\Theta_4)}{45\sqrt{3}},$$

$$M_c = \frac{m_{3/2}(1288\Theta_1 - 56\Theta_2 + 161\Theta_3 - 92\Theta_4)}{495\sqrt{3}}. \quad (4.84)$$

Next, to compute the trilinear coupling and the sleptons mass-squared we require the angles, the differences of angles and their first and second order derivatives with respect to the moduli. In table 13 we show the angles (3.16) made by the cycles wrapped by each stack of D6-branes with respect to the orientifold plane on each two-torus. The differences of the angles, $\theta_{xy}^i = \theta_y^i - \theta_x^i$ are,

$$\left[\begin{array}{ccc} \{0., 0., 0.\} & \{-0.217223, -0.492148, 0.70937\} & \{0.50991, -0.0776874, 0.850963\} \\ \{0.217223, 0.492148, -0.70937\} & \{0., 0., 0.\} & \{0.727132, 0.41446, 0.141593\} \\ \{-0.50991, 0.0776874, -0.850963\} & \{-0.727132, -0.41446, -0.141593\} & \{0., 0., 0.\} \end{array} \right] \quad (4.85)$$

To account for the negative angle differences we employ the sign function σ_{xy}^i , which is -1 only for negative angle difference and $+1$ otherwise,

$$\sigma_{xy}^i = \begin{pmatrix} \{1, 1, 1\} & \{-1, -1, 1\} & \{1, -1, 1\} \\ \{1, 1, -1\} & \{1, 1, 1\} & \{1, 1, 1\} \\ \{-1, 1, -1\} & \{-1, -1, -1\} & \{1, 1, 1\} \end{pmatrix}, \quad (4.86)$$

and the function η_{xy} is evaluated by taking the product on the torus index i as,

$$\eta_{xy} = \begin{pmatrix} 1 & 1 & -1 \\ -1 & 1 & 1 \\ 1 & -1 & 1 \end{pmatrix}. \quad (4.87)$$

Using the values of σ_{xy}^i and η_{xy} in (3.48) we can compute the four cases of functions $\Psi(\theta_{xy})$ defined in (3.43) and (3.44). Similarly we calculate the derivative $\Psi'(\theta_{xy}^j) = \frac{d\Psi(\theta_{xy}^j)}{d\theta_{xy}^j}$ using equations (3.51), (3.3), (3.53) and the properties of digamma function $\psi^{(0)}(z)$ (3.50) while neglecting the contribution of the t -moduli.

Utilizing above results while ignoring the CP-violating phases γ_m , the gaugino masses; the trilinear coupling (3.40); and the squared-masses of squarks and sleptons (3.42) are

obtained as,

$$\begin{aligned}
M_{\tilde{B}} &\equiv M_Y = m_{3/2} \left(\frac{5152\Theta_1 - 112\Theta_2 + 805\Theta_3 - 230\Theta_4}{2025\sqrt{3}} \right), \\
M_{\tilde{W}} &\equiv M_b = m_{3/2} \left(\frac{112\Theta_2 - 23\Theta_4}{45\sqrt{3}} \right), \\
M_{\tilde{g}} &\equiv M_a = m_{3/2} \left(\frac{644\Theta_1 + 28\Theta_2 + 23(7\Theta_3 + \Theta_4)}{270\sqrt{3}} \right), \\
A_0 &\equiv A_{abc} = m_{3/2} \left(-0.133497\Theta_1 - 1.55973\Theta_2 + 0.108067\Theta_3 - 0.146888\Theta_4 \right), \\
m_L^2 &\equiv m_{ab}^2 = m_{3/2}^2 \left(-1.92219\Theta_1^2 - 0.606279\Theta_1\Theta_2 + 0.894634\Theta_1\Theta_3 - 0.207461\Theta_1\Theta_4 \right. \\
&\quad \left. - 1.85446\Theta_2^2 + 0.894634\Theta_2\Theta_3 + 0.862019\Theta_2\Theta_4 - 0.50419\Theta_3^2 \right. \\
&\quad \left. + 0.239164\Theta_3\Theta_4 - 0.506606\Theta_4^2 + 1 \right), \\
m_R^2 &\equiv m_{ac}^2 = m_{3/2}^2 \left(-1.63243\Theta_1^2 + 1.90023\Theta_1\Theta_2 - 0.696574\Theta_1\Theta_3 + 1.49474\Theta_1\Theta_4 \right. \\
&\quad \left. + 0.770153\Theta_2^2 + 1.49862\Theta_2\Theta_3 - 1.898\Theta_2\Theta_4 - 1.96883\Theta_3^2 \right. \\
&\quad \left. + 1.08122\Theta_3\Theta_4 - 1.52482\Theta_4^2 + 1 \right). \tag{4.88}
\end{aligned}$$

All soft terms are subject to the constraint (3.27).

4.12 Model 19-dual

In Model 19-dual the three-point Yukawa couplings arise from the triplet intersections from the branes a , b and c on the first two-torus with 9 pairs of Higgs from the $\mathcal{N} = 2$ sector. Yukawa matrices for the Model 19-dual are of rank 3 and the three intersections required to form the disk diagrams for the Yukawa couplings all occur on the first torus as shown in figure 13.

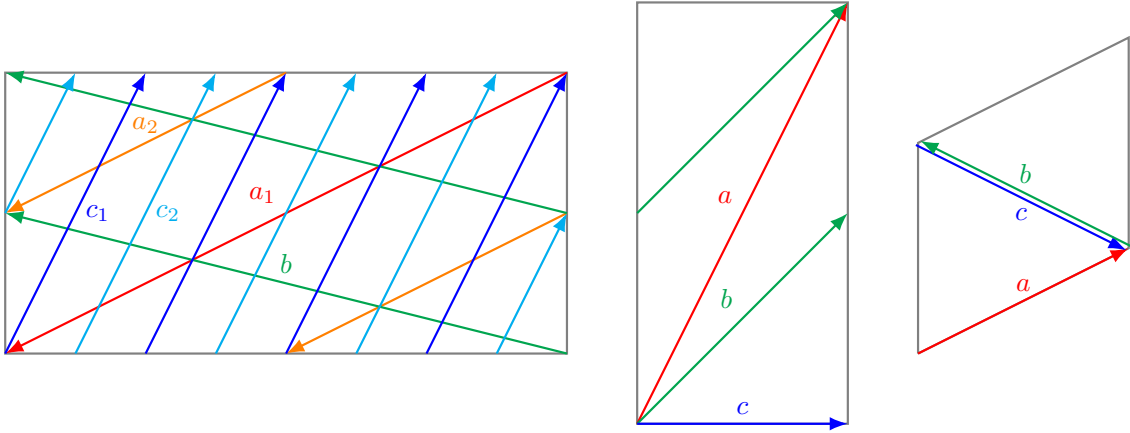


Figure 13: Brane configuration for the three two-tori in Model 19-dual where the third two-torus is tilted. Fermion mass hierarchies result from the intersections on the first two-torus.

19-dual	θ^1	θ^2	θ^3
a	$\tan^{-1}\left(\sqrt{\frac{7}{23}}\right)$	$-\tan^{-1}\left(\frac{\sqrt{\frac{7}{23}}}{2}\right)$	$\tan^{-1}\left(4\sqrt{\frac{7}{23}}\right)$
b	$\tan^{-1}\left(\sqrt{161}\right)$	$\tan^{-1}\left(\frac{\sqrt{161}}{2}\right)$	0
c	$\tan^{-1}\left(4\sqrt{\frac{7}{23}}\right)$	$-\tan^{-1}\left(4\sqrt{\frac{7}{23}}\right)$	$-\tan^{-1}\left(4\sqrt{\frac{7}{23}}\right)$

Table 14: The angles with respect to the orientifold plane made by the cycle wrapped by stack of D6-branes on each of the three two-tori in Model 19-dual.

The complex structure moduli U^i (3.5) are given as,

$$\{U^1, U^2, U^3\} = \left\{ i\sqrt{\frac{7}{23}}, i\sqrt{161}, \frac{8}{135} \left(28 + i\sqrt{161} \right) \right\}, \quad (4.89)$$

and the corresponding u -moduli and s -modulus in supergravity basis from (3.6) are,

$$\begin{aligned} \{u^1, u^2, u^3\} &= \left\{ \frac{\sqrt{2}\sqrt[4]{161}e^{-\phi_4}}{\pi}, \frac{\sqrt{2}\sqrt[4]{7}e^{-\phi_4}}{23^{3/4}\pi}, \frac{\sqrt[4]{161}e^{-\phi_4}}{4\sqrt{2}\pi} \right\}, \\ s &= \frac{\sqrt[4]{23}e^{-\phi_4}}{4\sqrt{2}7^{3/4}\pi}. \end{aligned} \quad (4.90)$$

Using (3.11) and the values from the table 47, the gauge kinetic function becomes,

$$\{f_a, f_b, f_c\} = \left\{ \frac{405e^{-\phi_4}}{8\sqrt{2}161^{3/4}\pi}, \frac{1485e^{-\phi_4}}{16\sqrt{2}161^{3/4}\pi}, \frac{135e^{-\phi_4}}{16\sqrt{2}161^{3/4}\pi} \right\}, \quad (4.91)$$

To calculate the gaugino masses $\{M_Y, M_b, M_a\}$ for the respective gauge groups $U(1)_Y$, $SU(2)_L$, and $SU(3)_C$, we first compute $\{M_a, M_b, M_c\}$ using (3.38) as,

$$\begin{aligned} M_a &= \frac{m_{3/2}(644\Theta_1 + 28\Theta_2 + 23(7\Theta_3 + \Theta_4))}{270\sqrt{3}}, \\ M_b &= \frac{m_{3/2}(1288\Theta_1 - 56\Theta_2 + 161\Theta_3 - 92\Theta_4)}{495\sqrt{3}}, \\ M_c &= \frac{m_{3/2}(112\Theta_2 - 23\Theta_4)}{45\sqrt{3}}. \end{aligned} \quad (4.92)$$

Next, to compute the trilinear coupling and the sleptons mass-squared we require the angles, the differences of angles and their first and second order derivatives with respect to the moduli. In table 14 we show the angles (3.16) made by the cycles wrapped by each stack of D6-branes with respect to the orientifold plane on each two-torus. The differences of the angles, $\theta_{xy}^i = \theta_y^i - \theta_x^i$ are,

$$\left[\begin{array}{ccc} \{0., 0., 0.\} & \{0.50991, -0.0776874, 0.850963\} & \{-0.217223, -0.492148, 0.70937\} \\ \{-0.50991, 0.0776874, -0.850963\} & \{0., 0., 0.\} & \{-0.727132, -0.41446, -0.141593\} \\ \{0.217223, 0.492148, -0.70937\} & \{0.727132, 0.41446, 0.141593\} & \{0., 0., 0.\} \end{array} \right] \quad (4.93)$$

To account for the negative angle differences we employ the sign function σ_{xy}^i , which is -1 only for negative angle difference and $+1$ otherwise,

$$\sigma_{xy}^i = \begin{pmatrix} \{1, 1, 1\} & \{1, -1, 1\} & \{-1, -1, 1\} \\ \{-1, 1, -1\} & \{1, 1, 1\} & \{-1, -1, -1\} \\ \{1, 1, -1\} & \{1, 1, 1\} & \{1, 1, 1\} \end{pmatrix}, \quad (4.94)$$

and the function η_{xy} is evaluated by taking the product on the torus index i as,

$$\eta_{xy} = \begin{pmatrix} 1 & -1 & 1 \\ 1 & 1 & -1 \\ -1 & 1 & 1 \end{pmatrix}. \quad (4.95)$$

Using the values of σ_{xy}^i and η_{xy} in (3.48) we can compute the four cases of functions $\Psi(\theta_{xy})$ defined in (3.43) and (3.44). Similarly we calculate the derivative $\Psi'(\theta_{xy}^j) = \frac{d\Psi(\theta_{xy}^j)}{d\theta_{xy}^j}$ using equations (3.51), (3.3), (3.53) and the properties of digamma function $\psi^{(0)}(z)$ (3.50) while neglecting the contribution of the t -moduli.

Utilizing above results while ignoring the CP-violating phases γ_m , the gaugino masses; the trilinear coupling (3.40); and the squared-masses of squarks and sleptons (3.42) are obtained as,

$$\begin{aligned} M_{\tilde{B}} &\equiv M_Y = m_{3/2} \left(\frac{1288\Theta_1 + 392\Theta_2 + 322\Theta_3 - 23\Theta_4}{675\sqrt{3}} \right), \\ M_{\tilde{W}} &\equiv M_b = m_{3/2} \left(\frac{1288\Theta_1 - 56\Theta_2 + 161\Theta_3 - 92\Theta_4}{495\sqrt{3}} \right), \\ M_{\tilde{g}} &\equiv M_a = m_{3/2} \left(\frac{644\Theta_1 + 28\Theta_2 + 23(7\Theta_3 + \Theta_4)}{270\sqrt{3}} \right), \\ A_0 &\equiv A_{abc} = m_{3/2} \left(-0.133497\Theta_1 - 1.55973\Theta_2 + 0.108067\Theta_3 - 0.146888\Theta_4 \right), \\ m_L^2 &\equiv m_{ab}^2 = m_{3/2}^2 \left(-1.63243\Theta_1^2 + 1.90023\Theta_1\Theta_2 - 0.696574\Theta_1\Theta_3 + 1.49474\Theta_1\Theta_4 \right. \\ &\quad \left. + 0.770153\Theta_2^2 + 1.49862\Theta_2\Theta_3 - 1.898\Theta_2\Theta_4 - 1.96883\Theta_3^2 \right. \\ &\quad \left. + 1.08122\Theta_3\Theta_4 - 1.52482\Theta_4^2 + 1 \right), \\ m_R^2 &\equiv m_{ac}^2 = m_{3/2}^2 \left(-1.92219\Theta_1^2 - 0.606279\Theta_1\Theta_2 + 0.894634\Theta_1\Theta_3 - 0.207461\Theta_1\Theta_4 \right. \\ &\quad \left. - 1.85446\Theta_2^2 + 0.894634\Theta_2\Theta_3 + 0.862019\Theta_2\Theta_4 - 0.50419\Theta_3^2 \right. \\ &\quad \left. + 0.239164\Theta_3\Theta_4 - 0.506606\Theta_4^2 + 1 \right). \end{aligned} \quad (4.96)$$

All soft terms are subject to the constraint (3.27).

4.13 Model 20

In Model 20 the three-point Yukawa couplings arise from the triplet intersections from the branes a , b and c on the second two-torus with 9 pairs of Higgs from the $\mathcal{N} = 2$ sector. Yukawa matrices for the Model 20 are of rank 3 and the three intersections required to

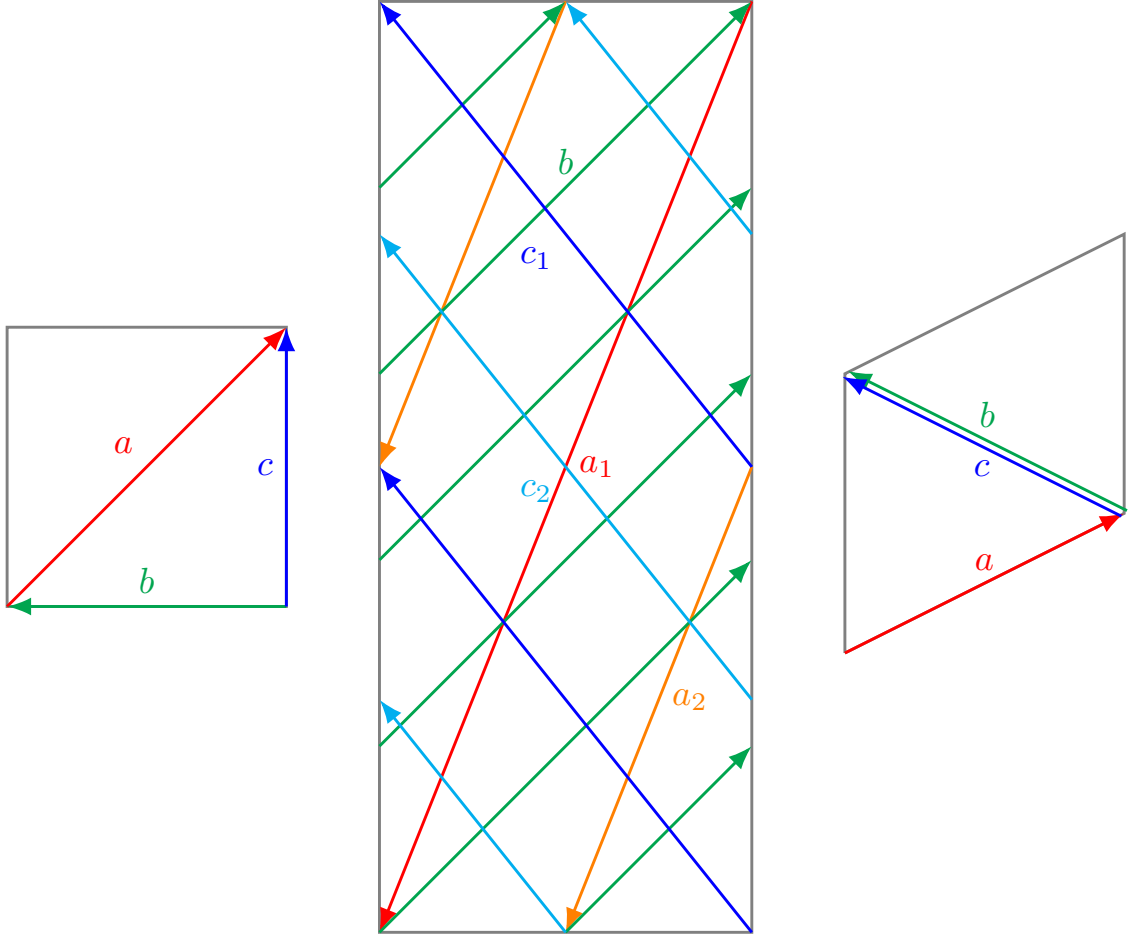


Figure 14: Brane configuration for the three two-tori in Model 20 where the third two-torus is tilted. Fermion mass hierarchies result from the intersections on the second two-torus.

20	θ^1	θ^2	θ^3
a	$\tan^{-1}\left(\frac{7}{\sqrt{5}}\right)$	0	$\frac{\pi}{2}$
b	$\tan^{-1}(\sqrt{5})$	$\tan^{-1}\left(\frac{2}{\sqrt{5}}\right)$	$-\tan^{-1}\left(\frac{\sqrt{5}}{2}\right)$
c	$\tan^{-1}\left(\frac{2}{\sqrt{5}}\right)$	$-\tan^{-1}\left(\frac{2}{\sqrt{5}}\right)$	$-\tan^{-1}\left(\frac{2}{\sqrt{5}}\right)$

Table 15: The angles with respect to the orientifold plane made by the cycle wrapped by stack of D6-branes on each of the three two-tori in Model 20.

form the disk diagrams for the Yukawa couplings all occur on the second torus as shown in figure 14.

The complex structure moduli U^i (3.5) are given as,

$$\{U^1, U^2, U^3\} = \left\{ \frac{7i}{\sqrt{5}}, i\sqrt{5}, \frac{4}{9} \left(2 + i\sqrt{5} \right) \right\}, \quad (4.97)$$

and the corresponding u -moduli and s -modulus in supergravity basis from (3.6) are,

$$\begin{aligned} \{u^1, u^2, u^3\} &= \left\{ \frac{\sqrt[4]{5}e^{-\phi_4}}{\sqrt{7}\pi}, \frac{\sqrt{7}e^{-\phi_4}}{5^{3/4}\pi}, \frac{\sqrt[4]{5}\sqrt{7}e^{-\phi_4}}{4\pi} \right\}, \\ s &= \frac{\sqrt[4]{5}e^{-\phi_4}}{4\sqrt{7}\pi}. \end{aligned} \quad (4.98)$$

Using (3.11) and the values from the table 48, the gauge kinetic function becomes,

$$\{f_a, f_b, f_c\} = \left\{ \frac{27e^{-\phi_4}}{8 \cdot 5^{3/4}\sqrt{7}\pi}, \frac{9\sqrt[4]{5}e^{-\phi_4}}{16\sqrt{7}\pi}, \frac{9\sqrt{7}e^{-\phi_4}}{16 \cdot 5^{3/4}\pi} \right\}, \quad (4.99)$$

To calculate the gaugino masses $\{M_Y, M_b, M_a\}$ for the respective gauge groups $U(1)_Y$, $SU(2)_L$, and $SU(3)_C$, we first compute $\{M_a, M_b, M_c\}$ using (3.38) as,

$$\begin{aligned} M_a &= \frac{m_{3/2}(10\Theta_1 + 14\Theta_2 + 5(7\Theta_3 + \Theta_4))}{18\sqrt{3}}, \\ M_b &= \frac{m_{3/2}(4\Theta_1 - 5\Theta_4)}{3\sqrt{3}}, \\ M_c &= \frac{m_{3/2}(4\Theta_2 + 5\Theta_3)}{3\sqrt{3}}. \end{aligned} \quad (4.100)$$

Next, to compute the trilinear coupling and the sleptons mass-squared we require the angles, the differences of angles and their first and second order derivatives with respect to the moduli. In table 15 we show the angles (3.16) made by the cycles wrapped by each stack of D6-branes with respect to the orientifold plane on each two-torus. The differences of the angles, $\theta_{xy}^i = \theta_y^i - \theta_x^i$ are,

$$\begin{bmatrix} \{0., 0., 0.\} & \{-0.12001, 0.721058, -0.317863\} & \{0.309193, 0.291855, -0.317863\} \\ \{0.12001, -0.721058, 0.317863\} & \{0., 0., 0.\} & \{0.429204, -0.429204, 0.\} \\ \{-0.309193, -0.291855, 0.317863\} & \{-0.429204, 0.429204, 0.\} & \{0., 0., 0.\} \end{bmatrix} \quad (4.101)$$

To account for the negative angle differences we employ the sign function σ_{xy}^i , which is -1 only for negative angle difference and $+1$ otherwise,

$$\sigma_{xy}^i = \begin{pmatrix} \{1, 1, 1\} & \{-1, 1, -1\} & \{1, 1, -1\} \\ \{1, -1, 1\} & \{1, 1, 1\} & \{1, -1, 1\} \\ \{-1, -1, 1\} & \{-1, 1, 1\} & \{1, 1, 1\} \end{pmatrix}, \quad (4.102)$$

and the function η_{xy} is evaluated by taking the product on the torus index i as,

$$\eta_{xy} = \begin{pmatrix} 1 & 1 & -1 \\ -1 & 1 & -1 \\ 1 & -1 & 1 \end{pmatrix}. \quad (4.103)$$

Using the values of σ_{xy}^i and η_{xy} in (3.48) we can compute the four cases of functions $\Psi(\theta_{xy})$ defined in (3.43) and (3.44). Similarly we calculate the derivative $\Psi'(\theta_{xy}^j) = \frac{d\Psi(\theta_{xy}^j)}{d\theta_{xy}^j}$ using equations (3.51), (3.3), (3.53) and the properties of digamma function $\psi^{(0)}(z)$ (3.50) while neglecting the contribution of the t -moduli.

Utilizing above results while ignoring the CP-violating phases γ_m , the gaugino masses; the trilinear coupling (3.40); and the squared-masses of squarks and sleptons (3.42) are obtained as,

$$\begin{aligned}
M_{\tilde{B}} &\equiv M_Y = m_{3/2} \left(\frac{20\Theta_1 + 112\Theta_2 + 175\Theta_3 + 10\Theta_4}{99\sqrt{3}} \right), \\
M_{\tilde{W}} &\equiv M_b = m_{3/2} \left(\frac{4\Theta_1 - 5\Theta_4}{3\sqrt{3}} \right), \\
M_{\tilde{g}} &\equiv M_a = m_{3/2} \left(\frac{10\Theta_1 + 14\Theta_2 + 5(7\Theta_3 + \Theta_4)}{18\sqrt{3}} \right), \\
A_0 &\equiv A_{abc} = m_{3/2} \left(-0.152188\Theta_1 - 1.57986\Theta_2 + 0.282383\Theta_3 - 0.282383\Theta_4 \right), \\
m_L^2 &\equiv m_{ab}^2 = m_{3/2}^2 \left(-0.399003\Theta_1^2 + 1.25156\Theta_1\Theta_2 - 0.666067\Theta_1\Theta_3 - 0.958492\Theta_1\Theta_4 \right. \\
&\quad \left. + 0.106172\Theta_2^2 + 0.163812\Theta_2\Theta_3 - 0.73081\Theta_2\Theta_4 - 2.07593\Theta_3^2 \right. \\
&\quad \left. + 1.71861\Theta_3\Theta_4 - 0.689841\Theta_4^2 + 1 \right), \\
m_R^2 &\equiv m_{ac}^2 = m_{3/2}^2 \left(-2.35521\Theta_1^2 - 1.21594\Theta_1\Theta_2 + 0.483768\Theta_1\Theta_3 + 1.51111\Theta_1\Theta_4 \right. \\
&\quad \left. - 0.387583\Theta_2^2 + 1.12751\Theta_2\Theta_3 + 0.178197\Theta_2\Theta_4 + 0.0690201\Theta_3^2 \right. \\
&\quad \left. - 1.68298\Theta_3\Theta_4 - 0.338871\Theta_4^2 + 1 \right). \tag{4.104}
\end{aligned}$$

All soft terms are subject to the constraint (3.27).

4.14 Model 20-dual

In Model 20-dual the three-point Yukawa couplings arise from the triplet intersections from the branes a , b and c on the second two-torus with 9 pairs of Higgs from the $\mathcal{N} = 2$ sector. Yukawa matrices for the Model 20-dual are of rank 3 and the three intersections required to form the disk diagrams for the Yukawa couplings all occur on the second torus as shown in figure 15.

20-dual	θ^1	θ^2	θ^3
a	$\tan^{-1} \left(\frac{7}{\sqrt{5}} \right)$	$\frac{\pi}{2}$	0
b	$\tan^{-1} (\sqrt{5})$	$-\tan^{-1} \left(\frac{\sqrt{5}}{2} \right)$	$\tan^{-1} \left(\frac{2}{\sqrt{5}} \right)$
c	$\tan^{-1} \left(\frac{2}{\sqrt{5}} \right)$	$-\tan^{-1} \left(\frac{2}{\sqrt{5}} \right)$	$-\tan^{-1} \left(\frac{2}{\sqrt{5}} \right)$

Table 16: The angles with respect to the orientifold plane made by the cycle wrapped by stack of D6-branes on each of the three two-tori in Model 20-dual.

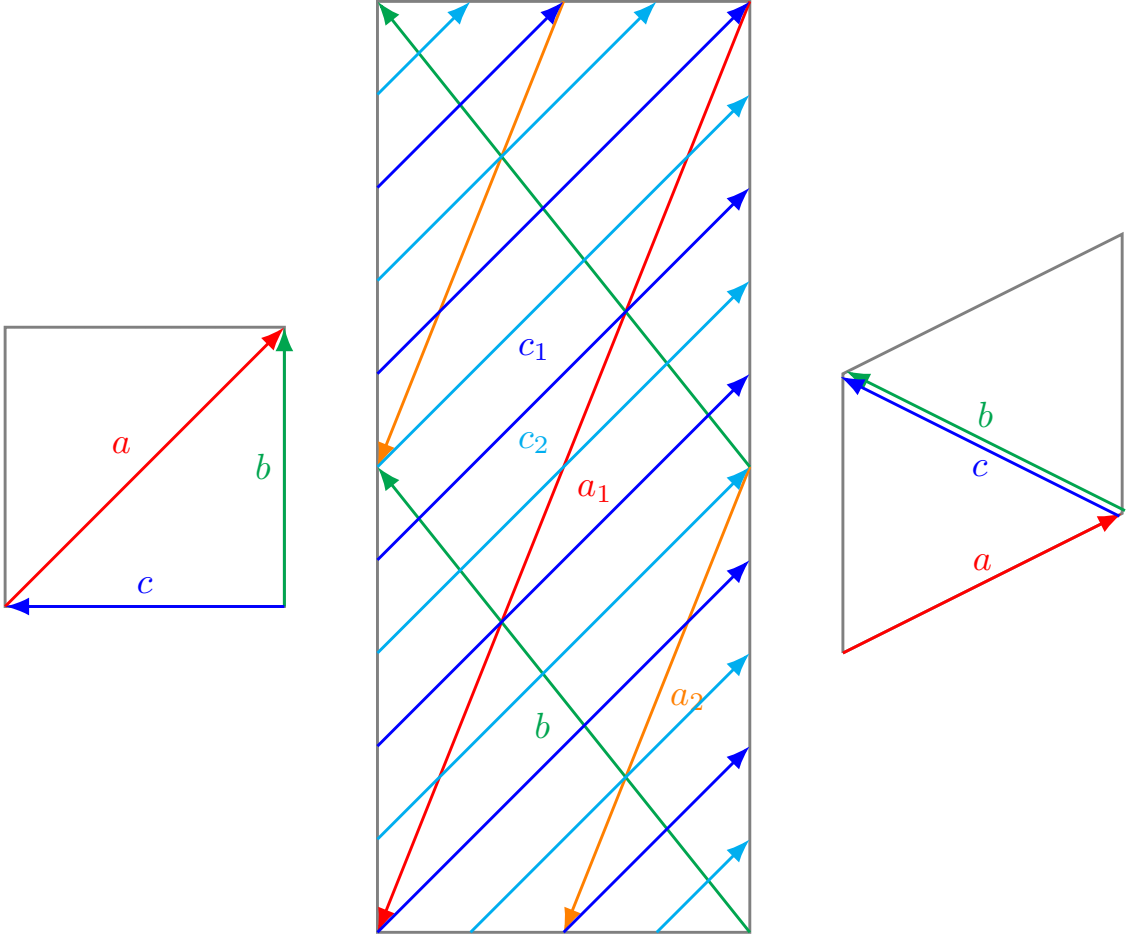


Figure 15: Brane configuration for the three two-tori in Model 20-dual where the third two-torus is tilted. Fermion mass hierarchies result from the intersections on the second two-torus.

The complex structure moduli U^i (3.5) are given as,

$$\{U^1, U^2, U^3\} = \left\{ \frac{7i}{\sqrt{5}}, i\sqrt{5}, \frac{4}{9} (2 + i\sqrt{5}) \right\}, \quad (4.105)$$

and the corresponding u -moduli and s -modulus in supergravity basis from (3.6) are,

$$\begin{aligned} \{u^1, u^2, u^3\} &= \left\{ \frac{\sqrt[4]{5}e^{-\phi_4}}{\sqrt{7}\pi}, \frac{\sqrt{7}e^{-\phi_4}}{5^{3/4}\pi}, \frac{\sqrt[4]{5}\sqrt{7}e^{-\phi_4}}{4\pi} \right\}, \\ s &= \frac{\sqrt[4]{5}e^{-\phi_4}}{4\sqrt{7}\pi}. \end{aligned} \quad (4.106)$$

Using (3.11) and the values from the table 49, the gauge kinetic function becomes,

$$\{f_a, f_b, f_c\} = \left\{ \frac{27e^{-\phi_4}}{8 \cdot 5^{3/4}\sqrt{7}\pi}, \frac{9\sqrt{7}e^{-\phi_4}}{16 \cdot 5^{3/4}\pi}, \frac{9\sqrt[4]{5}e^{-\phi_4}}{16\sqrt{7}\pi} \right\}, \quad (4.107)$$

To calculate the gaugino masses $\{M_Y, M_b, M_a\}$ for the respective gauge groups $U(1)_Y$, $SU(2)_L$, and $SU(3)_C$, we first compute $\{M_a, M_b, M_c\}$ using (3.38) as,

$$\begin{aligned} M_a &= \frac{m_{3/2}(10\Theta_1 + 14\Theta_2 + 5(7\Theta_3 + \Theta_4))}{18\sqrt{3}}, \\ M_b &= \frac{m_{3/2}(4\Theta_2 + 5\Theta_3)}{3\sqrt{3}}, \\ M_c &= \frac{m_{3/2}(4\Theta_1 - 5\Theta_4)}{3\sqrt{3}}. \end{aligned} \quad (4.108)$$

Next, to compute the trilinear coupling and the sleptons mass-squared we require the angles, the differences of angles and their first and second order derivatives with respect to the moduli. In table 16 we show the angles (3.16) made by the cycles wrapped by each stack of D6-branes with respect to the orientifold plane on each two-torus. The differences of the angles, $\theta_{xy}^i = \theta_y^i - \theta_x^i$ are,

$$\begin{bmatrix} \{0., 0., 0.\} & \{0.309193, 0.291855, -0.317863\} & \{-0.12001, 0.721058, -0.317863\} \\ \{-0.309193, -0.291855, 0.317863\} & \{0., 0., 0.\} & \{-0.429204, 0.429204, 0.\} \\ \{0.12001, -0.721058, 0.317863\} & \{0.429204, -0.429204, 0.\} & \{0., 0., 0.\} \end{bmatrix} \quad (4.109)$$

To account for the negative angle differences we employ the sign function σ_{xy}^i , which is -1 only for negative angle difference and $+1$ otherwise,

$$\sigma_{xy}^i = \begin{pmatrix} \{1, 1, 1\} & \{1, 1, -1\} & \{-1, 1, -1\} \\ \{-1, -1, 1\} & \{1, 1, 1\} & \{-1, 1, 1\} \\ \{1, -1, 1\} & \{1, -1, 1\} & \{1, 1, 1\} \end{pmatrix}, \quad (4.110)$$

and the function η_{xy} is evaluated by taking the product on the torus index i as,

$$\eta_{xy} = \begin{pmatrix} 1 & -1 & 1 \\ 1 & 1 & -1 \\ -1 & -1 & 1 \end{pmatrix}. \quad (4.111)$$

Using the values of σ_{xy}^i and η_{xy} in (3.48) we can compute the four cases of functions $\Psi(\theta_{xy})$ defined in (3.43) and (3.44). Similarly we calculate the derivative $\Psi'(\theta_{xy}^j) = \frac{d\Psi(\theta_{xy}^j)}{d\theta_{xy}^j}$ using equations (3.51), (3.3), (3.53) and the properties of digamma function $\psi^{(0)}(z)$ (3.50) while neglecting the contribution of the t -moduli.

Utilizing above results while ignoring the CP-violating phases γ_m , the gaugino masses; the trilinear coupling (3.40); and the squared-masses of squarks and sleptons (3.42) are

obtained as,

$$\begin{aligned}
M_{\tilde{B}} &\equiv M_Y = m_{3/2} \left(\frac{80\Theta_1 + 28\Theta_2 + 70\Theta_3 - 65\Theta_4}{81\sqrt{3}} \right), \\
M_{\tilde{W}} &\equiv M_b = m_{3/2} \left(\frac{4\Theta_2 + 5\Theta_3}{3\sqrt{3}} \right), \\
M_{\tilde{g}} &\equiv M_a = m_{3/2} \left(\frac{10\Theta_1 + 14\Theta_2 + 5(7\Theta_3 + \Theta_4)}{18\sqrt{3}} \right), \\
A_0 &\equiv A_{abc} = m_{3/2} \left(-0.152188\Theta_1 - 1.57986\Theta_2 + 0.282383\Theta_3 - 0.282383\Theta_4 \right), \\
m_L^2 &\equiv m_{ab}^2 = m_{3/2}^2 \left(-2.35521\Theta_1^2 - 1.21594\Theta_1\Theta_2 + 0.483768\Theta_1\Theta_3 + 1.51111\Theta_1\Theta_4 \right. \\
&\quad \left. - 0.387583\Theta_2^2 + 1.12751\Theta_2\Theta_3 + 0.178197\Theta_2\Theta_4 + 0.0690201\Theta_3^2 \right. \\
&\quad \left. - 1.68298\Theta_3\Theta_4 - 0.338871\Theta_4^2 + 1 \right), \\
m_R^2 &\equiv m_{ac}^2 = m_{3/2}^2 \left(-0.399003\Theta_1^2 + 1.25156\Theta_1\Theta_2 - 0.666067\Theta_1\Theta_3 - 0.958492\Theta_1\Theta_4 \right. \\
&\quad \left. + 0.106172\Theta_2^2 + 0.163812\Theta_2\Theta_3 - 0.73081\Theta_2\Theta_4 - 2.07593\Theta_3^2 \right. \\
&\quad \left. + 1.71861\Theta_3\Theta_4 - 0.689841\Theta_4^2 + 1 \right). \tag{4.112}
\end{aligned}$$

All soft terms are subject to the constraint (3.27).

4.15 Model 21

In Model 21 the three-point Yukawa couplings arise from the triplet intersections from the branes a , b and c on the second two-torus with 12 pairs of Higgs from the $\mathcal{N} = 2$ sector. Yukawa matrices for the Model 21 are of rank 3 and the three intersections required to form the disk diagrams for the Yukawa couplings all occur on the second torus as shown in figure 16.

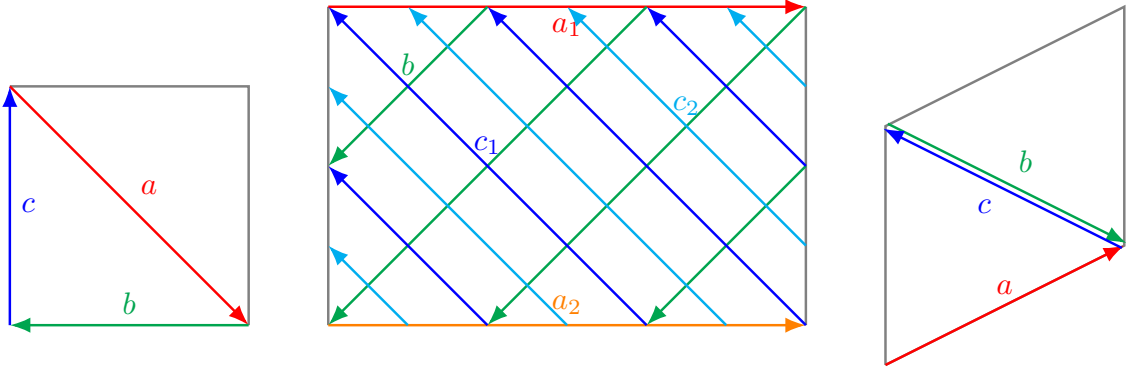


Figure 16: Brane configuration for the three two-tori in Model 21 where the third two-torus is tilted. Fermion mass hierarchies result from the intersections on the second two-torus.

The complex structure moduli U^i (3.5) are given as,

$$\{U^1, U^2, U^3\} = \left\{ i, \frac{2i}{3}, 1 + i \right\}, \tag{4.113}$$

21	θ^1	θ^2	θ^3
a	$\frac{3\pi}{4}$	0	$\frac{\pi}{2}$
b	0	$\frac{\pi}{4}$	$\frac{3\pi}{4}$
c	$\frac{\pi}{4}$	$\frac{3\pi}{4}$	$\frac{3\pi}{4}$

Table 17: The angles with respect to the orientifold plane made by the cycle wrapped by stack of D6-branes on each of the three two-tori in Model 21.

and the corresponding u -moduli and s -modulus in supergravity basis from (3.6) are,

$$\begin{aligned} \{u^1, u^2, u^3\} &= \left\{ \frac{e^{-\phi_4}}{\sqrt{3}\pi}, \frac{\sqrt{3}e^{-\phi_4}}{2\pi}, \frac{e^{-\phi_4}}{2\sqrt{3}\pi} \right\}, \\ s &= \frac{\sqrt{3}e^{-\phi_4}}{4\pi}. \end{aligned} \quad (4.114)$$

Using (3.11) and the values from the table 50, the gauge kinetic function becomes,

$$\{f_a, f_b, f_c\} = \left\{ \frac{\sqrt{3}e^{-\phi_4}}{8\pi}, \frac{\sqrt{3}e^{-\phi_4}}{4\pi}, \frac{\sqrt{3}e^{-\phi_4}}{4\pi} \right\}, \quad (4.115)$$

To calculate the gaugino masses $\{M_Y, M_b, M_a\}$ for the respective gauge groups $U(1)_Y$, $SU(2)_L$, and $SU(3)_C$, we first compute $\{M_a, M_b, M_c\}$ using (3.38) as,

$$\begin{aligned} M_a &= \frac{1}{2}\sqrt{3}m_{3/2}(\Theta_2 - \Theta_4), \\ M_b &= \frac{1}{2}\sqrt{3}m_{3/2}(\Theta_1 - \Theta_4), \\ M_c &= \frac{1}{2}\sqrt{3}m_{3/2}(\Theta_2 + \Theta_3). \end{aligned} \quad (4.116)$$

Next, to compute the trilinear coupling and the sleptons mass-squared we require the angles, the differences of angles and their first and second order derivatives with respect to the moduli. In table 17 we show the angles (3.16) made by the cycles wrapped by each stack of D6-branes with respect to the orientifold plane on each two-torus. The differences of the angles, $\theta_{xy}^i = \theta_y^i - \theta_x^i$ are,

$$\begin{bmatrix} \{0., 0., 0.\} & \{-0.0730092, 0.643806, -0.570796\} & \{0.356194, 0.356194, -0.429204\} \\ \{0.0730092, -0.643806, 0.570796\} & \{0., 0., 0.\} & \{0.429204, -0.287611, 0.141593\} \\ \{-0.356194, -0.356194, 0.429204\} & \{-0.429204, 0.287611, -0.141593\} & \{0., 0., 0.\} \end{bmatrix} \quad (4.117)$$

To account for the negative angle differences we employ the sign function σ_{xy}^i , which is -1 only for negative angle difference and $+1$ otherwise,

$$\sigma_{xy}^i = \begin{pmatrix} \{1, 1, 1\} & \{-1, 1, -1\} & \{1, 1, -1\} \\ \{1, -1, 1\} & \{1, 1, 1\} & \{1, -1, 1\} \\ \{-1, -1, 1\} & \{-1, 1, -1\} & \{1, 1, 1\} \end{pmatrix}, \quad (4.118)$$

and the function η_{xy} is evaluated by taking the product on the torus index i as,

$$\eta_{xy} = \begin{pmatrix} 1 & 1 & -1 \\ -1 & 1 & -1 \\ 1 & 1 & 1 \end{pmatrix}. \quad (4.119)$$

Using the values of σ_{xy}^i and η_{xy} in (3.48) we can compute the four cases of functions $\Psi(\theta_{xy})$ defined in (3.43) and (3.44). Similarly we calculate the derivative $\Psi'(\theta_{xy}^j) = \frac{d\Psi(\theta_{xy}^j)}{d\theta_{xy}^j}$ using equations (3.51), (3.3), (3.53) and the properties of digamma function $\psi^{(0)}(z)$ (3.50) while neglecting the contribution of the t -moduli.

Utilizing above results while ignoring the CP-violating phases γ_m , the gaugino masses; the trilinear coupling (3.40); and the squared-masses of squarks and sleptons (3.42) are obtained as,

$$\begin{aligned} M_{\tilde{B}} &\equiv M_Y = m_{3/2} \left(\frac{1}{8} \sqrt{3} (4\Theta_2 + 3\Theta_3 - \Theta_4) \right), \\ M_{\tilde{W}} &\equiv M_b = m_{3/2} \left(\frac{1}{2} \sqrt{3} (\Theta_1 - \Theta_4) \right), \\ M_{\tilde{g}} &\equiv M_a = m_{3/2} \left(\frac{1}{2} \sqrt{3} (\Theta_2 - \Theta_4) \right), \\ A_0 &\equiv A_{abc} = m_{3/2} \left(-0.444661\Theta_1 - 1.36219\Theta_2 + 0.260871\Theta_3 - 0.186075\Theta_4 \right), \\ m_L^2 &\equiv m_{ab}^2 = m_{3/2}^2 \left(-0.0689562\Theta_1^2 + 1.52807\Theta_1\Theta_2 - 0.25782\Theta_1\Theta_3 - 0.582907\Theta_1\Theta_4 \right. \\ &\quad \left. - 0.127855\Theta_2^2 + 0.31395\Theta_2\Theta_3 - 0.623439\Theta_2\Theta_4 - 2.04994\Theta_3^2 \right. \\ &\quad \left. + 1.23441\Theta_3\Theta_4 - 0.809377\Theta_4^2 + 1 \right), \\ m_R^2 &\equiv m_{ac}^2 = m_{3/2}^2 \left(-2.28519\Theta_1^2 - 1.00169\Theta_1\Theta_2 + 0.506454\Theta_1\Theta_3 + 1.26634\Theta_1\Theta_4 \right. \\ &\quad \left. - 0.637087\Theta_2^2 + 1.13601\Theta_2\Theta_3 + 0.140834\Theta_2\Theta_4 - 0.0262168\Theta_3^2 \right. \\ &\quad \left. - 1.1866\Theta_3\Theta_4 - 0.492648\Theta_4^2 + 1 \right). \end{aligned} \quad (4.120)$$

All soft terms are subject to the constraint (3.27).

4.16 Model 22

In Model 22 the three-point Yukawa couplings arise from the triplet intersections from the branes a , b and c on the first two-torus with 12 pairs of Higgs from the $\mathcal{N} = 2$ sector. Yukawa matrices for the Model 22 are of rank 3 and the three intersections required to form the disk diagrams for the Yukawa couplings all occur on the first torus as shown in figure 17.

The complex structure moduli U^i (3.5) are given as,

$$\{U^1, U^2, U^3\} = \left\{ i\sqrt{\frac{2}{5}}, \frac{1}{6}i\sqrt{\frac{5}{2}}, \frac{2}{7} \left(2 + i\sqrt{10} \right) \right\}, \quad (4.121)$$

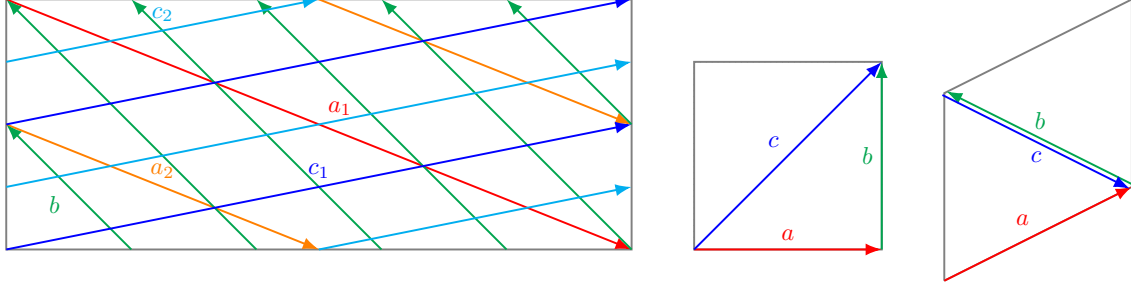


Figure 17: Brane configuration for the three two-tori in Model 22 where the third two-torus is tilted. Fermion mass hierarchies result from the intersections on the first two-torus.

22	θ^1	θ^2	θ^3
a	$-\tan^{-1}\left(\sqrt{\frac{2}{5}}\right)$	$-\tan^{-1}\left(\sqrt{\frac{5}{2}}\right)$	$\tan^{-1}\left(\frac{1}{\sqrt{10}}\right)$
b	0	$\frac{\pi}{2}$	$\tan^{-1}\left(\frac{\sqrt{\frac{5}{2}}}{6}\right)$
c	$\tan^{-1}\left(\sqrt{\frac{2}{5}}\right)$	$-\tan^{-1}\left(\sqrt{\frac{2}{5}}\right)$	$-\tan^{-1}\left(\sqrt{\frac{2}{5}}\right)$

Table 18: The angles with respect to the orientifold plane made by the cycle wrapped by stack of D6-branes on each of the three two-tori in Model 22.

and the corresponding u -moduli and s -modulus in supergravity basis from (3.6) are,

$$\{u^1, u^2, u^3\} = \left\{ \frac{\sqrt[4]{\frac{5}{2}}e^{-\phi_4}}{2\sqrt{3}\pi}, \frac{2^{3/4}\sqrt{3}e^{-\phi_4}}{5^{3/4}\pi}, \frac{\sqrt[4]{\frac{5}{2}}e^{-\phi_4}}{4\sqrt{3}\pi} \right\},$$

$$s = \frac{\sqrt[4]{\frac{5}{2}}\sqrt{3}e^{-\phi_4}}{2\pi}. \quad (4.122)$$

Using (3.11) and the values from the table 51, the gauge kinetic function becomes,

$$\{f_a, f_b, f_c\} = \left\{ \frac{7\sqrt{3}e^{-\phi_4}}{8\sqrt[4]{2}5^{3/4}\pi}, \frac{7\sqrt[4]{\frac{5}{2}}e^{-\phi_4}}{16\sqrt{3}\pi}, \frac{77e^{-\phi_4}}{16\sqrt[4]{2}\sqrt{3}5^{3/4}\pi} \right\}, \quad (4.123)$$

To calculate the gaugino masses $\{M_Y, M_b, M_a\}$ for the respective gauge groups $U(1)_Y$, $SU(2)_L$, and $SU(3)_C$, we first compute $\{M_a, M_b, M_c\}$ using (3.38) as,

$$M_a = \frac{1}{7}\sqrt{3}m_{3/2}(2\Theta_2 - 5\Theta_4),$$

$$M_b = \frac{1}{7}\sqrt{3}m_{3/2}(2\Theta_1 + 5\Theta_3),$$

$$M_c = \frac{1}{77}\sqrt{3}m_{3/2}(10\Theta_1 + 12\Theta_2 - 5(\Theta_3 + 12\Theta_4)). \quad (4.124)$$

Next, to compute the trilinear coupling and the sleptons mass-squared we require the angles, the differences of angles and their first and second order derivatives with respect

to the moduli. In table 18 we show the angles (3.16) made by the cycles wrapped by each stack of D6-branes with respect to the orientifold plane on each two-torus. The differences of the angles, $\theta_{xy}^i = \theta_y^i - \theta_x^i$ are,

$$\begin{bmatrix} \{0., 0., 0.\} & \{-0.301318, 0.570796, 0.0137074\} & \{-0.12978, 0.257665, -0.127885\} \\ \{0.301318, -0.570796, -0.0137074\} & \{0., 0., 0.\} & \{0.171538, -0.313131, -0.141593\} \\ \{0.12978, -0.257665, 0.127885\} & \{-0.171538, 0.313131, 0.141593\} & \{0., 0., 0.\} \end{bmatrix} \quad (4.125)$$

To account for the negative angle differences we employ the sign function σ_{xy}^i , which is -1 only for negative angle difference and $+1$ otherwise,

$$\sigma_{xy}^i = \begin{pmatrix} \{1, 1, 1\} & \{-1, 1, 1\} & \{-1, 1, -1\} \\ \{1, -1, -1\} & \{1, 1, 1\} & \{1, -1, -1\} \\ \{1, -1, 1\} & \{-1, 1, 1\} & \{1, 1, 1\} \end{pmatrix}, \quad (4.126)$$

and the function η_{xy} is evaluated by taking the product on the torus index i as,

$$\eta_{xy} = \begin{pmatrix} 1 & -1 & 1 \\ 1 & 1 & 1 \\ -1 & -1 & 1 \end{pmatrix}. \quad (4.127)$$

Using the values of σ_{xy}^i and η_{xy} in (3.48) we can compute the four cases of functions $\Psi(\theta_{xy})$ defined in (3.43) and (3.44). Similarly we calculate the derivative $\Psi'(\theta_{xy}^j) = \frac{d\Psi(\theta_{xy}^j)}{d\theta_{xy}^j}$ using equations (3.51), (3.3), (3.53) and the properties of digamma function $\psi^{(0)}(z)$ (3.50) while neglecting the contribution of the t -moduli.

Utilizing above results while ignoring the CP-violating phases γ_m , the gaugino masses; the trilinear coupling (3.40); and the squared-masses of squarks and sleptons (3.42) are obtained as,

$$\begin{aligned} M_{\tilde{B}} &\equiv M_Y = m_{3/2} \left(\frac{2\Theta_1 + 4\Theta_2 - \Theta_3 - 16\Theta_4}{7\sqrt{3}} \right), \\ M_{\tilde{W}} &\equiv M_b = m_{3/2} \left(\frac{1}{7} \sqrt{3} (2\Theta_1 + 5\Theta_3) \right), \\ M_{\tilde{g}} &\equiv M_a = m_{3/2} \left(\frac{1}{7} \sqrt{3} (2\Theta_2 - 5\Theta_4) \right), \\ A_0 &\equiv A_{abc} = m_{3/2} \left(-1.83963\Theta_1 - 1.52115\Theta_2 + 0.246437\Theta_3 + 1.38229\Theta_4 \right), \\ m_L^2 &\equiv m_{ab}^2 = m_{3/2}^2 \left(1.01495\Theta_1^2 - 0.356479\Theta_1\Theta_2 - 1.50575\Theta_1\Theta_3 - 0.924945\Theta_1\Theta_4 \right. \\ &\quad \left. + 0.41741\Theta_2^2 - 1.65173\Theta_2\Theta_3 - 1.24068\Theta_2\Theta_4 - 0.642555\Theta_3^2 \right. \\ &\quad \left. + 0.586882\Theta_3\Theta_4 - 0.632323\Theta_4^2 + 1 \right), \\ m_R^2 &\equiv m_{ac}^2 = m_{3/2}^2 \left(0.668817\Theta_1^2 + 0.0838741\Theta_1\Theta_2 - 2.13002\Theta_1\Theta_3 - 0.767052\Theta_1\Theta_4 \right. \\ &\quad \left. + 0.714726\Theta_2^2 - 0.702234\Theta_2\Theta_3 - 2.08352\Theta_2\Theta_4 + 0.213147\Theta_3^2 \right. \\ &\quad \left. + 1.43445\Theta_3\Theta_4 - 1.76444\Theta_4^2 + 1 \right). \end{aligned} \quad (4.128)$$

All soft terms are subject to the constraint (3.27).

4.17 Model 22-dual

In Model 22-dual the three-point Yukawa couplings arise from the triplet intersections from the branes a , b and c on the first two-torus with 12 pairs of Higgs from the $\mathcal{N} = 2$ sector. Yukawa matrices for the Model 22-dual are of rank 3 and the three intersections required to form the disk diagrams for the Yukawa couplings all occur on the first torus as shown in figure 18.

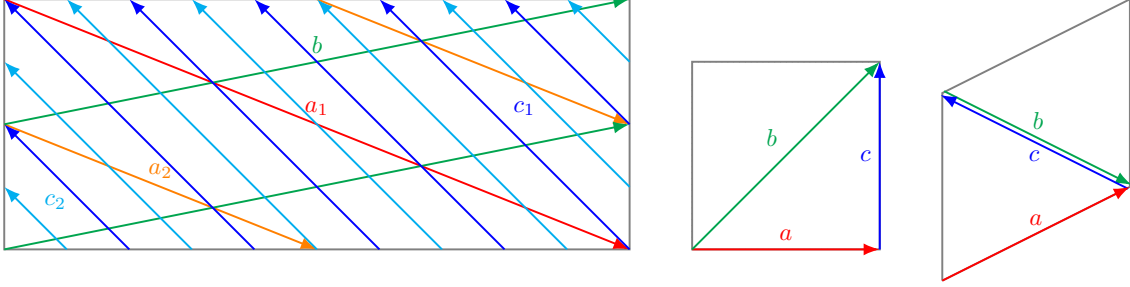


Figure 18: Brane configuration for the three two-tori in Model 22-dual where the third two-torus is tilted. Fermion mass hierarchies result from the intersections on the first two-torus.

22-dual	θ^1	θ^2	θ^3
a	$-\tan^{-1}\left(\sqrt{\frac{2}{5}}\right)$	$\tan^{-1}\left(\frac{1}{\sqrt{10}}\right)$	$-\tan^{-1}\left(\sqrt{\frac{5}{2}}\right)$
b	0	$\tan^{-1}\left(\frac{\sqrt{\frac{5}{2}}}{6}\right)$	$\frac{\pi}{2}$
c	$\tan^{-1}\left(\sqrt{\frac{2}{5}}\right)$	$-\tan^{-1}\left(\sqrt{\frac{2}{5}}\right)$	$-\tan^{-1}\left(\sqrt{\frac{2}{5}}\right)$

Table 19: The angles with respect to the orientifold plane made by the cycle wrapped by stack of D6-branes on each of the three two-tori in Model 22-dual.

The complex structure moduli U^i (3.5) are given as,

$$\{U^1, U^2, U^3\} = \left\{ i\sqrt{\frac{2}{5}}, \frac{1}{6}i\sqrt{\frac{5}{2}}, \frac{2}{7}(2 + i\sqrt{10}) \right\}, \quad (4.129)$$

and the corresponding u -moduli and s -modulus in supergravity basis from (3.6) are,

$$\begin{aligned} \{u^1, u^2, u^3\} &= \left\{ \frac{\sqrt[4]{\frac{5}{2}}e^{-\phi_4}}{2\sqrt{3}\pi}, \frac{2^{3/4}\sqrt{3}e^{-\phi_4}}{5^{3/4}\pi}, \frac{\sqrt[4]{\frac{5}{2}}e^{-\phi_4}}{4\sqrt{3}\pi} \right\}, \\ s &= \frac{\sqrt[4]{\frac{5}{2}}\sqrt{3}e^{-\phi_4}}{2\pi}. \end{aligned} \quad (4.130)$$

Using (3.11) and the values from the table 52, the gauge kinetic function becomes,

$$\{f_a, f_b, f_c\} = \left\{ \frac{7\sqrt{3}e^{-\phi_4}}{8\sqrt[4]{25^3/4}\pi}, \frac{77e^{-\phi_4}}{16\sqrt[4]{2}\sqrt{35^3/4}\pi}, \frac{7\sqrt[4]{\frac{5}{2}}e^{-\phi_4}}{16\sqrt{3}\pi} \right\}, \quad (4.131)$$

To calculate the gaugino masses $\{M_Y, M_b, M_a\}$ for the respective gauge groups $U(1)_Y$, $SU(2)_L$, and $SU(3)_C$, we first compute $\{M_a, M_b, M_c\}$ using (3.38) as,

$$\begin{aligned} M_a &= \frac{1}{7}\sqrt{3}m_{3/2}(2\Theta_2 - 5\Theta_4), \\ M_b &= \frac{1}{77}\sqrt{3}m_{3/2}(10\Theta_1 + 12\Theta_2 - 5(\Theta_3 + 12\Theta_4)), \\ M_c &= \frac{1}{7}\sqrt{3}m_{3/2}(2\Theta_1 + 5\Theta_3). \end{aligned} \quad (4.132)$$

Next, to compute the trilinear coupling and the sleptons mass-squared we require the angles, the differences of angles and their first and second order derivatives with respect to the moduli. In table 19 we show the angles (3.16) made by the cycles wrapped by each stack of D6-branes with respect to the orientifold plane on each two-torus. The differences of the angles, $\theta_{xy}^i = \theta_y^i - \theta_x^i$ are,

$$\left[\begin{array}{ccc} \{0., 0., 0.\} & \{-0.12978, 0.257665, -0.127885\} & \{-0.301318, 0.570796, 0.0137074\} \\ \{0.12978, -0.257665, 0.127885\} & \{0., 0., 0.\} & \{-0.171538, 0.313131, 0.141593\} \\ \{0.301318, -0.570796, -0.0137074\} & \{0.171538, -0.313131, -0.141593\} & \{0., 0., 0.\} \end{array} \right] \quad (4.133)$$

To account for the negative angle differences we employ the sign function σ_{xy}^i , which is -1 only for negative angle difference and $+1$ otherwise,

$$\sigma_{xy}^i = \begin{pmatrix} \{1, 1, 1\} & \{-1, 1, -1\} & \{-1, 1, 1\} \\ \{1, -1, 1\} & \{1, 1, 1\} & \{-1, 1, 1\} \\ \{1, -1, -1\} & \{1, -1, -1\} & \{1, 1, 1\} \end{pmatrix}, \quad (4.134)$$

and the function η_{xy} is evaluated by taking the product on the torus index i as,

$$\eta_{xy} = \begin{pmatrix} 1 & 1 & -1 \\ -1 & 1 & -1 \\ 1 & 1 & 1 \end{pmatrix}. \quad (4.135)$$

Using the values of σ_{xy}^i and η_{xy} in (3.48) we can compute the four cases of functions $\Psi(\theta_{xy})$ defined in (3.43) and (3.44). Similarly we calculate the derivative $\Psi'(\theta_{xy}^j) = \frac{d\Psi(\theta_{xy}^j)}{d\theta_{xy}^j}$ using equations (3.51), (3.3), (3.53) and the properties of digamma function $\psi^{(0)}(z)$ (3.50) while neglecting the contribution of the t -moduli.

Utilizing above results while ignoring the CP-violating phases γ_m , the gaugino masses; the trilinear coupling (3.40); and the squared-masses of squarks and sleptons (3.42) are

obtained as,

$$\begin{aligned}
M_{\tilde{B}} &\equiv M_Y = m_{3/2} \left(\frac{10\Theta_1 + 8\Theta_2 + 25\Theta_3 - 20\Theta_4}{21\sqrt{3}} \right), \\
M_{\tilde{W}} &\equiv M_b = m_{3/2} \left(\frac{1}{77} \sqrt{3} (10\Theta_1 + 12\Theta_2 - 5(\Theta_3 + 12\Theta_4)) \right), \\
M_{\tilde{g}} &\equiv M_a = m_{3/2} \left(\frac{1}{7} \sqrt{3} (2\Theta_2 - 5\Theta_4) \right), \\
A_0 &\equiv A_{abc} = m_{3/2} \left(-1.83963\Theta_1 - 1.52115\Theta_2 + 0.246437\Theta_3 + 1.38229\Theta_4 \right), \\
m_L^2 &\equiv m_{ab}^2 = m_{3/2}^2 \left(0.668817\Theta_1^2 + 0.0838741\Theta_1\Theta_2 - 2.13002\Theta_1\Theta_3 - 0.767052\Theta_1\Theta_4 \right. \\
&\quad \left. + 0.714726\Theta_2^2 - 0.702234\Theta_2\Theta_3 - 2.08352\Theta_2\Theta_4 + 0.213147\Theta_3^2 \right. \\
&\quad \left. + 1.43445\Theta_3\Theta_4 - 1.76444\Theta_4^2 + 1 \right), \\
m_R^2 &\equiv m_{ac}^2 = m_{3/2}^2 \left(1.01495\Theta_1^2 - 0.356479\Theta_1\Theta_2 - 1.50575\Theta_1\Theta_3 - 0.924945\Theta_1\Theta_4 \right. \\
&\quad \left. + 0.41741\Theta_2^2 - 1.65173\Theta_2\Theta_3 - 1.24068\Theta_2\Theta_4 - 0.642555\Theta_3^2 \right. \\
&\quad \left. + 0.586882\Theta_3\Theta_4 - 0.632323\Theta_4^2 + 1 \right). \tag{4.136}
\end{aligned}$$

All soft terms are subject to the constraint (3.27).

5 Discussion and conclusion

We have studied the supersymmetry breaking soft terms for all the viable models in the complete landscape of three-family supersymmetric Pati-Salam models arising from intersecting D6-branes on a $\mathbb{T}^6/(\mathbb{Z}_2 \times \mathbb{Z}_2)$ orientifold in type IIA string theory, comprising 33 independent models with distinct string-scale gauge coupling relations. It is found that only 17 models contain viable Yukawa textures. We have focused on the u -moduli dominated case together with the s -moduli turned on, where the soft terms remain independent of the Yukawa couplings and the Wilson lines. The results for the trilinear coupling, gaugino-masses, squared-mass parameters of squarks, sleptons and Higgs depend on the brane wrapping numbers as well as supersymmetry breaking parameters which include the gravitino-mass parameter $m_{3/2}$ and the goldstino angles Θ_m , $m = 1, 2, 3, 4$.

In particular for the case of dual models under the exchange of two $SU(2)$ sectors, the Yukawa couplings remain unchanged as discussed in [15], however, the corresponding soft term parameters only match for the trilinear coupling and the mass of the gluino. This can be explained by the internal geometry of the compact space where the Yukawa interactions depend only on the triangular area of the worldsheet instantons while the soft term parameters have an additional dependence on the orientation-angles of D6-branes in the three two-tori. Thus, the dual models besides having different gauge coupling relations also possess distinct masses of gauginos and squared-masses of squarks and sleptons. While it was already clear from the analysis of the Yukawa coupling [15] that the best performing models in the entire landscape are the models 22 and 22-dual, the different result for susy breaking soft terms combined with experimental data for superpartners can in principle distinguish between the two models.

Our analysis reveals that the susy breaking soft terms are in general highly model dependent as evident from the results of section 4. Nonetheless, we have found a special limit under which the Higgs and the gaugino-masses in all of the models become degenerate. This limit corresponds to setting three goldstino angles to be equal to $1/2$ and taking dilaton angle to be $-1/2$, i.e. $\Theta_1 = \Theta_2 = \Theta_3 = -\Theta_s = 1/2$, provided that all CP-violating phases γ_i are set to zero. Note that the special limit satisfies the crucial constraint (3.27) on the values of Θ_i . This results in the following universal masses for the gauginos (viz. bino, wino and gluino) and the Higgs,

$$\begin{aligned} m_{1/2} \equiv M_{\tilde{B}} = M_{\tilde{W}} = M_{\tilde{g}} &= \frac{\sqrt{3}}{2} m_{3/2}, \\ m_H &= \frac{m_{3/2}}{2} = \frac{m_{1/2}}{\sqrt{3}}. \end{aligned} \tag{5.1}$$

Unlike the gaugino masses, the trilinear coupling A_0 and the scalar squared-mass parameters of squarks and the sleptons, m_L^2 and m_R^2 , do not exhibit such universality and in general depend on the specific model parameters.

Given that the precise scale of supersymmetry remains uncertain, we defer further empirical investigations into supersymmetric partner spectra and the resultant neutralino relic density to future studies. It is noteworthy that string theory offers insights into the intricate phenomenology of superpartners through the wrapping numbers and the angles of intersecting D6-branes in the internal compact dimensions. However, additional experimental input is essential to fully leverage this mathematical framework.

Acknowledgments

TL is supported in part by the National Key Research and Development Program of China Grant No. 2020YFC2201504, by the Projects No. 11875062, No. 11947302, No. 12047503, and No. 12275333 supported by the National Natural Science Foundation of China, by the Key Research Program of the Chinese Academy of Sciences, Grant No. XDPB15, by the Scientific Instrument Developing Project of the Chinese Academy of Sciences, Grant No. YJKYYQ20190049, and by the International Partnership Program of Chinese Academy of Sciences for Grand Challenges, Grant No. 112311KYSB20210012. Z.-W. Wang is supported in part by the hundred talented program at University of Electronic Science and Technology of China. AM is supported by the Guangdong Basic and Applied Basic Research Foundation (Grant No. 2021B1515130007), Shenzhen Natural Science Fund (the Stable Support Plan Program 20220810130956001).

A Independent supersymmetric Pati-Salam models

We tabulate the 33 independent models with distinct allowed gauge coupling relations in the three-family $\mathcal{N} = 1$ supersymmetric Pati-Salam landscape arising from intersecting D6-branes on a type IIA $\mathbb{T}^6/(\mathbb{Z}_2 \times \mathbb{Z}_2)$ orientifold [14, 15].

Model 1		$U(4)_C \times U(2)_L \times U(2)_R \times USp(4)_2 \times USp(4)_4$								
stack	N	$(n^1, l^1) \times (n^2, l^2) \times (n^3, l^3)$	$n_{\square\square}$	n_{\square}	b	b'	c	c'	2	4
a	8	$(1, -1) \times (1, 0) \times (1, 1)$	0	0	3	0	-3	0	-1	1
b	4	$(0, 1) \times (-1, 3) \times (-1, 1)$	2	-2	-	-	0	-4	1	0
c	4	$(-2, -1) \times (-1, -1) \times (1, -1)$	2	6	-	-	-	-	1	-2
2	4	$(1, 0) \times (0, -1) \times (0, 2)$	$x_A = \frac{1}{3}x_B = x_C = \frac{1}{3}x_D$ $\beta_2^g = -2, \beta_4^g = -2,$ $\chi_1 = 1, \chi_2 = \frac{1}{3}, \chi_3 = 2$							
4	4	$(0, -1) \times (0, 1) \times (2, 0)$								

Table 20: D6-brane configurations and intersection numbers of Model 1, and its MSSM gauge coupling relation is $g_a^2 = g_b^2 = \frac{5}{3}g_c^2 = \frac{25}{19}\frac{5g_Y^2}{3} = 4\sqrt{\frac{2}{3}}\pi e^{\phi_4}$.

Model 1-dual		$U(4)_C \times U(2)_L \times U(2)_R \times USp(4)_2 \times USp(4)_4$								
stack	N	$(n^1, l^1) \times (n^2, l^2) \times (n^3, l^3)$	$n_{\square\square}$	n_{\square}	b	b'	c	c'	2	4
a	8	$(1, -1) \times (1, 0) \times (1, 1)$	0	0	-3	0	3	0	-1	1
b	4	$(-2, -1) \times (-1, -1) \times (1, -1)$	2	6	-	-	0	-4	1	-2
c	4	$(0, 1) \times (-1, 3) \times (-1, 1)$	2	-2	-	-	-	-	1	0
2	4	$(1, 0) \times (0, -1) \times (0, 2)$	$x_A = \frac{1}{3}x_B = x_C = \frac{1}{3}x_D$ $\beta_2^g = -2, \beta_4^g = -2,$ $\chi_1 = 1, \chi_2 = \frac{1}{3}, \chi_3 = 2$							
4	4	$(0, -1) \times (0, 1) \times (2, 0)$								

Table 21: D6-brane configurations and intersection numbers of Model 1-dual, and its MSSM gauge coupling relation is $g_a^2 = \frac{5}{3}g_b^2 = g_c^2 = \frac{5g_Y^2}{3} = 4\sqrt{\frac{2}{3}}\pi e^{\phi_4}$.

Model 2		$U(4)_C \times U(2)_L \times U(2)_R \times USp(2)_1 \times USp(2)_2 \times USp(2)_3 \times USp(2)_4$										
stack	N	$(n^1, l^1) \times (n^2, l^2) \times (n^3, l^3)$	$n_{\square\square}$	n_{\square}	b	b'	c	c'	1	2	3	4
a	8	$(1, -1) \times (1, 0) \times (1, 1)$	0	0	-2	-1	3	0	0	-1	0	1
b	4	$(-1, 0) \times (-1, -1) \times (1, -3)$	2	-2	-	-	-4	-4	0	0	1	-3
c	4	$(0, 1) \times (-1, 3) \times (-1, 1)$	2	-2	-	-	-	-	-3	1	0	0
1	2	$(1, 0) \times (1, 0) \times (2, 0)$	$x_A = \frac{1}{3}x_B = \frac{1}{3}x_C = \frac{1}{3}x_D$ $\beta_1^g = -3, \beta_2^g = -3, \beta_3^g = -5, \beta_4^g = -1,$ $\chi_1 = \frac{1}{3}, \chi_2 = 1, \chi_3 = \frac{2}{3}$									
2	2	$(1, 0) \times (0, -1) \times (0, 2)$										
3	2	$(0, -1) \times (1, 0) \times (0, 2)$										
4	2	$(0, -1) \times (0, 1) \times (2, 0)$										

Table 22: D6-brane configurations and intersection numbers of Model 2, and its MSSM gauge coupling relation is $g_a^2 = \frac{9}{5}g_b^2 = g_c^2 = \frac{5g_Y^2}{3} = \frac{12}{5}\sqrt{2}\pi e^{\phi_4}$.

Model 3		$U(4)_C \times U(2)_L \times U(2)_R \times USp(4)_4$							
stack	N	$(n^1, l^1) \times (n^2, l^2) \times (n^3, l^3)$	$n_{\square\square}$	n_{\square}	b	b'	c	c'	4
a	8	$(-2, 1) \times (-1, 0) \times (1, 1)$	-1	1	-3	0	3	0	2
b	4	$(1, 0) \times (1, 3) \times (1, -1)$	-2	2	-	-	0	4	-1
c	4	$(-1, 2) \times (-1, 1) \times (-1, 1)$	2	6	-	-	-	-	1
4	4	$(0, -1) \times (0, 1) \times (2, 0)$	$x_A = \frac{4}{3}x_B = 8x_C = \frac{8}{3}x_D$ $\beta_4^g = 0,$ $\chi_1 = 4, \chi_2 = \frac{2}{3}, \chi_3 = 4$						

Table 23: D6-brane configurations and intersection numbers of Model 3, and its MSSM gauge coupling relation is $g_a^2 = \frac{1}{2}g_b^2 = \frac{13}{6}g_c^2 = \frac{65}{44}\frac{5g_Y^2}{3} = \frac{16}{5}\sqrt{\frac{2}{3}}\pi e^{\phi_4}$.

Model 3-dual		$U(4)_C \times U(2)_L \times U(2)_R \times USp(4)_4$							
stack	N	$(n^1, l^1) \times (n^2, l^2) \times (n^3, l^3)$	$n_{\square\square}$	n_{\square}	b	b'	c	c'	4
a	8	$(-2, 1) \times (-1, 0) \times (1, 1)$	-1	1	3	0	-3	0	2
b	4	$(-1, 2) \times (-1, 1) \times (-1, 1)$	2	6	-	-	0	4	1
c	4	$(1, 0) \times (1, 3) \times (1, -1)$	-2	2	-	-	-	-	-1
4	4	$(0, -1) \times (0, 1) \times (2, 0)$	$x_A = \frac{4}{3}x_B = 8x_C = \frac{8}{3}x_D$ $\beta_4^g = 0,$ $\chi_1 = 4, \chi_2 = \frac{2}{3}, \chi_3 = 4$						

Table 24: D6-brane configurations and intersection numbers of Model 3-dual, and its MSSM gauge coupling relation is $g_a^2 = \frac{13}{6}g_b^2 = \frac{1}{2}g_c^2 = \frac{5}{8}\frac{5g_Y^2}{3} = \frac{16}{5}\sqrt{\frac{2}{3}}\pi e^{\phi_4}$.

Model 4		$U(4)_C \times U(2)_L \times U(2)_R \times USp(4)_4$							
stack	N	$(n^1, l^1) \times (n^2, l^2) \times (n^3, l^3)$	$n_{\square\square}$	n_{\square}	b	b'	c	c'	4
a	8	$(2, -1) \times (1, 0) \times (1, 1)$	-1	1	-2	-1	3	0	2
b	4	$(1, 0) \times (1, 1) \times (1, -3)$	2	-2	-	-	-4	0	-3
c	4	$(-1, 2) \times (-1, 1) \times (-1, 1)$	2	6	-	-	-	-	1
4	4	$(0, -1) \times (0, 1) \times (2, 0)$	$x_A = 2x_B = \frac{4}{3}x_C = 4x_D$ $\beta_4^g = 2,$ $\chi_1 = 2\sqrt{\frac{2}{3}}, \chi_2 = \sqrt{6}, \chi_3 = 2\sqrt{\frac{2}{3}}$						

Table 25: D6-brane configurations and intersection numbers of Model 4, and its MSSM gauge coupling relation is $g_a^2 = \frac{21}{10}g_b^2 = \frac{7}{2}g_c^2 = \frac{7}{4}\frac{5g_Y^2}{3} = \frac{8}{5}6^{3/4}\pi e^{\phi_4}$.

Model 5		$U(4)_C \times U(2)_L \times U(2)_R \times USp(2)_1 \times USp(2)_2 \times USp(2)_4$									
stack	N	$(n^1, l^1) \times (n^2, l^2) \times (n^3, l^3)$	$n_{\square\square}$	n_{\square}	b	b'	c	c'	1	2	4
a	8	$(1, -1) \times (1, 0) \times (1, 1)$	0	0	-2	-1	3	0	0	-1	1
b	4	$(-1, 0) \times (-1, -1) \times (1, -3)$	2	-2	-	-	-5	-2	0	0	-3
c	4	$(0, 1) \times (-2, 3) \times (-1, 1)$	1	-1	-	-	-	-	-3	2	0
1	2	$(1, 0) \times (1, 0) \times (2, 0)$	$x_A = \frac{2}{3}x_B = \frac{2}{9}x_C = \frac{2}{3}x_D$ $\beta_1^g = -3, \beta_2^g = -2, \beta_4^g = -1,$ $\chi_1 = \frac{\sqrt{2}}{3}, \chi_2 = \sqrt{2}, \chi_3 = \frac{2\sqrt{2}}{3}$								
2	2	$(1, 0) \times (0, -1) \times (0, 2)$									
4	2	$(0, -1) \times (0, 1) \times (2, 0)$									

Table 26: D6-brane configurations and intersection numbers of Model 5, and its MSSM gauge coupling relation is $g_a^2 = \frac{27}{11}g_b^2 = 2g_c^2 = \frac{10}{7}\frac{5g_Y^2}{3} = \frac{48}{11}\sqrt{2}\pi e^{\phi_4}$.

Model 6		$U(4)_C \times U(2)_L \times U(2)_R \times USp(2)_2 \times USp(2)_3 \times USp(2)_4$									
stack	N	$(n^1, l^1) \times (n^2, l^2) \times (n^3, l^3)$	$n_{\square\square}$	n_{\square}	b	b'	c	c'	2	3	4
a	8	$(1, -1) \times (1, 0) \times (1, 1)$	0	0	-2	-1	3	0	-1	0	1
b	4	$(-1, 0) \times (-2, -1) \times (1, -3)$	5	-5	-	-	-7	-10	0	1	-6
c	4	$(0, 1) \times (-1, 3) \times (-1, 1)$	2	-2	-	-	-	-	1	0	0
2	2	$(1, 0) \times (0, -1) \times (0, 2)$	$x_A = \frac{1}{3}x_B = \frac{1}{18}x_C = \frac{1}{3}x_D$ $\beta_2^g = -3, \beta_3^g = -5, \beta_4^g = 2,$ $\chi_1 = \frac{1}{3\sqrt{2}}, \chi_2 = \sqrt{2}, \chi_3 = \frac{\sqrt{2}}{3}$								
3	2	$(0, -1) \times (1, 0) \times (0, 2)$									
4	2	$(0, -1) \times (0, 1) \times (2, 0)$									

Table 27: D6-brane configurations and intersection numbers of Model 6, and its MSSM gauge coupling relation is $g_a^2 = \frac{54}{19}g_b^2 = g_c^2 = \frac{5g_Y^2}{3} = \frac{48}{19}\sqrt{2}\pi e^{\phi_4}$.

Model 7		$U(4)_C \times U(2)_L \times U(2)_R \times USp(2)_2 \times USp(2)_4$								
stack	N	$(n^1, l^1) \times (n^2, l^2) \times (n^3, l^3)$	$n_{\square\square}$	n_{\square}	b	b'	c	c'	2	4
a	8	$(1, -1) \times (1, 0) \times (1, 1)$	0	0	-2	-1	3	0	-1	1
b	4	$(-1, 0) \times (-2, -1) \times (1, -3)$	5	-5	-	-	-8	-8	0	-6
c	4	$(0, 1) \times (-2, 3) \times (-1, 1)$	1	-1	-	-	-	-	2	0
2	2	$(1, 0) \times (0, -1) \times (0, 2)$	$x_A = \frac{2}{3}x_B = \frac{1}{9}x_C = \frac{2}{3}x_D$ $\beta_2^g = -2, \beta_4^g = 2,$ $\chi_1 = \frac{1}{3}, \chi_2 = 2, \chi_3 = \frac{2}{3}$							
4	2	$(0, -1) \times (0, 1) \times (2, 0)$								

Table 28: D6-brane configurations and intersection numbers of Model 7, and its MSSM gauge coupling relation is $g_a^2 = \frac{18}{5}g_b^2 = 2g_c^2 = \frac{10}{7}\frac{5g_Y^2}{3} = \frac{24\pi e^{\phi_4}}{5}$.

Model 8		$U(4)_C \times U(2)_L \times U(2)_R \times USp(2)_1 \times USp(4)_3$								
stack	N	$(n^1, l^1) \times (n^2, l^2) \times (n^3, l^3)$	$n_{\square\square}$	n_{\square}	b	b'	c	c'	1	3
a	8	$(1, -1) \times (-1, 0) \times (-1, -1)$	0	0	-2	-1	3	0	0	0
b	4	$(1, 0) \times (1, 1) \times (1, -3)$	2	-2	-	-	-4	-8	0	1
c	4	$(-1, 4) \times (0, 1) \times (-1, 1)$	3	-3	-	-	-	-	-4	1
1	2	$(1, 0) \times (1, 0) \times (2, 0)$	$x_A = \frac{3}{4}x_B = \frac{1}{4}x_C = \frac{3}{4}x_D$ $\beta_1^g = -2, \beta_3^g = -4,$ $\chi_1 = \frac{1}{2}, \chi_2 = \frac{3}{2}, \chi_3 = 1$							
3	4	$(0, -1) \times (1, 0) \times (0, 2)$								

Table 29: D6-brane configurations and intersection numbers of Model 8, and its MSSM gauge coupling relation is $g_a^2 = \frac{13}{5}g_b^2 = 3g_c^2 = \frac{5}{3}\frac{5g_Y^2}{3} = \frac{16}{5}\sqrt{3}\pi e^{\phi_4}$.

Model 9		$U(4)_C \times U(2)_L \times U(2)_R \times USp(2)_1 \times USp(4)_3$								
stack	N	$(n^1, l^1) \times (n^2, l^2) \times (n^3, l^3)$	$n_{\square\square}$	n_{\square}	b	b'	c	c'	1	3
a	8	$(-1, 1) \times (-1, 0) \times (1, 1)$	0	0	3	0	-3	0	0	0
b	4	$(-1, 4) \times (0, 1) \times (-1, 1)$	3	-3	-	-	0	-4	-4	1
c	4	$(1, 0) \times (1, 3) \times (1, -1)$	-2	2	-	-	-	-	0	3
1	2	$(1, 0) \times (1, 0) \times (2, 0)$	$x_A = \frac{1}{12}x_B = \frac{1}{4}x_C = \frac{1}{12}x_D$ $\beta_1^g = -2, \beta_3^g = -2,$ $\chi_1 = \frac{1}{2}, \chi_2 = \frac{1}{6}, \chi_3 = 1$							
3	4	$(0, -1) \times (1, 0) \times (0, 2)$								

Table 30: D6-brane configurations and intersection numbers of Model 9, and its MSSM gauge coupling relation is $g_a^2 = \frac{1}{3}g_b^2 = g_c^2 = \frac{5g_Y^2}{3} = \frac{16\pi e^{\phi_4}}{5\sqrt{3}}$.

Model 9-dual		$U(4)_C \times U(2)_L \times U(2)_R \times USp(2)_1 \times USp(4)_3$								
stack	N	$(n^1, l^1) \times (n^2, l^2) \times (n^3, l^3)$	$n_{\square\square}$	n_{\square}	b	b'	c	c'	1	3
a	8	$(-1, 1) \times (-1, 0) \times (1, 1)$	0	0	-3	0	3	0	0	0
b	4	$(1, 0) \times (1, 3) \times (1, -1)$	-2	2	-	-	0	-4	0	3
c	4	$(-1, 4) \times (0, 1) \times (-1, 1)$	3	-3	-	-	-	-	-4	1
1	2	$(1, 0) \times (1, 0) \times (2, 0)$	$x_A = \frac{1}{12}x_B = \frac{1}{4}x_C = \frac{1}{12}x_D$ $\beta_1^g = -2, \beta_3^g = -2,$ $\chi_1 = \frac{1}{2}, \chi_2 = \frac{1}{6}, \chi_3 = 1$							
3	4	$(0, -1) \times (1, 0) \times (0, 2)$								

Table 31: D6-brane configurations and intersection numbers of Model 9-dual, and its MSSM gauge coupling relation is $g_a^2 = g_b^2 = \frac{1}{3}g_c^2 = \frac{5}{11}\frac{5g_Y^2}{3} = \frac{16\pi e^{\phi_4}}{5\sqrt{3}}$.

Model 10		$U(4)_C \times U(2)_L \times U(2)_R \times USp(4)_3$							
stack	N	$(n^1, l^1) \times (n^2, l^2) \times (n^3, l^3)$	$n_{\square\square}$	n_{\square}	b	b'	c	c'	3
a	8	$(1, -1) \times (-1, 0) \times (-1, -1)$	0	0	-2	-1	3	0	0
b	4	$(1, 0) \times (2, 1) \times (1, -3)$	5	-5	-	-	-8	-16	1
c	4	$(-1, 4) \times (0, 1) \times (-1, 1)$	3	-3	-	-	-	-	1
3	4	$(0, -1) \times (1, 0) \times (0, 2)$	$x_A = \frac{3}{2}x_B = \frac{1}{4}x_C = \frac{3}{2}x_D$ $\beta_3^g = -4,$ $\chi_1 = \frac{1}{2}, \chi_2 = 3, \chi_3 = 1$						

Table 32: D6-brane configurations and intersection numbers of Model 10, and its MSSM gauge coupling relation is $g_a^2 = \frac{26}{5}g_b^2 = 6g_c^2 = 2\frac{5g_Y^2}{3} = \frac{16}{5}\sqrt{6}\pi e^{\phi_4}$.

Model 11		$U(4)_C \times U(2)_L \times U(2)_R \times USp(4)_3$							
stack	N	$(n^1, l^1) \times (n^2, l^2) \times (n^3, l^3)$	$n_{\square\square}$	n_{\square}	b	b'	c	c'	3
a	8	$(1, -1) \times (-1, 0) \times (-1, -1)$	0	0	3	0	-3	0	0
b	4	$(-1, 4) \times (0, 1) \times (-1, 1)$	3	-3	-	-	0	-8	1
c	4	$(1, 0) \times (2, 3) \times (1, -1)$	-1	1	-	-	-	-	3
3	4	$(0, -1) \times (1, 0) \times (0, 2)$	$x_A = \frac{1}{6}x_B = \frac{1}{4}x_C = \frac{1}{6}x_D$ $\beta_3^g = -2,$ $\chi_1 = \frac{1}{2}, \chi_2 = \frac{1}{3}, \chi_3 = 1$						

Table 33: D6-brane configurations and intersection numbers of Model 11, and its MSSM gauge coupling relation is $g_a^2 = \frac{2}{3}g_b^2 = 2g_c^2 = \frac{10}{7}\frac{5g_Y^2}{3} = \frac{16}{5}\sqrt{\frac{2}{3}}\pi e^{\phi_4}$.

Model 11-dual		$U(4)_C \times U(2)_L \times U(2)_R \times USp(4)_3$							
stack	N	$(n^1, l^1) \times (n^2, l^2) \times (n^3, l^3)$	$n_{\square\square}$	n_{\square}	b	b'	c	c'	3
a	8	$(1, -1) \times (-1, 0) \times (-1, -1)$	0	0	-3	0	3	0	0
b	4	$(1, 0) \times (2, 3) \times (1, -1)$	-1	1	-	-	0	-8	3
c	4	$(-1, 4) \times (0, 1) \times (-1, 1)$	3	-3	-	-	-	-	1
3	4	$(0, -1) \times (1, 0) \times (0, 2)$	$x_A = \frac{1}{6}x_B = \frac{1}{4}x_C = \frac{1}{6}x_D$ $\beta_3^g = -2,$ $\chi_1 = \frac{1}{2}, \chi_2 = \frac{1}{3}, \chi_3 = 1$						

Table 34: D6-brane configurations and intersection numbers of Model 11-dual, and its MSSM gauge coupling relation is $g_a^2 = 2g_b^2 = \frac{2}{3}g_c^2 = \frac{10}{13}\frac{5g_Y^2}{3} = \frac{16}{5}\sqrt{\frac{2}{3}}\pi e^{\phi_4}$.

Model 12		$U(4)_C \times U(2)_L \times U(2)_R \times USp(2)_3$							
stack	N	$(n^1, l^1) \times (n^2, l^2) \times (n^3, l^3)$	$n_{\square\square}$	n_{\square}	b	b'	c	c'	3
a	8	$(1, 1) \times (1, 0) \times (1, -1)$	0	0	3	-6	3	0	0
b	4	$(-2, -1) \times (0, -1) \times (-5, -1)$	9	-9	-	-	-8	0	-10
c	4	$(-2, 1) \times (-1, 1) \times (1, 1)$	-2	-6	-	-	-	-	-2
3	2	$(0, -1) \times (1, 0) \times (0, 2)$	$x_A = \frac{5}{6}x_B = 10x_C = \frac{5}{6}x_D$ $\beta_3^g = 6,$ $\chi_1 = \sqrt{10}, \chi_2 = \frac{\sqrt{\frac{5}{2}}}{6}, \chi_3 = 2\sqrt{10}$						

Table 35: D6-brane configurations and intersection numbers of Model 12, and its MSSM gauge coupling relation is $g_a^2 = \frac{35}{66}g_b^2 = \frac{7}{6}g_c^2 = \frac{35}{32}\frac{5g_Y^2}{3} = \frac{8\sqrt[4]{25^{3/4}}\pi e^{\phi_4}}{11\sqrt{3}}$.

Model 13		$U(4)_C \times U(2)_L \times U(2)_R \times USp(2)_1 \times USp(2)_4$								
stack	N	$(n^1, l^1) \times (n^2, l^2) \times (n^3, l^3)$	$n_{\square\square}$	n_{\square}	b	b'	c	c'	1	4
a	8	$(-1, -1) \times (1, 1) \times (1, 1)$	0	-4	6	-3	-3	0	1	-1
b	4	$(-1, 2) \times (-1, 0) \times (5, 1)$	9	-9	-	-	-9	-10	0	1
c	4	$(-2, 1) \times (0, -1) \times (1, -1)$	-1	1	-	-	-	-	-1	0
1	2	$(1, 0) \times (1, 0) \times (2, 0)$	$x_A = 22x_B = 2x_C = \frac{11}{5}x_D$ $\beta_1^g = -3, \beta_4^g = -3,$ $\chi_1 = \frac{1}{\sqrt{5}}, \chi_2 = \frac{11}{\sqrt{5}}, \chi_3 = 4\sqrt{5}$							
4	2	$(0, -1) \times (0, 1) \times (2, 0)$								

Table 36: D6-brane configurations and intersection numbers of Model 13, and its MSSM gauge coupling relation is $g_a^2 = \frac{5}{14}g_b^2 = \frac{11}{6}g_c^2 = \frac{11}{8}\frac{5g_Y^2}{3} = \frac{8}{63}5^{3/4}\sqrt{11}\pi e^{\phi_4}$.

Model 14		$U(4)_C \times U(2)_L \times U(2)_R \times USp(2)_1 \times USp(2)_2 \times USp(2)_3 \times USp(2)_4$										
stack	N	$(n^1, l^1) \times (n^2, l^2) \times (n^3, l^3)$	$n_{\square\square}$	n_{\square}	b	b'	c	c'	1	2	3	4
a	8	$(1, -1) \times (1, 0) \times (1, 1)$	0	0	-3	0	3	0	0	-1	0	1
b	4	$(-1, 0) \times (-1, -3) \times (1, -1)$	-2	2	-	-	0	0	0	0	3	-1
c	4	$(0, 1) \times (-1, 3) \times (-1, 1)$	2	-2	-	-	-	-	-3	1	0	0
1	2	$(1, 0) \times (1, 0) \times (2, 0)$	$x_A = \frac{1}{3}x_B = x_C = \frac{1}{3}x_D$ $\beta_1^g = -3, \beta_2^g = -3, \beta_3^g = -3, \beta_4^g = -3,$ $\chi_1 = 1, \chi_2 = \frac{1}{3}, \chi_3 = 2$									
2	2	$(1, 0) \times (0, -1) \times (0, 2)$										
3	2	$(0, -1) \times (1, 0) \times (0, 2)$										
4	2	$(0, -1) \times (0, 1) \times (2, 0)$										

Table 37: D6-brane configurations and intersection numbers of Model 14, and its MSSM gauge coupling relation is $g_a^2 = g_b^2 = g_c^2 = \frac{5g_Y^2}{3} = 4\sqrt{\frac{2}{3}}\pi e^{\phi_4}$.

Model 15		$U(4)_C \times U(2)_L \times U(2)_R \times USp(4)_1 \times USp(2)_3 \times USp(2)_4$									
stack	N	$(n^1, l^1) \times (n^2, l^2) \times (n^3, l^3)$	$n_{\square\square}$	n_{\square}	b	b'	c	c'	1	3	4
a	8	$(-1, 1) \times (1, -1) \times (1, -1)$	0	4	-3	0	3	0	-1	1	1
b	4	$(-4, 1) \times (-1, 0) \times (1, 1)$	-3	3	-	-	0	2	0	0	4
c	4	$(-2, -1) \times (0, 1) \times (1, 1)$	1	-1	-	-	-	-	1	-2	0
1	4	$(1, 0) \times (1, 0) \times (2, 0)$	$x_A = \frac{5}{2}x_B = 2x_C = 10x_D$ $\beta_1^g = -3, \beta_3^g = -2, \beta_4^g = 0,$ $\chi_1 = 2\sqrt{2}, \chi_2 = \frac{5}{\sqrt{2}}, \chi_3 = \sqrt{2}$								
3	2	$(0, -1) \times (1, 0) \times (0, 2)$									
4	2	$(0, -1) \times (0, 1) \times (2, 0)$									

Table 38: D6-brane configurations and intersection numbers of Model 15, and its MSSM gauge coupling relation is $g_a^2 = \frac{4}{9}g_b^2 = \frac{10}{9}g_c^2 = \frac{50}{47}\frac{5g_Y^2}{3} = \frac{16}{27}2^{3/4}\sqrt{5}\pi e^{\phi_4}$.

Model 15-dual		$U(4)_C \times U(2)_L \times U(2)_R \times USp(4)_1 \times USp(2)_2 \times USp(2)_4$									
stack	N	$(n^1, l^1) \times (n^2, l^2) \times (n^3, l^3)$	$n_{\square\square}$	n_{\square}	b	b'	c	c'	1	2	4
a	8	$(1, 1) \times (-1, -1) \times (1, 1)$	0	-4	-3	0	3	0	1	-1	-1
b	4	$(0, 1) \times (-2, 1) \times (-1, 1)$	-1	1	-	-	0	-2	-1	2	0
c	4	$(-1, 0) \times (4, 1) \times (-1, 1)$	3	-3	-	-	-	-	0	0	-4
1	4	$(1, 0) \times (1, 0) \times (2, 0)$	$x_A = 2x_B = \frac{5}{2}x_C = 10x_D$ $\beta_1^g = -3, \beta_2^g = -2, \beta_4^g = 0,$ $\chi_1 = \frac{5}{\sqrt{2}}, \chi_2 = 2\sqrt{2}, \chi_3 = \sqrt{2}$								
2	2	$(1, 0) \times (0, -1) \times (0, 2)$									
4	2	$(0, -1) \times (0, 1) \times (2, 0)$									

Table 39: D6-brane configurations and intersection numbers of Model 15-dual, and its MSSM gauge coupling relation is $g_a^2 = \frac{10}{9}g_b^2 = \frac{4}{9}g_c^2 = \frac{4}{7}\frac{5g_Y^2}{3} = \frac{16}{27}2^{3/4}\sqrt{5}\pi e^{\phi_4}$.

Model 16		U(4) _C × U(2) _L × U(2) _R × USp(4) ₁ × USp(2) ₄								
stack	N	(n ¹ , l ¹) × (n ² , l ²) × (n ³ , l ³)	n _{□□}	n _□	b	b'	c	c'	1	4
a	8	(1, 1) × (−2, −1) × (1, 1)	0	−8	3	0	−3	0	1	−2
b	4	(−4, −1) × (1, 0) × (−1, 1)	3	−3	-	-	0	−2	0	−4
c	4	(−2, 1) × (1, 1) × (−1, 1)	−2	−6	-	-	-	-	−1	−2
1	4	(1, 0) × (1, 0) × (2, 0)	$x_A = \frac{13}{2}x_B = \frac{13}{8}x_C = 26x_D$ $\beta_1^g = -3, \beta_4^g = 4,$ $\chi_1 = \sqrt{\frac{13}{2}}, \chi_2 = 2\sqrt{26}, \chi_3 = \frac{\sqrt{13}}{2}$							
4	2	(0, −1) × (0, 1) × (2, 0)								

Table 40: D6-brane configurations and intersection numbers of Model 16, and its MSSM gauge coupling relation is $g_a^2 = \frac{1}{6}g_b^2 = \frac{7}{6}g_c^2 = \frac{35}{32}\frac{5g_Y^2}{3} = \frac{16}{135}26^{3/4}\pi e^{\phi_4}$.

Model 16-dual		$U(4)_C \times U(2)_L \times U(2)_R \times USp(4)_1 \times USp(2)_4$								
stack	N	$(n^1, l^1) \times (n^2, l^2) \times (n^3, l^3)$	$n_{\square\square}$	n_{\square}	b	b'	c	c'	1	4
a	8	$(1, 1) \times (-2, -1) \times (1, 1)$	0	-8	-3	0	3	0	1	-2
b	4	$(-2, 1) \times (1, 1) \times (-1, 1)$	-2	-6	-	-	0	-2	-1	-2
c	4	$(-4, -1) \times (1, 0) \times (-1, 1)$	3	-3	-	-	-	-	0	-4
1	4	$(1, 0) \times (1, 0) \times (2, 0)$	$x_A = \frac{13}{2}x_B = \frac{13}{8}x_C = 26x_D$ $\beta_1^g = -3, \beta_4^g = 4,$ $\chi_1 = \sqrt{\frac{13}{2}}, \chi_2 = 2\sqrt{26}, \chi_3 = \frac{\sqrt{13}}{2}$							
4	2	$(0, -1) \times (0, 1) \times (2, 0)$								

Table 41: D6-brane configurations and intersection numbers of Model 16-dual, and its MSSM gauge coupling relation is $g_a^2 = \frac{7}{6}g_b^2 = \frac{1}{6}g_c^2 = \frac{1}{4}\frac{5g_Y^2}{3} = \frac{16}{135}26^{3/4}\pi e^{\phi_4}$.

Model 17		$U(4)_C \times U(2)_L \times U(2)_R \times USp(2)_2 \times USp(2)_3 \times USp(2)_4$									
stack	N	$(n^1, l^1) \times (n^2, l^2) \times (n^3, l^3)$	$n_{\square\square}$	n_{\square}	b	b'	c	c'	2	3	4
a	8	$(1, -1) \times (1, 0) \times (1, 1)$	0	0	-3	0	3	0	-1	0	1
b	4	$(-1, 0) \times (-2, -3) \times (1, -1)$	-1	1	-	-	0	-3	0	3	-2
c	4	$(0, 1) \times (-1, 3) \times (-1, 1)$	2	-2	-	-	-	-	1	0	0
2	2	$(1, 0) \times (0, -1) \times (0, 2)$	$x_A = \frac{1}{3}x_B = \frac{1}{2}x_C = \frac{1}{3}x_D$ $\beta_2^g = -3, \beta_3^g = -3, \beta_4^g = -2,$ $\chi_1 = \frac{1}{\sqrt{2}}, \chi_2 = \frac{\sqrt{2}}{3}, \chi_3 = \sqrt{2}$								
3	2	$(0, -1) \times (1, 0) \times (0, 2)$									
4	2	$(0, -1) \times (0, 1) \times (2, 0)$									

Table 42: D6-brane configurations and intersection numbers of Model 17, and its MSSM gauge coupling relation is $g_a^2 = 2g_b^2 = g_c^2 = \frac{5g_Y^2}{3} = \frac{16\sqrt[4]{2}\pi e^{\phi_4}}{3\sqrt{3}}$.

Model 17-dual		$U(4)_C \times U(2)_L \times U(2)_R \times USp(2)_2 \times USp(2)_3 \times USp(2)_4$									
stack	N	$(n^1, l^1) \times (n^2, l^2) \times (n^3, l^3)$	$n_{\square\square}$	n_{\square}	b	b'	c	c'	2	3	4
a	8	$(1, -1) \times (1, 0) \times (1, 1)$	0	0	3	0	-3	0	-1	0	1
b	4	$(0, 1) \times (-1, 3) \times (-1, 1)$	2	-2	-	-	0	-3	1	0	0
c	4	$(-1, 0) \times (-2, -3) \times (1, -1)$	-1	1	-	-	-	-	0	3	-2
2	2	$(1, 0) \times (0, -1) \times (0, 2)$	$x_A = \frac{1}{3}x_B = \frac{1}{2}x_C = \frac{1}{3}x_D$ $\beta_2^g = -3, \beta_3^g = -3, \beta_4^g = -2,$ $\chi_1 = \frac{1}{\sqrt{2}}, \chi_2 = \frac{\sqrt{2}}{3}, \chi_3 = \sqrt{2}$								
3	2	$(0, -1) \times (1, 0) \times (0, 2)$									
4	2	$(0, -1) \times (0, 1) \times (2, 0)$									

Table 43: D6-brane configurations and intersection numbers of Model 17-dual, and its MSSM gauge coupling relation is $g_a^2 = g_b^2 = 2g_c^2 = \frac{10}{7}\frac{5g_Y^2}{3} = \frac{16\sqrt[4]{2}\pi e^{\phi_4}}{3\sqrt{3}}$.

Model 18		$U(4)_C \times U(2)_L \times U(2)_R \times USp(2)_2 \times USp(2)_3 \times USp(2)_4$									
stack	N	$(n^1, l^1) \times (n^2, l^2) \times (n^3, l^3)$	$n_{\square\square}$	n_{\square}	b	b'	c	c'	2	3	4
a	8	$(1, -1) \times (1, 0) \times (1, 1)$	0	0	3	0	-3	0	-1	0	1
b	4	$(-1, 4) \times (0, 1) \times (-1, 1)$	3	-3	-	-	0	-7	0	1	0
c	4	$(2, 1) \times (1, 1) \times (1, -1)$	2	6	-	-	-	-	1	2	-2
2	2	$(1, 0) \times (0, -1) \times (0, 2)$	$x_A = \frac{1}{9}x_B = \frac{1}{4}x_C = \frac{1}{9}x_D$ $\beta_2^g = -3, \beta_3^g = -3, \beta_4^g = -2,$ $\chi_1 = \frac{1}{2}, \chi_2 = \frac{2}{9}, \chi_3 = 1$								
3	2	$(0, -1) \times (1, 0) \times (0, 2)$									
4	2	$(0, -1) \times (0, 1) \times (2, 0)$									

Table 44: D6-brane configurations and intersection numbers of Model 18, and its MSSM gauge coupling relation is $g_a^2 = \frac{4}{9}g_b^2 = \frac{17}{9}g_c^2 = \frac{85}{61}\frac{5g_Y^2}{3} = \frac{32\pi e^{\phi_4}}{15}$.

Model 18-dual		$U(4)_C \times U(2)_L \times U(2)_R \times USp(2)_2 \times USp(2)_3 \times USp(2)_4$									
stack	N	$(n^1, l^1) \times (n^2, l^2) \times (n^3, l^3)$	$n_{\square\square}$	n_{\square}	b	b'	c	c'	2	3	4
a	8	$(1, -1) \times (1, 0) \times (1, 1)$	0	0	-3	0	3	0	-1	0	1
b	4	$(2, 1) \times (1, 1) \times (1, -1)$	2	6	-	-	0	-7	1	2	-2
c	4	$(-1, 4) \times (0, 1) \times (-1, 1)$	3	-3	-	-	-	-	0	1	0
2	2	$(1, 0) \times (0, -1) \times (0, 2)$	$x_A = \frac{1}{9}x_B = \frac{1}{4}x_C = \frac{1}{9}x_D$ $\beta_2^g = -3, \beta_3^g = -3, \beta_4^g = -2,$ $\chi_1 = \frac{1}{2}, \chi_2 = \frac{2}{9}, \chi_3 = 1$								
3	2	$(0, -1) \times (1, 0) \times (0, 2)$									
4	2	$(0, -1) \times (0, 1) \times (2, 0)$									

Table 45: D6-brane configurations and intersection numbers of Model 18-dual, and its MSSM gauge coupling relation is $g_a^2 = \frac{17}{9}g_b^2 = \frac{4}{9}g_c^2 = \frac{4}{7}\frac{5g_Y^2}{3} = \frac{32\pi e^{\phi_4}}{15}$.

Model 19		$U(4)_C \times U(2)_L \times U(2)_R \times USp(2)_1 \times USp(2)_4$								
stack	N	$(n^1, l^1) \times (n^2, l^2) \times (n^3, l^3)$	$n_{\square\square}$	n_{\square}	b	b'	c	c'	1	4
a	8	$(-1, -1) \times (1, 1) \times (1, 1)$	0	-4	-3	0	3	0	1	-1
b	4	$(1, 4) \times (1, 0) \times (1, -1)$	-3	3	-	-	0	7	0	-1
c	4	$(-2, 1) \times (2, 1) \times (-1, 1)$	-3	-13	-	-	-	-	-1	-4
1	2	$(1, 0) \times (1, 0) \times (2, 0)$	$x_A = 28x_B = \frac{28}{23}x_C = 7x_D$ $\beta_1^g = -3, \beta_4^g = 1,$ $\chi_1 = \sqrt{\frac{7}{23}}, \chi_2 = \sqrt{161}, \chi_3 = 8\sqrt{\frac{7}{23}}$							
4	2	$(0, -1) \times (0, 1) \times (2, 0)$								

Table 46: D6-brane configurations and intersection numbers of Model 19, and its MSSM gauge coupling relation is $g_a^2 = \frac{1}{6}g_b^2 = \frac{11}{6}g_c^2 = \frac{11}{8}\frac{5g_Y^2}{3} = \frac{8}{405}\sqrt{2161}^{3/4}\pi e^{\phi_4}$.

Model 19-dual		$U(4)_C \times U(2)_L \times U(2)_R \times USp(2)_1 \times USp(2)_4$								
stack	N	$(n^1, l^1) \times (n^2, l^2) \times (n^3, l^3)$	$n_{\square\square}$	n_{\square}	b	b'	c	c'	1	4
a	8	$(-1, -1) \times (1, 1) \times (1, 1)$	0	-4	3	0	-3	0	1	-1
b	4	$(-2, 1) \times (2, 1) \times (-1, 1)$	-3	-13	-	-	0	7	-1	-4
c	4	$(1, 4) \times (1, 0) \times (1, -1)$	-3	3	-	-	-	-	0	-1
1	2	$(1, 0) \times (1, 0) \times (2, 0)$	$x_A = 28x_B = \frac{28}{23}x_C = 7x_D$ $\beta_1^g = -3, \beta_4^g = 1,$ $\chi_1 = \sqrt{\frac{7}{23}}, \chi_2 = \sqrt{161}, \chi_3 = 8\sqrt{\frac{7}{23}}$							
4	2	$(0, -1) \times (0, 1) \times (2, 0)$								

Table 47: D6-brane configurations and intersection numbers of Model 19-dual, and its MSSM gauge coupling relation is $g_a^2 = \frac{11}{6}g_b^2 = \frac{1}{6}g_c^2 = \frac{1}{4}\frac{5g_Y^2}{3} = \frac{8}{405}\sqrt{2161}^{3/4}\pi e^{\phi_4}$.

Model 20		$U(4)_C \times U(2)_L \times U(2)_R \times USp(2)_1 \times USp(2)_4$								
stack	N	$(n^1, l^1) \times (n^2, l^2) \times (n^3, l^3)$	$n_{\square\square}$	n_{\square}	b	b'	c	c'	1	4
a	8	$(1, 1) \times (-1, -1) \times (1, 1)$	0	-4	3	0	-3	0	1	-1
b	4	$(-1, 0) \times (5, 2) \times (-1, 1)$	3	-3	-	-	0	-1	0	-5
c	4	$(0, 1) \times (-2, 1) \times (-1, 1)$	-1	1	-	-	-	-	-1	0
1	2	$(1, 0) \times (1, 0) \times (2, 0)$	$x_A = 2x_B = \frac{14}{5}x_C = 7x_D$ $\beta_1^g = -3, \beta_4^g = 1,$ $\chi_1 = \frac{7}{\sqrt{5}}, \chi_2 = \sqrt{5}, \chi_3 = \frac{4}{\sqrt{5}}$							
4	2	$(0, -1) \times (0, 1) \times (2, 0)$								

Table 48: D6-brane configurations and intersection numbers of Model 20, and its MSSM gauge coupling relation is $g_a^2 = \frac{5}{6}g_b^2 = \frac{7}{6}g_c^2 = \frac{35}{32}\frac{5g_Y^2}{3} = \frac{8}{27}5^{3/4}\sqrt{7}\pi e^{\phi_4}$.

Model 20-dual		$U(4)_C \times U(2)_L \times U(2)_R \times USp(2)_1 \times USp(2)_4$								
stack	N	$(n^1, l^1) \times (n^2, l^2) \times (n^3, l^3)$	$n_{\square\square}$	n_{\square}	b	b'	c	c'	1	4
a	8	$(1, 1) \times (-1, -1) \times (1, 1)$	0	-4	-3	0	3	0	1	-1
b	4	$(0, 1) \times (-2, 1) \times (-1, 1)$	-1	1	-	-	0	-1	-1	0
c	4	$(-1, 0) \times (5, 2) \times (-1, 1)$	3	-3	-	-	-	-	0	-5
1	2	$(1, 0) \times (1, 0) \times (2, 0)$	$x_A = 2x_B = \frac{14}{5}x_C = 7x_D$ $\beta_1^g = -3, \beta_4^g = 1,$ $\chi_1 = \frac{7}{\sqrt{5}}, \chi_2 = \sqrt{5}, \chi_3 = \frac{4}{\sqrt{5}}$							
4	2	$(0, -1) \times (0, 1) \times (2, 0)$								

Table 49: D6-brane configurations and intersection numbers of Model 20-dual, and its MSSM gauge coupling relation is $g_a^2 = \frac{7}{6}g_b^2 = \frac{5}{6}g_c^2 = \frac{25}{28}\frac{5g_Y^2}{3} = \frac{8}{27}5^{3/4}\sqrt{7}\pi e^{\phi_4}$.

Model 21		$U(4)_C \times U(2)_L \times U(2)_R \times USp(2)_2 \times USp(2)_4$								
stack	N	$(n^1, l^1) \times (n^2, l^2) \times (n^3, l^3)$	$n_{\square\square}$	n_{\square}	b	b'	c	c'	2	4
a	8	$(1, -1) \times (1, 0) \times (1, 1)$	0	0	-3	0	3	0	-1	1
b	4	$(-1, 0) \times (-2, -3) \times (1, -1)$	-1	1	-	-	0	0	0	-2
c	4	$(0, 1) \times (-2, 3) \times (-1, 1)$	1	-1	-	-	-	-	2	0
2	2	$(1, 0) \times (0, -1) \times (0, 2)$	$x_A = \frac{2}{3}x_B = x_C = \frac{2}{3}x_D$ $\beta_2^g = -2, \beta_4^g = -2,$ $\chi_1 = 1, \chi_2 = \frac{2}{3}, \chi_3 = 2$							
4	2	$(0, -1) \times (0, 1) \times (2, 0)$								

Table 50: D6-brane configurations and intersection numbers of Model 21, and its MSSM gauge coupling relation is $g_a^2 = 2g_b^2 = 2g_c^2 = \frac{10}{7} \frac{5g_Y^2}{3} = \frac{8\pi e^{\phi_4}}{\sqrt{3}}$.

Model 22		$U(4)_C \times U(2)_L \times U(2)_R \times USp(2)_3$								
stack	N	$(n^1, l^1) \times (n^2, l^2) \times (n^3, l^3)$	$n_{\square\square}$	n_{\square}	b	b'	c	c'	3	
a	8	$(1, -1) \times (1, 0) \times (1, 1)$	0	0	3	0	-3	0	0	
b	4	$(-2, 5) \times (0, 1) \times (-1, 1)$	3	-3	-	-	0	-8	2	
c	4	$(2, 1) \times (1, 1) \times (1, -1)$	2	6	-	-	-	-	2	
3	2	$(0, -1) \times (1, 0) \times (0, 2)$	$x_A = \frac{1}{6}x_B = \frac{2}{5}x_C = \frac{1}{6}x_D$ $\beta_3^g = -2,$ $\chi_1 = \sqrt{\frac{2}{5}}, \chi_2 = \frac{\sqrt{\frac{5}{2}}}{6}, \chi_3 = 2\sqrt{\frac{2}{5}}$							

Table 51: D6-brane configurations and intersection numbers of Model 22, and its MSSM gauge coupling relation is $g_a^2 = \frac{5}{6}g_b^2 = \frac{11}{6}g_c^2 = \frac{11}{8} \frac{5g_Y^2}{3} = \frac{8\sqrt[4]{25^{3/4}}\pi e^{\phi_4}}{7\sqrt{3}}$.

Model 22-dual		$U(4)_C \times U(2)_L \times U(2)_R \times USp(2)_3$								
stack	N	$(n^1, l^1) \times (n^2, l^2) \times (n^3, l^3)$	$n_{\square\square}$	n_{\square}	b	b'	c	c'	3	
a	8	$(1, -1) \times (1, 0) \times (1, 1)$	0	0	-3	0	3	0	0	
b	4	$(2, 1) \times (1, 1) \times (1, -1)$	2	6	-	-	0	-8	2	
c	4	$(-2, 5) \times (0, 1) \times (-1, 1)$	3	-3	-	-	-	-	2	
3	2	$(0, -1) \times (1, 0) \times (0, 2)$	$x_A = \frac{1}{6}x_B = \frac{2}{5}x_C = \frac{1}{6}x_D$ $\beta_3^g = -2,$ $\chi_1 = \sqrt{\frac{2}{5}}, \chi_2 = \frac{\sqrt{\frac{5}{2}}}{6}, \chi_3 = 2\sqrt{\frac{2}{5}}$							

Table 52: D6-brane configurations and intersection numbers of Model 22-dual, and its MSSM gauge coupling relation is $g_a^2 = \frac{11}{6}g_b^2 = \frac{5}{6}g_c^2 = \frac{25}{28} \frac{5g_Y^2}{3} = \frac{8\sqrt[4]{25^{3/4}}\pi e^{\phi_4}}{7\sqrt{3}}$.

References

- [1] M. Berkooz, M. R. Douglas and R. G. Leigh, *Branes intersecting at angles*, *Nucl. Phys. B* **480** (1996) 265 [[hep-th/9606139](#)].
- [2] G. Aldazabal, S. Franco, L. E. Ibanez, R. Rabadan and A. M. Uranga, *Intersecting brane worlds*, *JHEP* **02** (2001) 047 [[hep-ph/0011132](#)].
- [3] E. Witten, *D-branes and K-theory*, *JHEP* **12** (1998) 019 [[hep-th/9810188](#)].
- [4] A. M. Uranga, *D-brane probes, RR tadpole cancellation and K-theory charge*, *Nucl. Phys. B* **598** (2001) 225 [[hep-th/0011048](#)].
- [5] A. Mansha, T. Li and M. Sabir, *Revisiting the supersymmetric trinification models from intersecting D6-branes*, *Commun. Theor. Phys.* **76** (2024) 095201 [[2406.07586](#)].
- [6] M. Cvetič, T. Li and T. Liu, *Supersymmetric Pati-Salam models from intersecting D6-branes: A Road to the standard model*, *Nucl. Phys. B* **698** (2004) 163 [[hep-th/0403061](#)].
- [7] R. Blumenhagen, B. Kors, D. Lust and S. Stieberger, *Four-dimensional String Compactifications with D-Branes, Orientifolds and Fluxes*, *Phys. Rept.* **445** (2007) 1 [[hep-th/0610327](#)].
- [8] R. Blumenhagen, M. Cvetič, P. Langacker and G. Shiu, *Toward realistic intersecting D-brane models*, *Ann. Rev. Nucl. Part. Sci.* **55** (2005) 71 [[hep-th/0502005](#)].
- [9] T. Li, A. Mansha and R. Sun, *Revisiting the supersymmetric Pati-Salam models from intersecting D6-branes*, *Eur. Phys. J. C* **81** (2021) 82 [[1910.04530](#)].
- [10] T. Li, A. Mansha, R. Sun, L. Wu and W. He, *$N=1$ supersymmetric $SU(12)_C \times SU(2)_L \times SU(2)_R$ models, $SU(4)_C \times SU(6)_L \times SU(2)_R$ models, and $SU(4)_C \times SU(2)_L \times SU(6)_R$ models from intersecting D6-branes*, *Phys. Rev. D* **104** (2021) 046018 [[1912.11633](#)].
- [11] A. Mansha, T. Li, M. Sabir and L. Wu, *Three-family supersymmetric Pati-Salam models with symplectic groups from intersecting D6-branes*, *Eur. Phys. J. C* **84** (2024) 151 [[2212.09644](#)].
- [12] M. Sabir, T. Li, A. Mansha and X.-C. Wang, *The supersymmetry breaking soft terms, and fermion masses and mixings in the supersymmetric Pati-Salam model from intersecting D6-branes*, *JHEP* **04** (2022) 089 [[2202.07048](#)].
- [13] A. Mansha, T. Li and L. Wu, *The hidden sector variations in the $\mathcal{N} = 1$ supersymmetric three-family Pati-Salam models from intersecting D6-branes*, *Eur. Phys. J. C* **83** (2023) 1067 [[2303.02864](#)].
- [14] W. He, T. Li and R. Sun, *The complete search for the supersymmetric Pati-Salam models from intersecting D6-branes*, *JHEP* **08** (2022) 044 [[2112.09632](#)].
- [15] M. Sabir, A. Mansha, T. Li and Z.-W. Wang, *Fermion masses and mixings in the supersymmetric Pati-Salam landscape from Intersecting D6-Branes*, *JHEP* **10** (2024) 252 [[2409.09110](#)].
- [16] M. Sabir, T. Li, A. Mansha and Z.-W. Wang, *Fermion Masses and Mixings in String Theory with Dirac Neutrinos*, [2407.19458](#).
- [17] E. G. Gimon and J. Polchinski, *Consistency conditions for orientifolds and D-manifolds*, *Phys. Rev. D* **54** (1996) 1667 [[hep-th/9601038](#)].

- [18] M. B. Green and J. H. Schwarz, *Anomaly Cancellation in Supersymmetric D=10 Gauge Theory and Superstring Theory*, *Phys. Lett. B* **149** (1984) 117.
- [19] J. F. G. Cascales and A. M. Uranga, *Chiral 4d string vacua with D branes and NSNS and RR fluxes*, *JHEP* **05** (2003) 011 [[hep-th/0303024](#)].
- [20] F. Marchesano and G. Shiu, *MSSM vacua from flux compactifications*, *Phys. Rev. D* **71** (2005) 011701 [[hep-th/0408059](#)].
- [21] F. Marchesano and G. Shiu, *Building MSSM flux vacua*, *JHEP* **11** (2004) 041 [[hep-th/0409132](#)].
- [22] C.-M. Chen, T. Li and D. V. Nanopoulos, *Type IIA Pati-Salam flux vacua*, *Nucl. Phys. B* **740** (2006) 79 [[hep-th/0601064](#)].
- [23] M. Cvetič, P. Langacker, T. Li and T. Liu, *D6-brane splitting on type IIA orientifolds*, *Nucl. Phys. B* **709** (2005) 241 [[hep-th/0407178](#)].
- [24] M. Cvetič, R. Richter and T. Weigand, *Computation of D-brane instanton induced superpotential couplings: Majorana masses from string theory*, *Phys. Rev. D* **76** (2007) 086002 [[hep-th/0703028](#)].
- [25] C.-M. Chen, T. Li, V. E. Mayes and D. V. Nanopoulos, *Towards realistic supersymmetric spectra and Yukawa textures from intersecting branes*, *Phys. Rev. D* **77** (2008) 125023 [[0711.0396](#)].
- [26] R. Blumenhagen, M. Cvetič and T. Weigand, *Spacetime instanton corrections in 4D string vacua: The Seesaw mechanism for D-Brane models*, *Nucl. Phys. B* **771** (2007) 113 [[hep-th/0609191](#)].
- [27] M. Haack, D. Krefl, D. Lust, A. Van Proeyen and M. Zagermann, *Gaugino Condensates and D-terms from D7-branes*, *JHEP* **01** (2007) 078 [[hep-th/0609211](#)].
- [28] B. Florea, S. Kachru, J. McGreevy and N. Saulina, *Stringy Instantons and Quiver Gauge Theories*, *JHEP* **05** (2007) 024 [[hep-th/0610003](#)].
- [29] E. Cremmer, S. Ferrara, L. Girardello and A. Van Proeyen, *Yang-Mills Theories with Local Supersymmetry: Lagrangian, Transformation Laws and SuperHiggs Effect*, *Nucl. Phys. B* **212** (1983) 413.
- [30] D. Lust, P. Mayr, R. Richter and S. Stieberger, *Scattering of gauge, matter, and moduli fields from intersecting branes*, *Nucl. Phys. B* **696** (2004) 205 [[hep-th/0404134](#)].
- [31] I. R. Klebanov and E. Witten, *Proton decay in intersecting D-brane models*, *Nucl. Phys. B* **664** (2003) 3 [[hep-th/0304079](#)].
- [32] R. Blumenhagen, D. Lust and S. Stieberger, *Gauge unification in supersymmetric intersecting brane worlds*, *JHEP* **07** (2003) 036 [[hep-th/0305146](#)].
- [33] L. E. Ibanez, F. Marchesano and R. Rabadan, *Getting just the standard model at intersecting branes*, *JHEP* **11** (2001) 002 [[hep-th/0105155](#)].
- [34] R. Blumenhagen, M. Cvetič, F. Marchesano and G. Shiu, *Chiral D-brane models with frozen open string moduli*, *JHEP* **03** (2005) 050 [[hep-th/0502095](#)].
- [35] A. Font and L. E. Ibanez, *SUSY-breaking soft terms in a MSSM magnetized D7-brane model*, *JHEP* **03** (2005) 040 [[hep-th/0412150](#)].
- [36] M. Cvetič and I. Papadimitriou, *Conformal field theory couplings for intersecting D-branes on orientifolds*, *Phys. Rev. D* **68** (2003) 046001 [[hep-th/0303083](#)].

- [37] Y. Kawamura, T. Kobayashi and T. Komatsu, *Specific scalar mass relations in $SU(3) \times SU(2) \times U(1)$ orbifold model*, *Phys. Lett. B* **400** (1997) 284 [[hep-ph/9609462](#)].
- [38] Z. Komargodski and N. Seiberg, *Comments on the Fayet-Iliopoulos Term in Field Theory and Supergravity*, *JHEP* **06** (2009) 007 [[0904.1159](#)].
- [39] G. L. Kane, P. Kumar, J. D. Lykken and T. T. Wang, *Some phenomenology of intersecting D-brane models*, *Phys. Rev. D* **71** (2005) 115017 [[hep-ph/0411125](#)].
- [40] A. Brignole, L. E. Ibanez and C. Munoz, *Soft supersymmetry breaking terms from supergravity and superstring models*, *Adv. Ser. Direct. High Energy Phys.* **18** (1998) 125 [[hep-ph/9707209](#)].
- [41] A. Brignole, L. E. Ibanez and C. Munoz, *Towards a theory of soft terms for the supersymmetric Standard Model*, *Nucl. Phys. B* **422** (1994) 125 [[hep-ph/9308271](#)].
- [42] S.-J. Lee, W. Lerche and T. Weigand, *Emergent strings from infinite distance limits*, *JHEP* **02** (2022) 190 [[1910.01135](#)].
- [43] G. F. Casas, L. E. Ibáñez and F. Marchesano, *Yukawa couplings at infinite distance and swampland towers in chiral theories*, *JHEP* **09** (2024) 170 [[2403.09775](#)].